Theory of Partial Discharge and Arc Formation

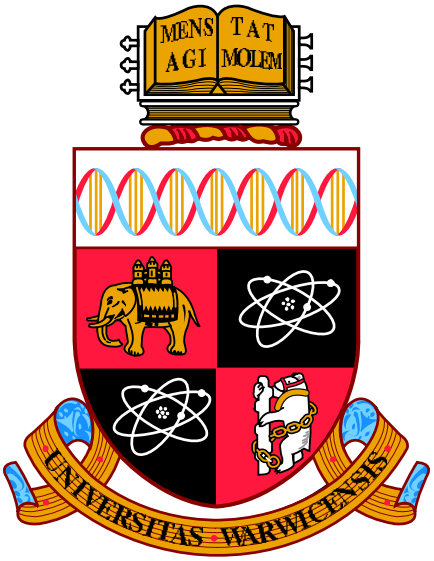

A Shipley

School of Engineering

University of Warwick

Dissertation submitted for the degree of

Doctor of Philosophy

October 2011

Declaration

The author wishes to declare that, except for commonly understood and accepted ideas or where reference is made to the work of others, the work in this dissertation is his own, and includes nothing which is the outcome of work done in collaboration. It has not been submitted in part, or in whole, to any other university for a degree, diploma or other qualification.
Adrian Shipley
July 2012

Acknowledgements

I would like to thank my supervisor, Professor Phil Mawby and also Dr Angus Bryant, who was originally my Co-Supervisor prior to leaving the University. Both have provided great help and guidance and helped shape the original ideas behind this work. Phil has continued to help steer my work and this thesis for which I am extremely grateful.

I would also like to give my sincere thanks to Steve Miles for his support and encouragement from the beginning, when I was only discussing the notional idea of undertaking a PhD to the present day, this level of support was a great help during the formative periods of this research. This thanks also extends to Simon Linacre, Joe Krisciunas and Steve Carlson who have also been very supportive during my studies.

Thanks also to Sam Jeffries who has made the challenges associated with my working life and studies so much easier and enabled me to focus on any given task at hand.

Additionally thanks to Jonathan Grylls, who gave up a lot of his personal time in proof reading various chapters of this thesis this was very much appreciated.

Finally I would like to thank my wife Nicole for her patience and support over these past few years. Also my father Ken who has been an inspiration and a hero throughout my life, but sadly past away during the writing of this thesis.

To my wife Nicole and children Daniel, Martin, Lauren and Paul
Also to my Parents, Doreen and Ken

Abstract

The demand for electrical power has consistently risen over time, whether it be to support the development and expansion of cities or because traditional approaches to societies solutions are being replaced by their electrical equivalent. The automotive industry is beginning to introduce more electric, greener vehicles. The aviation industry is also being challenged with the same issues. Whatever the motivation, this rising demand for power is always facilitated by employing higher and higher voltage levels.

It is well understood that if the voltage is too high for a given air gap, electric breakdown will occur. this effect is exacerbated by increases in altitude, resulting in constant challenges in aviation to satisfy the contradictory demands for smaller/lighter compact solutions against the biggest possible air gaps necessary to prevent electric breakdown.

An experimental curve by Louis Karl Heinrich Friedrich Paschen was developed, which relates the voltage at which electric breakdown would be expected to that of the product of gas pressure (p) and distance (d). The aviation industry does not use this curve directly as alternate guidance documents are used. These documents are extremely conservative, sometimes overly so, as will be seen in the thesis. Mathematical attempts have been provided to try and explain the Paschen curve, based on Townsend Primary and secondary ionisation. However, the variable 'pd' does not get explicitly linked and a type of mathematical fudge becomes incorporated.

This thesis attempts to provide a theory of the minimum electric breakdown curve and fundamentally link he 'pd' product. by experimental validation of the theory, with the accepted standards included. A basis for challenging these standards may result and prevent potential over engineering in the future in this continually challenging environment. This theory will then go on to explain arc formation by providing a treatment to a paradox that occurs at the point of breakdown.

Contents

List of Figures

Chapter

1 General Introduction

-

1.1 History of Electrification

1.1.1 Terrestrial

The building of the first electrical transmission grid in the UK was completed in 1933. It was an early example of a nationalised public service industry and of large-scale industrial management in Britain. In any history of the Grid it is necessary to touch on many historical aspects political, economic, environmental and commercial). Other than the main technical theme. Nevertheless in his paper the emphasis is on the technical history [1].

The reason why the UK electrical transmission grid was built goes back many years. A short summary of the background is given here. During the 1914-18 War the deficiencies of the numerous electricity networks meeting the national need were widely recognised.

Consequently, in 1919 an Act of Parliament was passed which appointed Electricity Commissioners to supervise electricity supply. The Commission was expected to encourage independent undertakings to form the Joint Electricity Authorities (JEA). Each JEA would supply electricity to all the users in a large area, e.g. Greater London, from a small number of large and hence economic power stations. For several reasons this voluntary scheme failed to reform generation: it failed to standardise the frequency of supply, it failed to make cheaper electricity widely available and it failed to encourage the electrification of industry, homes and offices. In 1926 Parliament tried again. However this time it proposed a Central Electricity Board (CEB) with powers to select efficient power stations, to buy and sell wholesale electricity and to economise on both capital and running costs. Some of these undertakings would own and operate one or more selected stations which would be under the operational control of the CEB; other undertakings would take a bulk supply from the Grid, at-Grid tariff, which they would retail to their customers. The proposed grid network of 1927 is shown below

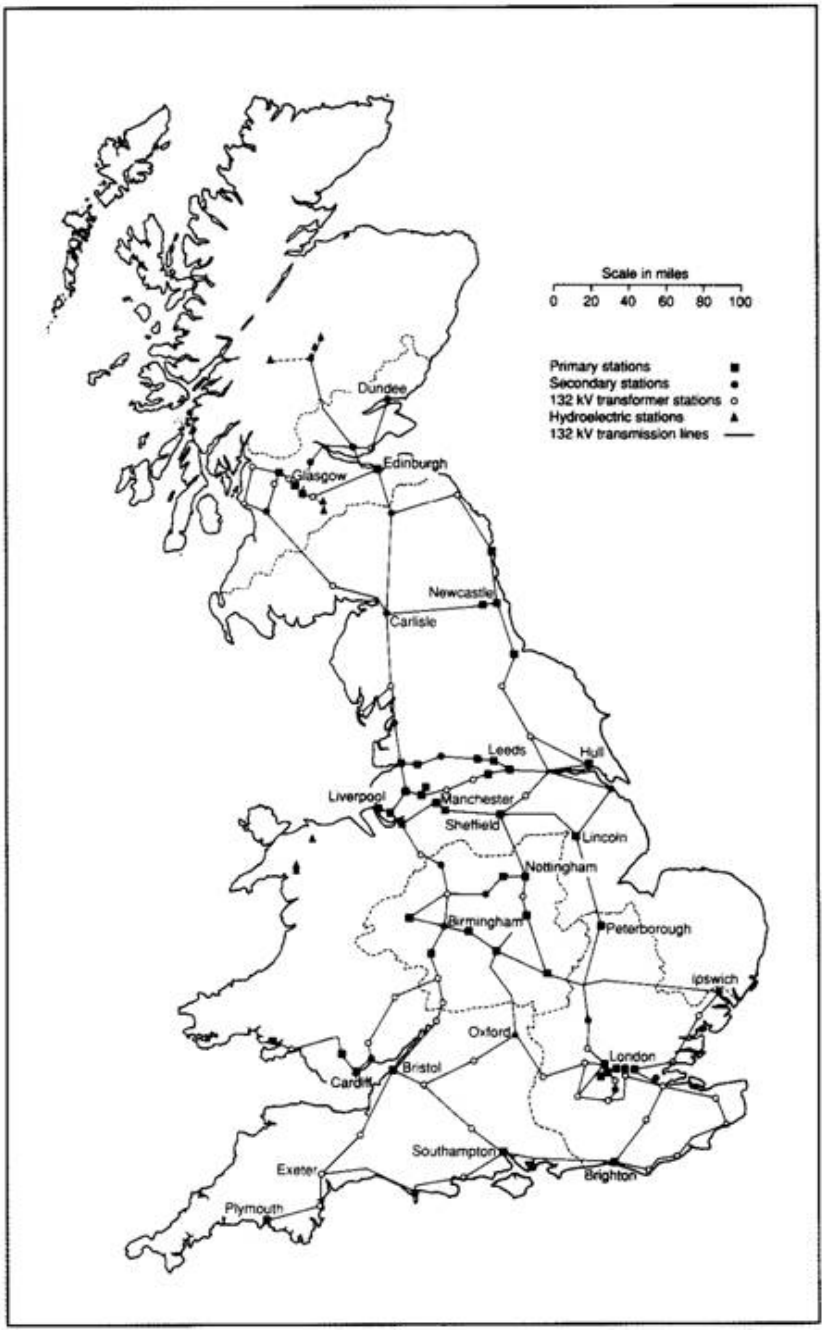

Figure 1.1: Proposed Grid network in 1927 [1]

The design of each scheme area was based on the principle of interconnecting power

stations in a ring main. The design criteria used were both technical and economic. Comments written by Kennedy on four schemes have survived and show how carefully the schemes were scrutinised [11]. These notes show that great attention was paid to the selection of the power stations and their interconnection by the ring mains of the 132kV overhead transmission lines.

The 1926 act was set up by the Central Electricity Board (CEB) and standardised the transmission voltage at 132kV at 50Hz. However, in 1949, the British Electricity Authority decided to upgrade the grid by adding 275 kV links. In 1965 the grid voltage was further raised to 400kV, transmitting over 221km over what is now referred to as the super-grid, from Sundon to West Burton. 500kV is now regularly used in China, however, 800kV distribution is seriously being considered also. [1]

1.1.2 Aerospace

Early aircraft were considered mechanical machines where the battery only provided power for the spark plugs within the engine, which was very similar to that of car, an early example of this is shown below in figure 1.2. Instrumentation and navigational aids where mechanical with very little demand to move towards electrification, a trend seen also in the automotive industry of the time. During the 1910's the need to communicate became essential and so electronic equipment was finding its way onto aircraft as communication could only be done by electronics [2].

The communication equipment derived its power from the 12V - 14V battery that was already on the aircraft providing electrical power for the spark plugs within the engine.

1913 saw the first aircraft with an electronic compass fitted and soon after more and more mechanical functions were replaced by their electronic equivalent. This increase in the number of electronic loads meant that the power demand raised accordingly. It was during this time that the first deviation away from automotive architectures occurred where the battery voltage was raised from 12V - 14V to 28V, to help minimise the weight of the wiring system.

With the increase in electrical loads, more and more wiring was required and to provide power to these loads at 14V would require thick and heavy gauge wiring. Raising the supply voltage to 28V meant that the wiring would not need to increase in gauge. Increasing the gauge of the wiring would have a two fold effect on the manufacture of the aircraft. First, wiring of the aircraft becomes more difficult due to the wiring not being as flexible, secondly, the weight of the aircraft increases and this has a direct impact on the fuel required for flight.

Figure 1.2: Autochrome Lumiere circa 1917 [2]

The energy taken from the battery needs to be replenished and magneto's using permanent magnets were deployed on aircraft in 1914. Under normal operation the electrical loads will receive their power from the magneto's and the batteries are now only used for engine start and to provide power to the loads while the engine is getting up to speed.

As the quantity and power demand of the electrical loads increases further, greater demand to increase the gauge of the wiring would have been felt. To restrain further wiring gauge increases a new higher voltage bus was employed. In 1946 The Convair 36 Peacemaker shown below in figure 1.3 employed the first 115V AC generator.

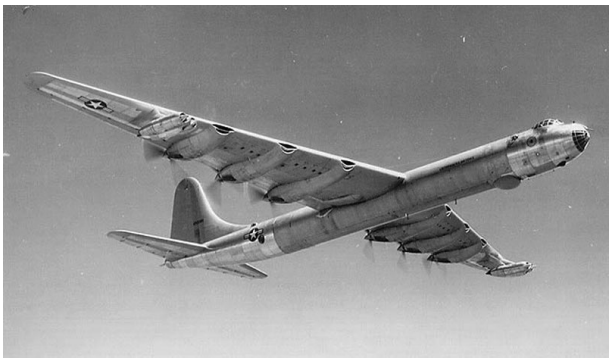

Figure 1.3: Convair B36 Peacemaker 1946 [2]

This new 115V AC power bus, came with its own problems, namely weight and size. If this bus adopted the frequency of that used by household electrical systems (i.e. 50/60Hz), the size of the generator would have been very large and would have meant that this method of electrification was prohibitive. Instead the aviation generator operated at 400Hz and this increase of frequency meant that the size and weight of the generator could be reduced to an acceptable value for aviation purposes. The 400Hz was kept con-

stant by the inclusion of power electronics (e.g. cycloconverter). This combination of 115V AC and 28V DC supply voltages became the main stay of aviation power systems for many years after, in fact the only change to the electrical system occurred in 1996. The Global Express chose Variable Frequency (VF) over the traditional Constant Frequency (CF). The decision to employ 'VF' over 'CF' was primarily due to weight. VF is a simpler and lighter solution, but it took many years of persuasion and scrutiny by the aviation industry, by what at the time was considered a huge technological leap as it was of the opinion that electrical equipment would not be able to handle what is still termed 'frequency wild' electrical generation.

Since 1996 all AC power sources adopt a frequency wild output. The term 'frequency wild' is a little misleading as the frequency range is actually between 360Hz and 800Hz, however, its nominal frequency is still around 400Hz.

At every junction any decision to change anything on the aircraft or employ different architectures and technologies will have weight challenges against it. In fact employing what is considered as high voltage (115V AC) has been challenged as the volume and weight of this bus has been scrutinised. Now the three phase 115V AC system would normally require four cables, namely each of the three phases and its associated neutral. In order to save weight the neutral cable is dispensed with and neutral return currents through the fuselage are permitted. But still the aircraft is carrying three cables. If a 270V DC systems was to be employed and the current return path was still the fuselage then this would mean that the original three cables routing the three phases around the aircraft could be reduced to just one. Further, being at a higher voltage, less current is required for the same power. Moreover, in what was a surprise to all in the industry of

the time 'skin effect' was having an effect and the cables where required to be oversized by 15% to accommodate the losses due to skin effect. Employing a DC system provides greater cable utilisation as skin effects only impact AC systems. The JSF F-35 is the first aircraft to employ a 270V DC architecture as wiring volume and weight are at a premium on such an aircraft. The 270V DC is derived from the rectified 115V AC generator voltage.

Figure 1.4: JSF F-35 circa 2006 [2]

The latest civil aircraft to adopt high voltage DC electrical systems as part of it's architecture is the Boeing 787 [12]. This aircraft is the first aircraft to employ a bleed-less engine technology, bleed-less means that pneumatic air is no longer taken (bled) off the engine. The two principle reasons for going bleed-less are to reduce the weight of the overall system, by removing the heavy pneumatic pipe-work and replace it with electrical cables. Moving to more electrical solutions will improve the speed of manufacture which will reduce the None Recoverable Expenditure (NRE) that it takes to produce the aircraft in the first place.

For the Boeing 787, in addition to raising the generator output AC supply voltage even higher to 230V, it also takes advantage of the further weight savings that DC architectures offer and this aircraft also utilises a ± 270V DC power bus, again derived by rectifying

the 230V AC generator voltage. Previously, aircraft's electrical system used about 220kW of electrical power, however, the Boeing 787, with a majority of it's pneumatic functions now being completed electrically, the electrical power for this aircraft has risen to 1.4MW.

Figure 1.5: Boeing 787 at the Paris Air Show 2011, Image courtesy of The Boeing Company.

Although 1.4MW appears very large, in comparison to the thrust output of the engine the electrical system still only uses 3% of the thrust power available from the engine which is approximately 40MW! in total. Most of the electrical energy is used for passenger comfort, (i.e. Cabin pressurisation, heating, lighting, In Flight Entertainment (IFE) and Galleys) most of which are not required for the F-35.

The range of voltages employed on the Boeing 787 are; 230V AC, ±270V DC, 115V AC and 28V DC. Some of the voltages used are for legacy reasons and others, mainly the higher voltage buses are to facilitate the need for more powerful electrical loads, whilst maintaining attempts to drive weight down as pneumatic systems are replaced with electrical equivalents.

1.2 Market Trends in Electrification

1.2.1 Terrestrial

From a household perspective the supply voltage to the home has always been a low voltage operating at a modest frequency; UK and Europe 230V @ 50Hz (originally 240V, but reduced in the early 1990's), US 115V @ 60Hz for single phase outlets. These voltages are derived at a local sub-station (transformer). The input supply to the sub-station, however, is from a far higher voltage, initially in 1926 distribution was at 132kV @ 50Hz. However, In 1949, the British Electricity Authority decided to upgrade the grid by adding 275kV links. In 1965 the grid voltage was further raised to 400kV, transmitting over 221km over what is now referred to as the super-grid. 500kV is now regularly used in China, however, 800kV distribution is seriously being considered. So the trend appears to be very clear, higher voltage.

1.2.2 Aerospace

As discussed in Section 1.1.2, there has been an upward trend in the magnitude of the electrical systems supply voltage dating back from 1913, when the first electronic compass was employed in aircraft right up to current days on the Boeing 787.

Each time aircraft tries to exploit a technological advantage, it is quite common for it to be in the form of an electrical load. The drive to reduce the reliance on pneumatic and hydraulic systems, has been accommodated by replacing them with the electrical equivalents. It is perceived that applying electrical systems to areas where pneumatic and hydraulic systems once where the main stay will realise an overall system weight

reduction. Weight and volume are the two main key market drivers for aviation to keep running costs as low as possible, this in turn will drive down, or at least limit the rise of ticket costs. Manufacturing cost is also a key driver as this impacts the initial cost of the aircraft, which is also a factor in the ticket price. As some of the technological advancements remove components, these have been further realised as cost saving enhancements. For example, the incorporation of High Voltage DC (HVDC) architectures such as +270V and $\pm 270V$ which have reduced the number of cables required to route the same amount of power around the aircraft, this is a cost, weight and volume saving.

1.3 Limitations for Future Trends in Electrification

1.3.1 Financial

New technologies very rarely get introduced to the market without first going through extensive de-risking or trials in order to validate the design. Substantial investment is made into all new technologies prior to deployment, however, to secure the investment required for research and development the cost benefit to the various industrial sectors needs to be clearly understood, in other words a 'business case' will be required to justify any investment required.

The financial picture often comes in two parts Non-Recurring Expenditure (NRE) and Recurring costs. NRE is further broken down in to two; there is the NRE associated with doing the research and development in order to de-risk the new technology to an appropriate technology maturity. The other part associated with NRE is the cost to man-

ufacture the solution. All of this investment and cost needs to be recovered and is either paid for up front by a customer, or the cost is amortised over the future sales of equipment.

Recurring costs are those of the materials used to implement this new technology, for the terrestrial transmission grid it is the cost to lay out all of the cables and sub-stations around the country. Sub-sea requires a similar infrastructure with laying out of cables and implementing various levels of power conversion. Fundamentally aerospace has similar requirements, however, some of the terms are different for example, aerospace does not have power plants and sub-stations. Aerospace has electrical generators and power conversion, the functionality of these are the same.

With the cost of copper being high, any reduction on the quantity and cross sectional area needed to implement the electrical power infrastructure will certainly help reduce NRE and recurring costs. If the weight is able to be reduced with regards to the domestic electrical transmission grid, the physical capability of the pylons required to hold up the cables reduces again helping reduce cost. As aluminum is over three times lighter than copper, but has only 61% of the conductivity, it is the material of choice for overhead cables for the grid. For aviation, any weight reduction of the cabling, not only eases the manufacture of the aircraft but also reduces the amount of fuel that is required for each flight, this in turn is realised as a cost saving at the ticket price. The domestic grid has for some time used aluminum as part of the cable alloy, due to it being cheaper than copper, only recently has aerospace applied the same technique. However, it is not being applied to the whole aircraft due to the fact that copper is by far the better material to route electricity as it has a lower resistivity.

1.3.2 Technological

As stated previously, any technologies attempting to be employed as part of an electrical distribution system, whether it be terrestrial electrical transmission grid, sub-sea or aviation, will have been scrutinised for its financial merit and form part of an overall business case. Regardless of the specific technology developed, the environment in which the technologies must operate will be described in the following sections. It is the environment in which the technologies must operate (e.g. altitude, temperature, voltage) that this thesis will focus its attention on.

1.3.2.1 Voltage Level

The advantage of transmitting and distributing electricity using high voltage has been widely exploited since the first grid was deployed in 1933, here 132kV was used to distribute electricity over long distances. Typically a sub-station would locally convert the voltage to 240V AC originally at 40Hz, it wasn't until later that the frequency of transmission was raise to 50Hz (as it currently stands in the UK). Again the raising of the electrical transmission grid frequency was born out of the need to contain/reduce the volume and weight of the switchgear, increasing the frequency meant that any magnetic components would also reduce in size, due to the fact that the eddy current heating effects in the magnetic material are inversely proportional to the frequency in which they operate.

Aerospace has followed a similar trend to the domestic electrical transmission grid and subsea, however, its voltage levels appear humble in comparison. starting originally at 14V DC, but steadily progressing to 115V AC then to 270V DC, closely followed by

230V AC then ±270V DC. The main issue for aerospace is and has always been volume and weight, both of which are constantly being challenged to reduce and if supply voltages are constantly rising then the probability of electrical discharge or corona is raised considerably. So if we are attempting to reduce the volume of cabling in an aircraft then the separation between the cables is also reduced, increasing the probability of electrical discharge. Another phenomena that affects aerospace and not sub-sea or the terrestrial grid is that of the effects of altitude on electric breakdown or partial discharge, here the voltage capable of causing disruptive discharge at sea level is greatly increased at altitudes of 18km (65000ft). Fortunately there is an experimental curve validated by Friedrich Paschen [13]. Who verified that there is a minimum breakdown curve that can be observed at any elevation for a given separation between conductors in a gas (e.g. Air). These mutually exclusive requirements to reduce volume and thus separation also for further increases in system voltage further has and continues to plague aerospace and restricts the further rise of system voltage, from a safety standpoint with respect to electric breakdown and partial discharge, the widest possible gap between conductors is desirable, however, from a weight and volume perspective the opposite is required. A fundamental understanding of the physics behind Paschens' experimental curve is therefore required, applied to aerospace as discharges over varying altitudes only occur in this sector.

1.3.2.2 AC versus DC

The AC versus DC debate has been ongoing since the 19th Century. Electric power transmission frequencies have long been debated over the last 100 years. Transmission systems have evolved from Thomas Edison's direct current (DC) systems in 1880's, to Nikola Tesla's and George Westinghouse's variety of transmission system frequencies of 25 Hz to

as high as 133 Hz. Systems running at 25 Hz have lower line losses than higher frequency systems but pay a price of significantly larger transformers and noticeable light flicker [14].

Basically this issue divides into two parts, namely the cabling required for the distribution and the power conversion required for the system. DC systems offer by far the lowest Cost, Volume and Weight cabling solution for the distribution system. However, AC systems offer the simplest power conversion and generation. Power conversion is accomplished by using transformers and generation is performed simply by securing a permanent magnet to the shaft of a rotating machine (rotor) and inducing electrical power into the surrounding coils into some static fixings (stator). In the 19th century technology was not sufficient to support DC power conversion at the powers required for a national grid, however, 130 years on, Power electronics has moved on sufficiently to enable high voltage DC architectures to be re-evaluated for its deployment.

But regardless of whether an AC or DC system is adopted, the increase in the supply voltage is inevitable due to the economic pressures that the world of electrical power distribution are put under. To minimise the losses in the cables in an AC system, preference for the lowest frequency possible would be desired (25Hz), however, this only passes the problem to that of the conversion (e.g. transformer).

For aerospace applications, in order to ensure that the stresses experienced by the generator and engine are minimised, power quality requirements are placed on all electrical loads. Single phase equipment is limited to 500W and anything greater must derive its power from a three phase supply, as laid out in the aviation standard document RTCA-DO160F. Also any power demand greater than 50W will mandate 'Power Factor

Correction'. This requirement makes all loads appear as resistors with respect to the generator. This is turn maximises the power utilisation out of the generator, however, all of the loads now have to carry the burden of carrying extra electronics and thus weight and volume to meet the power factor requirement. Employing DC architectures negates the need for power factor correction, therefore from a load perspective adopting a DC architecture can provide the smallest possible solution [5].

Example: Motor drive actuator.

A motor drive actuator is the system that converts the electrical power into mechanical force for the purpose of moving a flight surface such as a flap, (actuation). As with all equipment on aircraft volume and weight of the solution must be minimised.

If an AC system is adopted, then the motor drive electronics will require three phases (assuming a power requirement greater than 500W), and the associated power electronics will now require an active front end in order to satisfy the power factor correction requirement. As in most motor topologies the output of the active front end will supply a DC link bus, which will then be inverted to create a new three phase AC output to be able to control/drive the motor shaft. The motor shaft will be mechanically linked through some gearing to the flight surface that is to moved or actuated. Whereas if a DC system is adopted, only one or two supply cables are required (depending on whether a +270V or a $\pm$270V is used respectively), so there is already a wiring weight saving. With the motor drive electronics the front end rectifier is no longer required to create a DC link as the supply voltage itself will provide the DC link, thus only the output inverter is required to perform the motor control as described previously. Therefore adopting a DC architecture can prove to be the lightest and smallest solution, the only problem is in creating the DC source in the first place. As described previously generating AC sources is the simplest

approach, in order to create a DC source in aviation, currently AC generators are used, the AC is then passed through a Transformer Rectifier Unit (TRU) to create DC. Aviation standards dictate that a minimum of a 12 pulse TRU will be acceptable for aviation purposes, however, 18-pulse and 24-pulse are in common place now.

1.3.3 Arc Formation During Circuit Interruption

The act of interrupting an electrical circuit by inserting an air gap in series with the flow of current, will cause an arc to form, this may be achieved by opening a contactor, as shown below in figure 1.6

Figure 1.6: Aviation Standard Contactor

The above contactor is applied to the below simple circuit below, in which a power source passes power through a circuit interruption device (in this example a contactor)

to supply power to a resistor. Parasitic inductances have been included in the circuit to reflect reality.

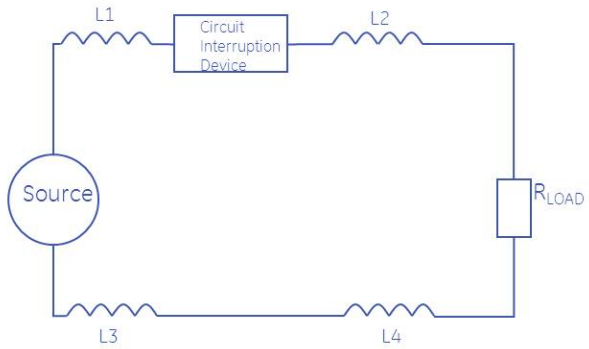

Figure 1.7: Simple Electrical Circuit, including parasitic inductances

If we now assume that the source voltage is 12V and is passing approximately 200A, then if the voltage across the contacts of the contactor were monitored along with the current passing through the load (before, during and after the opening of the contacts), then the following V-I curves would result.

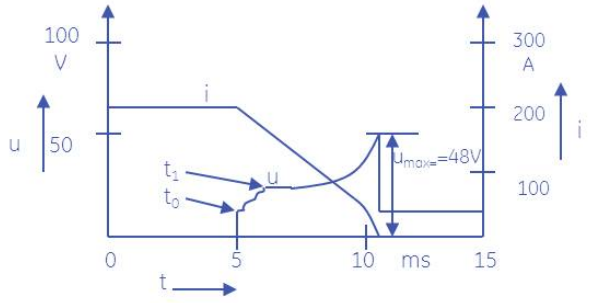

Figure 1.8: V-I curves resulting from Circuit Breaker interruption

From the above figure a typical voltage/current versus time is given. Time t_0 shows the point in time that the contacts begin to separate, whereby all of the current passes

through a much reduced surface area of the contact from when it was originally under pressure. This very high current density causes an abrupt rise in temperature resulting in the metal over heating and a metallic explosion between the contacts, where an arc will form. A voltage will establish across the arc, however, due to the metalised gas between the contacts the arc voltage will be lower than normal arc voltage, only when the metal within the gas has migrated under the influence of the electric field to one of the contacts will the arc voltage rise to typical values of approximately 20V. The time at which all of the metal has migrated from the space between the contacts is given by time t_1. This will be explained further later in this section.

Similar results also been observed in other papers, such as [15] which observe V-I circuit interruption curves as shown below [16] .

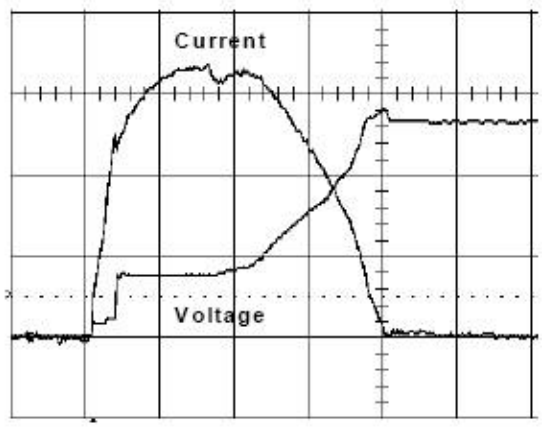

Figure 1.9: Measured V-I curves for a 125A Circuit Breaker operating in 54VDC. The above test circuit was configured with a 5.2kA prospective current and 0.25ms prospective time constant; 1kA/div current, 20V/div voltage and 0.5ms/div.

Both figures 1.8 & 1.9 demonstrate the same circuit interrupting phenomenon in which current will continue to flow across the contacts of the circuit breaker even though its con-

tacts are no longer touching one another. There is a finite voltage across these contacts which is different to that of the system voltage proving evidence to support the presence of an arc. The duration of the arc is dependant on the stored energy within the system, the rate at which the contacts open, the arc voltage across the contacts, the system voltage and the source resistance. Referring to figure 1.7 the energy stored in the system will be that stored in the parasitic inductances shown as L1 through L4, where the total energy will be equal to; $E = \frac{1}{2}L_{total}I^2$ where $L_{total} = L_1 + L_2 + L_3 + L_4$.

The arc may be thought of as converting the stored energy in the circuit to heat in the arc itself, The load voltage will reduce when the arc is present which is approximately 20V initially, (figure 1.8) and as the circuit energy is being '*burnt up*' the arc voltage appears to exhibit a negative impedance and the arc voltage begins to rise. However, this negative impedance effect only exists when a majority of the system energy has been used up. The arc voltage now continues to rise until the arc voltage becomes greater than the system voltage and the circuit is finally interrupted.

In an AC system the arc is quenched many times during the zero crossing of the circuit current. However, it must be noted that even though the arc has been quenched at a zero crossing, if the $\frac{1}{2}L_{total}I^2$ has not been completely dissipated an arc will re-establish on the next half cycle and the arc quenching process will begin all over again. In a DC system, however, this auto-quenching phenomenon does not exist and the arc will remain until all the energy has been dissipated. To explain the arc quenching and re-establishing mechanism, the system capacitance must be recognised. The total system capacitance, which is distributed, also stores energy and the $\frac{1}{2}C_{total}V^2$ must be taken into account. The inductive energy is far, far greater than that of the capacitive which is why it can

often be ignored, but is required here to explain the arc quenching and re-establishing mechanism in an AC system.

As the current approaches zero the inductive energy begins to be transfered to the system capacitance. But as the inductive energy is much greater than that of the capacitive, the voltage begins to rise. When the current reaches zero the arc will be quenched, however, the voltage across the contacts will continue to rise, until a voltage is achieved that will cause breakdown to occur. At this point the arc is re-established and the capacitive energy is transfered back to the system inductance and the whole cycle begins again. This process will continue until the system energy is dissipated, both capacitive and inductive, but it is the inductive energy that is the most dominant.

This is one of the main reasons why AC is still favored over DC. The temperatures that the contacts of the contactor experience are very high indeed, to the point that small pieces of the contacts melt every time the contactor is operated. This molten metal will experience forces due to the E-field across the contacts and small pieces of metal will be forced over to the other contact. In an AC system, on average, as much flows away from one contact as it receives, but this is not true for a DC system, metal will always migrate from one contact to the other, impacting the reliability of DC contactors considerably compared to their AC counterparts. It is for this reason that relays and contactors are able to handle much higher power levels in AC systems as opposed to DC.

Referring back to figure 1.8 there is further phenomenon occurring between times t_o&t_1. As the contactor attempts to interrupt the circuit, contact pressure is reduced between the contact faces. the contact faces are never perfect and only a portion of the

total surface area ever conducts the current. But as the contact pressure is reduced the surface area over which current will conduct will reduce meaning the current density over the contact face will rise, this will continue until all of the current supplying the circuit is passing across an infinitesimally small area of the contact, the current density will be that high that the contact material will melt. During this high temperature event the arc will be initiated. So each time the contactor or relay is being used to interrupt a circuit small deformations are occurring at the face of the contact material. In AC systems the deformation occurs on both faces equally, however, in a DC system the deformation occur predominately on just one face [17].

The arc is only a phenomenon if the circuit interruption method is by that of an air gap, or other form of gas. If an alternative interruption method was employed the arc may not develop. If solid-state switching was adopted in the form of a MOSFET, then an arc will be negated. The $\frac{1}{2}L_{total}I^2$ circuit energy will still need to be dissipated, however, this will now be accommodated in the form of re-combination energy within the MOSFET itself, providing it can withstand it.

1.3.4 Electric Breakdown

This will refer to uncontrolled current flow as a result of excessive electric field strength in the area that the current flow is occurring. The electric field strength will be such that electrons will accelerate under it's influence and collide with other molecules/atoms with enough force to in turn dislodge electrons from the impacted molecule/atom (Townsend primary ionisation). In addition to the dislodged electron from the impacted molecule/atom

which will act under the influence of the applied electric field. A positive ion will result from the collision, which will also act under the electric fields influence, however, the positive ion will accelerate in the opposite direction to that of the electron as it has the opposite charge. The positive ion will accelerate towards the negative charge of the electric field and should it collide with anything along its path, such as a metallic plate, the ion, being much heavier than that of the electron will cause an impact that will dislodge further electrons from this weakly bound structure (Townsend secondary ionisation). Townsend secondary ionisation will permit subsequent primary ionisation to take place. With both Townsend's primary and secondary ionisation mechanism's taking place an avalanche effect will result. It is this avalanche effect that is responsible for the uncontrolled current flow that is akin to thyristor action, where it is the system impedance that will be the only limiting factor for current flow. In addition, the only mechanism to halt the current flow is to reduce it to zero.

Electric breakdown should be avoided under all conditions and appropriate spacings and insulation material should be used to prevent such an effect. Everything can ultimately breakdown under electric forces. It is just a matter of how much electric force (i.e. Voltage) is required for a given material.

This thesis will take no account of the breakdown phenomenon of solid dielectrics and will concentrate on effects on gaseous dielectrics such as air. The reason for this is because the breakdown of solid insulation appears to be invariant to altitude, whereas when using a gaseous dielectric variation due to altitude will be observed. Solid dielectric material exhibits a much higher electric breakdown potential compared to air, therefore air is being considered as the worst case [18].

Although the domestic grid is tied to the earth, there is height variability especially when routing the grid up a mountain. Admittedly these altitudes are not as high as those experienced in aviation but care must be taken to not ignore this effect. The domestic grid is reliant on air gap dielectric spacing when distributing power over the various countries and this must be considered when designing a pylon, for example. The domestic grid does not use insulation on its transmission cables due primarily to cost, therefore good design practices and applying appropriate de-rating to the dielectric air gap spacing is what is relied upon.

1.3.4.1 Partial Discharge and Corona

Guidelines and definitions are given in [19]. However, I would like to add some further clarification of the definitions here, it is these definitions that will be used throughout this thesis. It must be noted here that thesis definition for partial discharge is not consistent with the industry definition, however, I believe the term correctly describes the phenomena detailed in this thesis and should be added to the industrial definition.

Corona - When a gas is exposed to an electric field of sufficient magnitude, any free electrons will accelerate under its influence. These accelerating electrons may collide with the gas molecules and dislodge weakly bound electrons (Townsend primary ionisation), producing an electron and positive gas ion pair. This is quite often visible, this phenomenon is called **corona**. Corona is often observed near to sharp edges or points that have a voltage attributed to them, as treated in Gauss' Law, for a given voltage the electric field is inversely proportional to the area at any given point where the E-field

exists, implying that the E-field can be highly non-uniform over a given path, due to the geometries of the conductors over which the E-field traverses. This means that corona is often localised to the sharp edge and doesn't normally propagate over the entire E-field length.

Partial Discharge - partial discharge (PD) is a localised dielectric breakdown of a small portion of a solid or fluid electrical insulation system under high voltage stress, which does not bridge the space between two conductors. Partial discharge usually occurs in voids located within the material and is usually non-sustaining.

It is the non-sustaining characteristic of partial discharge that this thesis treats as key and not the fact that partial discharge occurs in localised areas/voids between conductors. With this in mind, this thesis offers an addition to the definition that also includes bridging mechanisms between conductors.

Alternate definition. Partial discharge (PD) is a transitory discharge mechanism that can occur in voids in dielectric material or between the conductors across the dielectric material which provide electric field stress between these two conductors.

As it will be described in much greater detail in Chapters 4 and 5, mechanisms are proposed that will cause the void to grow and extend the whole length between the conductors, causing a transitional (partial) discharge.

With such an electric field described above, electrons would also be expected to be dislodged from the metal conductor itself as this will require much less energy than that

required to ionize the gas. If, however, the electric field is lowered even further so that the gas does not become ionized, but sufficient electrons are still able to be liberated from the metallic conductor, then a plasma may form and if the plasma was able to bridge the gap of the E-field, then **partial discharge** would be observed. Partial discharge requires an E-field for the plasma to propagate, so once the plasma has bridged the gap the E-field collapses, resulting in the plasma dispersing and the whole partial discharge process would need to repeat again. Partial discharge is non-visible, but can still cause damage to equipment. [20]

1.3.4.2 Effects of Altitude on Partial Discharge

As the formation of a plasma responsible for partial discharge is closely related to the gas in which the plasma propagates, it necessarily follows that the air pressure, or the pressure of the gas is related to the plasma propagation and thus partial discharge. As plasma formation comprises of accelerating electrons in an electric field, then the less collisions that the electrons have to make with the air molecules coupled with the fact that the accelerated electrons will achieve much higher velocities as they have been able to travel further distances means that a lower electric field will be required to observe partial discharge.

Therefore as altitude is increased and air pressure reduces, meaning that the 'mean free path' λ between adjacent air molecules increases it follows that the electric field required for partial discharge to occur reduces and if the E-field is uniform as it would be if two parallel plates where used to create the electric field, then this translates directly to the voltage required to cause partial discharge. i.e. the voltage required to cause partial discharge at altitude will be lower than that required at sea level.

1.3.4.3 Paschen Curve

Louis Karl Heinrich Friedrich Paschen (January 22, 1865 - February 25, 1947), was a German physicist, known for his work on electrical discharges. During his work into electrical discharges he experimentally verified that the Voltage (V) required for partial discharge to be observed was directly related to the product of both the air pressure (**p**) and the distance of the air gap (**d**), forming the product (**pd**).The experimental curve that Paschen was able to verify is given below [18].

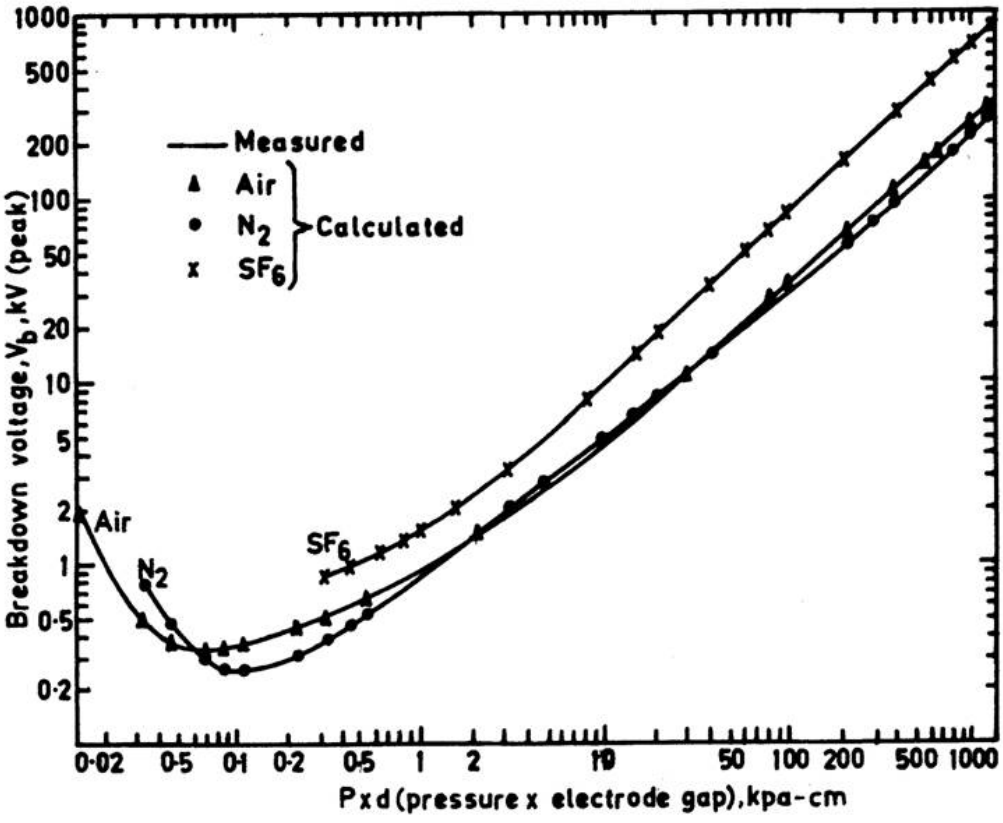

Figure 1.10: Measured Paschen curves for air, N2 and SF6

It can be seen from the above graph that it is non-monotonic and at very low 'pd' products the voltage required for electrical discharge rises. In order to interpret this curve, if we assume that a test set up is at sea level, then we are highlighting the far right hand side of the curve and a rather high voltage will be required for electric discharge to be observed. If now the altitude is increased, which is achieved by lowering the pressure, we then begin to move leftwards across the curve, this in turn reduces the amount of voltage required for electric discharges to be observed. If we now continue rising in altitude (thereby reducing the air pressure), there comes a point when we are at the minimum of the curve (known as the Paschen minimum) and any further reduction in air pressure (further increase in altitude) requires a rise in voltage for electric discharge to be observed. The accepted reason for this is that these extremely low pressures we are creating a vacuum where there are no air molecules capable of transporting the plasma or being ionised. Any observed discharges beyond this point are probably due to other phenomenon such as vacuum discharge or even quantum tunneling.

1.4 Future Benefit of High Voltage Architectures

As the demand for electricity continues to rise, not just in its existing locations around the globe, but rather new and developing areas, the need for globalised electrification means that more and more power is required to more and more destinations. The cost of implementing such an infrastructure will in most cases prove prohibitively expensive. The cost of the raw material (e.g. cables) and the labour to install them will always prove barriers to entry. As power demand goes up the losses in the cables also rises, this creates extra heat, due to I^2R losses and the volt drop over long lengths of cable may

prove problematic in some circumstances.

All of the above issues are directly impacted by implementing a high voltage architecture, cable weight and thus costs are reduced so too are the cable losses. If a DC architecture is employed then the cable weight and quantity will be further reduced, which will have an impact on the implementation costs of building such an infrastructure.

For aerospace the same is true, as more and more loads are required for future aircraft architectures due to the fact that much effort is being put on realising the 'All Electric Aircraft' (AEA), which as an end goal has all systems being electrical with the removal of Hydraulic and Pneumatic systems.

As electrical discharge requirements for aerospace applications have to deal with two separate but apparently related variables, namely air pressure (**p**) and gap distance (**d**), this is considered worst case from a theoretical standpoint and is therefore considered the main topic for the remainder of this thesis.

1.5 Motivation

The current accepted design guidelines for clearance separation between electrical conductors to ensure that electric breakdown will not occur when operated at altitude have worked well for many years. with the increasing demand for more and more electrical power in aviation, system voltages have persistently risen over the years. The constant demand for aviation equipment to be as small and light as possible is now being im-

pacted by adherence to these guidelines. Although a majority of aircraft operate below the Paschen minimum, natural threats such as lightning are above this minimum. As lightning is a natural phenomenon for aircraft, equipment must be designed to meet these levels and the guidelines must be applied. Current aircraft naturally operate above the Paschen minimum and the lightning threats are much higher due to the introduction of composite materials, therefore the design guidelines are being applied throughout the design life-cycle of the equipment and not just as transient disturbance considerations during operation.

The original data from which the guidelines (IPC-2221A EN-60664) were compiled from is unable to be obtained and only the guidelines themselves remain. These guidelines attempt to account for partial discharge in air as well as other methods of breakdown which are not detailed, however, it is impossible to separate out these failure mechanisms. This has directly led to many products being over sized or over engineered, as no credit can be taken for advancements in coating technologies and/or advancements in PCB technologies providing di-electric withstand strength superior to those at the time the guidelines where written.

Should engineering design practices be applied that result in electric discharges in air being the only mechanism by which breakdown can occur, then an experimental curve exists, known as the Paschen curve [18]. This experimental curve relates the minimum voltage by which electric discharges can occur to that of the pressure, distance product as shown in figure 1.10. The problem now is that if the accepted guidelines are overlaid on this curve (As will be shown in Section 7), the guidelines request much larger air gaps than those required of the Paschen minimum.

After much investigation, many attempts have been made to analyse this electrical discharge phenomenon, most of which adopt a similar approach. None, however, result directly with the Paschen curve and curve fitting constants are applied to the equations to make them fit. If it could be proved that there is indeed a minimum electric breakdown curve in a gas and that the *pd* product is the only variable that correlates to the minimum breakdown voltage, then divergence away from the guidelines may be accepted where appropriate, allowing lighter and smaller equipment to be achieved.

Therefore the current accepted theory of electric breakdown does not provide us with a fundamental understanding of breakdown phenomenon and this is the main drive behind the research detailed in this thesis. Aerospace specifically is only being considered as it is understood that this is the worst case environment.

1.6 Thesis Outline

In the next chapter the electrical systems for aerospace are first detailed, to provide an understanding of the environment in which electrical equipment must be able to operate. The chapter following that explains the current accepted theory of electric breakdown.

The following three chapters are the main body of research. Firstly, plasma formation and it effects on polarisation in a gaseous dielectric will be explained, it is intended for this to provide an understand of the fundamental mechanisms behind electric breakdown, which will be given in the following chapter. Here the specific conditions will be detailed

that will result in electric breakdown and the 'proposed theory of partial discharge' will be given. The final of these three chapters will explain a consequence of partial discharge taking place and will explain how a 'transition from partial discharge to arc' may result.

Experimental test results will then be provided. Here the results of much testing will be overlaid with the proposed theoretical curve. Partial discharge is probabilistic in nature as a discharge at a given voltage is not deterministic, so the curve should be interpreted as the minimum at which the probability of partial discharge becomes non-zero. Finally the 'conclusions' of the thesis 'and further work' will be detailed.

Chapter 2

High Voltage Architectures and the More Electric Aircraft

2.1 The More Electric Aircraft

The transmission and distribution of power is most easily implemented if done using electrical cables over hydraulic or pneumatic pipework. Passing wires around complicated structures and through bulk heads is much easier and simpler than the routing of pipework. Pipe-work has the added complication of the need for it to remain leak free and maintain pressure inside the pipes whether they be for pneumatic systems or hydraulic systems. No pneumatic or hydraulic system can be truly leak free, therefore, a maintenance infrastructure needs to be put into place in airports across the globe so as to check and top up the pressures of these two systems.

Electrical wiring does not suffer from the maintenance issues associated with those of pneumatic and hydraulic systems. Electrical systems do not need to be maintained to have it's pressure or voltage topped up, the only issue for electrical wiring is to maintain good electrical connectivity. Electrical wiring offers another benefit over pipe-work in that if properly installed, electrical wiring can survive harsher environments such as vibration,

temperature cycling, altitude variation.

Vibration - Wiring can be installed in just one piece and discontinuities are only required at termination points, whereas pipe-work usually comprises of sections that are bonded together (e.g. welded joints) in order to create a longer pipe length, in addition to the termination points. Wiring is much more flexible than pipe-work and much more flexible over long lengths.

Temperature cycling- Outside of the cabin area of civil airliners, where the temperature is kept at a comfortable level for onboard passengers and crew, temperature is left uncontrolled and is open to the outside temperatures and variations caused by any of the onboard equipment, this could be from additional heat being generated by onboard fuel pumps that need to continually operate under normal conditions. If the aircraft could be deployed to Alaska and left over night on the runway, it could be expected to start at -55^{o}C. If however, under the same scenario but with this time the destination of the dessert, start up temperatures of +75^{o}C would equally be expected. Systems providers to the aerospace industry will not be given destination or route information regarding any aircraft, so inevitably, both extremes have to be catered for. But -55^{o}C $<$ T$_{ambiant}$ $<$ +75^{o}C is only the start up requirement, consideration needs to be given to the self heating that the on board equipment will provide. It is conceivable that at further +30^{o}C rise maybe experienced inside the onboard equipment also the the cabling could experience similar temperature rises. Some equipment may not be able to contain the temperature rise to just +30^{o}C and higher temperature rises would need to be catered for. +50^{o}C may be the limit, as this would give rise to a component temperature of +125^{o}C, which is the highest temperature rating for a commercially available electronic component. Elec-

tronic component temperature ratings of -55^{o}C < $T_{component}$ < +125^{o}C are often referred to as aerospace or space temperature ranges. For much of the onboard equipment the -55^{o}C requirement has often been contested and for many of the on board equipment this requirement is relaxed and -40^{o}C is imposed. If the temperature rise within any of the electronic equipment can be contained to just a 30^{o}C rise then the temperature variation is reduced to -40^{o}C < $T_{component}$ < +105^{o}C, this temperature range is commonly referred to as automotive, which has a higher temperature range that standard Commercial Off the Shelf (COTs) components which is -40^{o}C < $T_{component}$ < +85^{o}C. Some equipment, however, are not able to have any of the temperature requirements relaxed, such as those associated with the engine (e.g.The Full Authority Digital Engine Control - FADEC), which is the electronic control equipment for the engine and have to operate over the full -55^{o}C < $T_{ambiant}$ < +75^{o}C, which in turn often requires components to operate over -55^{o}C < $T_{component}$ < +125^{o}C. The distribution of power in the aircraft is also unable to have any temperature variation requirements relaxed and is also expected to operate over these wide temperature ranges, which is why electrical cables are preferred over pipe-work, however, both methods of power distribution suffer from ageing due to the temperature cycling that they experience, especially as civil aircraft are expected to operate for up to 20 years or more.

Altitude - Obviously aircraft have to fly so altitude needs to be considered for its effects on equipment and power distribution, whether that be electrical, pneumatic or hydraulic. As altitude rises the air pressure reduces, as shown below;

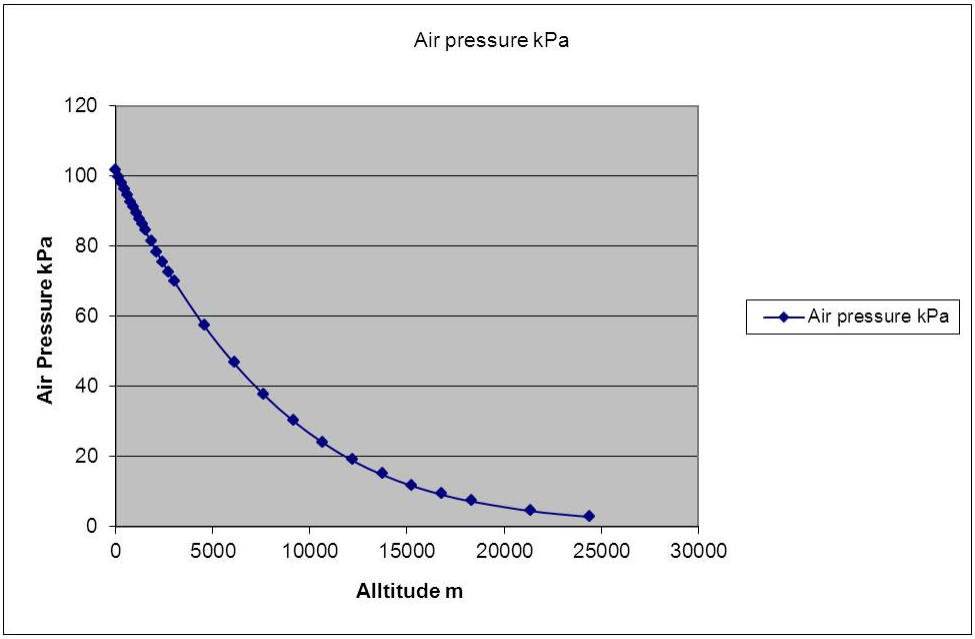

Figure 2.1: Graph of pressure variation with Altitude

Figure 2.1 was derived from a table in [21]

As air pressure reduces with increasing altitude and a couple of effects are experienced by the various equipment. For pneumatic and hydraulic equipment the reduction in air pressure can increase the probability of leaks to occur, this in turn can cause pressure to be lost in either the hydraulic or pneumatic systems and impede flight functionality. Clearly these systems will have been designed to cater for the altitude effects, however, what is being described here are the stresses that these systems must endure naturally.

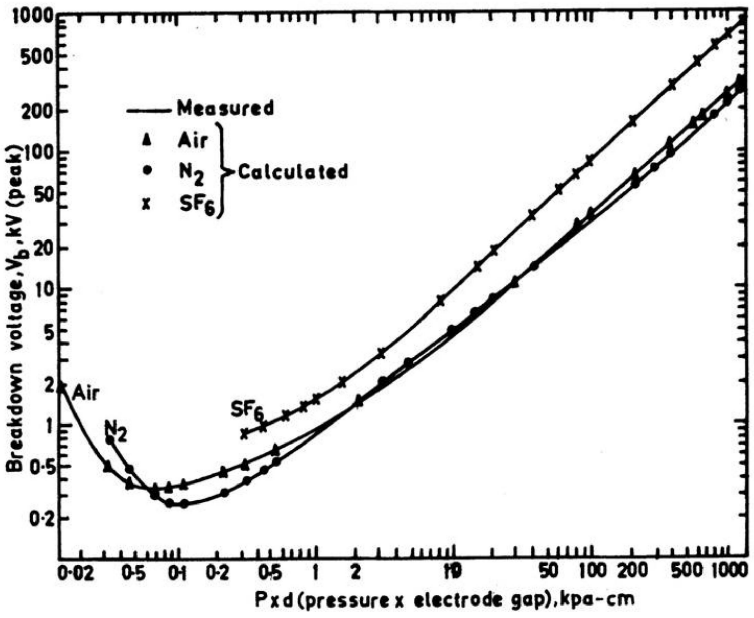

Figure 2.2: Measured Paschen curves for air, N2 and SF6

The effect of air pressure reduction on the electrical system is to increase the probability of electrical discharges occurring in the electrical system, as shown above in figure 2.2. Again, the electrical system will have been designed to cater for these effects due to

altitude variation. However, this does mean that an electrical system has to be physically designed for a given aircrafts intended fight envelope. Typically Civil aircraft fly at around 10000m (30000ft), however, the design standards of RTCA-DO-160F will require designs to be qualified to altitudes of 15000m (50000ft). However, military platforms will often have 20000m (65000ft) as a design requirement (e.g. MIL-STD-810). But, as one would expect in the world of aviation, with the correct dielectric spacing mandated throughout the electrical system design, the system effects due to altitude variation are accommodated [5] [22].

2.1.1 The Bleed-less Engine

As described previously, a huge maintenance infrastructure is required to maintain all of the aircraft and keep them running throughout their operable life. There is also still high demand for new aircraft, so the pressures to reduce it's cost of production and reduce the time it takes to build the aircraft in the first place are also quite onerous on the aircraft manufactures.

The first system to be challenged to help meet these market forces is the pneumatic system. If the pneumatic system can be dispensed with then all the pipe-work can be removed, the mechanical fixings required to allow the pipe-work to operate and survive the harsh aviation environment can also be removed. The pipe-work will then be replaced with electrical cable, which is lighter and cheaper than the pneumatic pipe-work and also much easier to install on the aircraft, aiding construction time demands. In short migrating the pneumatic system to that of an equivalent electrical system will provide ease of

manufacture and expected efficiency benefits are also expected. The first aircraft to move to a bleed-less architecture is the Boeing 787, shown below.

Figure 2.3: Boeing 787

2.1.2 Impact of a Bleed-less Engine on Aircraft Architectures

With the removal of the pneumatic system, migration to an electrical equivalent is required. The three main systems that the pneumatic system provide function for are;

- Cabin pressurisation

- Air Conditioning
- Ice-Protection

High pressure compressed air in the engine is ignited with kerosene fuel to provide thrust. This high pressure air was '*bled*' off the engine, which is why we refer to traditional engines as bleed engines and the engine for the Boeing 787 as no-bleed. The bleed air was then routed to the cabin environment and effectively pressurised the cabin in order for passengers and crew to experience the pressures associated with a much lower altitude, in fact the pressure that are experienced by passengers are that of about 2000m (7000ft), this pressurised air was also warm enough to provide adequate heating, conditioning the air suitable for passenger comfort.

Another important function that was required by the pneumatic system, was that of ice-protection. As aircraft take-off and land, they must pass through moist atmosphere at low altitude <1200m (<4000ft), this moist atmosphere can also experience low temperatures. These two factors can allow ice to form on the leading edge of the wing and the nacelle as the aircraft fly through this region. This ice formation can have dramatic effects on the aerodynamics and the overall controllability of the aircraft. In fact there have been fatal and near fatal air incidents attributed to icing incidents during take off and landing.

Below is excerpt from a report from CNN regarding a plane that was due to fly from Newark Airport to Buffalo Niagara International Airport February 13, 2009

BUFFALO NIAGARA INTERNATIONAL AIRPORT

Search for answers begins in Buffalo plane crash

February 13, 2009

Share Mixx Twitter Email

The pilots of a commuter airliner that crashed late Thursday about 6 miles from a Buffalo, New York, airport discussed "significant ice buildup" on the plane's wings and windshields before the plane plunged to the ground, killing 50.

Continental Connection Flight 3407 was en route from Newark, New Jersey, to Buffalo Niagara International Airport when it went down about 10:20 p.m. ET Thursday.

Firefighters from nine volunteer fire departments battled the flames at the crash site.

Preliminary information recovered from the flight's cockpit voice and data recorders indicated that the plane underwent "severe" pitching and rolling motions after the landing gear was lowered and wing flaps were set for the approach, Steve Chealander of the National Transportation Safety Board said Friday afternoon.

Figure 2.4: CNN report 13th February 2009

The way in which the ice protection is performed on a bleed air system is to route the high pressure warm air off the engine and route it down through tubes that are in close proximity to the leading edge of the wings and also the nacelles. These tube have small vent holes to let the warm air escape and provide heat to the leading edge of the wings and nacelle. These tubes with the holes in them are commonly referred to as '***piccolo tubes***' as this is what they resemble. This warm air is applied during take off and landing to prevent ice from forming in the first place, this is referred to as ***anti-ice*** functionality.

2.1.3 Impact on the Aircrafts Electrical System

In order to replace the aviation functions as described in the previous section with their electrical equivalents, new equipment is required to be designed for the aircraft that had not previously been seen. In order to provide the cabin pressure and temperature control,

a combined Environmental Control System (ECS) was employed. As this is a critical system, two ECS systems are incorporated into the aircraft, each requiring approximately 220kW each! The ECS system is essentially an air-conditioning unit that operates at much higher pressure differentials than domestic appliances.

The electric de-ice heater mats were inserted in to the leading edge of the wing and nacelle. These heater mats are essentially film resistors, arranged possibly as shown below.

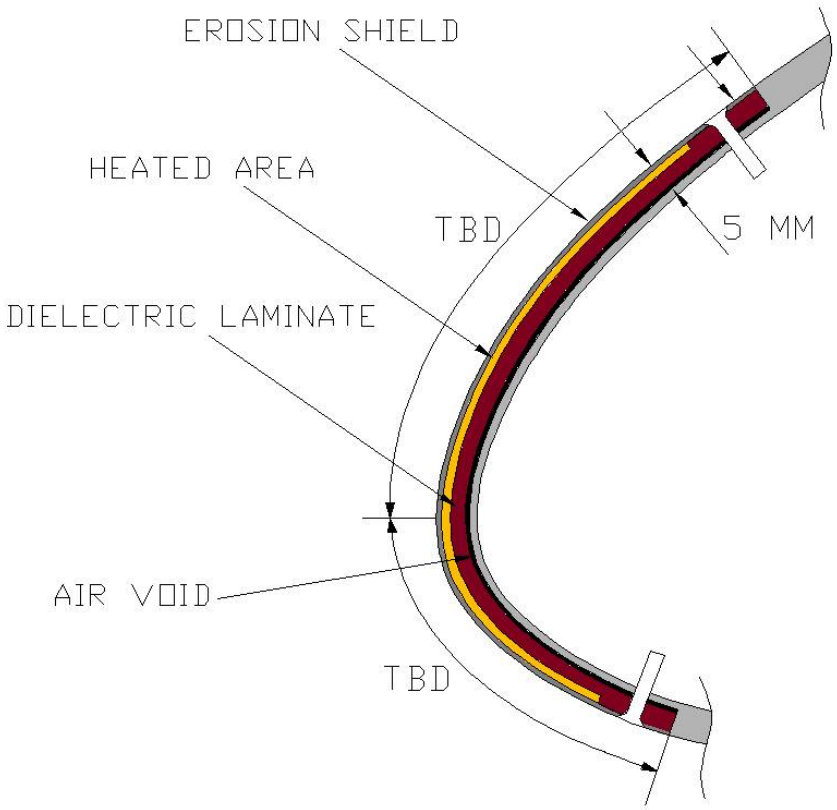

Figure 2.5: Possible physical arrangement of electric wing leading edge [3]

The heated area is further divided into about six zones, in order to help reduce the power required for de-ice. The power is reduced by only heating one of the heating zones

at a time, in a type of pulse width modulated (PWM) fashion. The power demanded by just one of the heater mats is of the order of 4kW and if there are five of these per half slat and three full slats per wing, this adds up to a total electrical power requirement of 240kW if all heater mats where commanded on at the same time. Therefore applying a time division multiplexed approach to the de-ice system will greatly constrain the amount of power required under de-ice conditions.

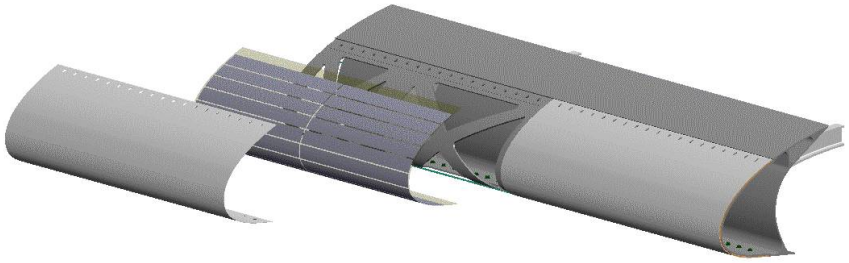

Figure 2.6: view of heater mat zoning in the leading edge [3]

The Boeing 787 Dreamliner's electrical system now requires approximately 1.4MW to perform the original functions and the additional functions that are no longer powered from pneumatic sources.

2.1.3.1 Electrical Power Distribution

With the electrical system now demanding 1.4MW as opposed to the 220kW originally required for previous aircraft (e.g. Boeing 777), alterations to the the electrical system must be incorporated so as to minimise the weight and volume of the wiring. The vol-

ume of the wiring comes in two forms, first the quantity of wires required to supply the electrical loads and also the thickness of the wire itself.

To help reduce the thickness of the wiring and applying previous solutions to the same problem, raising the electrical supply voltage will go a long way to help this. In fact the Boeing 787 now generates electrical power at 230V AC, the new Airbus A350 XWB (eXtra Wide Body) also uses 230V AC generators to supply power for that aircraft, which also has adopted a no-bleed architecture for its electrical system.

In order to help minimise the size of the ECS system and to reduce the quantity and size of the cables feeding power to it, employing a DC architecture was adopted. In order to supply potentially 440kW of power to just two units and to reduce the levels of power conversion required in the ECS, $\pm$270V can be used, this will provide the best cable area utilisation as a DC system does not suffer from skin effects, the cable itself will be at its smallest cross sectional area, as the ECS system will be provided power continuously by the highest voltage available, (as opposed to the peak voltages in the 230VAC system). The ECS system will not require a front end rectifier to create the necessary DC link bus, prior to the voltage being inverted again for subsequent motor drive electronics to supply the various pumps required for ECS operation. In fact this is exactly the approach Boeing have taken on the 787 [12].

2.2 Trends in Aviation Systems Supply Voltage

It is evident that the aerospace industry has been able to exploit the advantages that higher system voltages offer, ranging from a humble 14V supply used to power navigational aids, right up to current times when 230VAC and ±270VDC is used to distribute 1.4MW of power. aircraft are now operating like 'flying villages'. and the displacement of the pneumatic system may just be the first of many movements to a future More Electric Aircraft (MEA) concept, see below for an MEA concept.

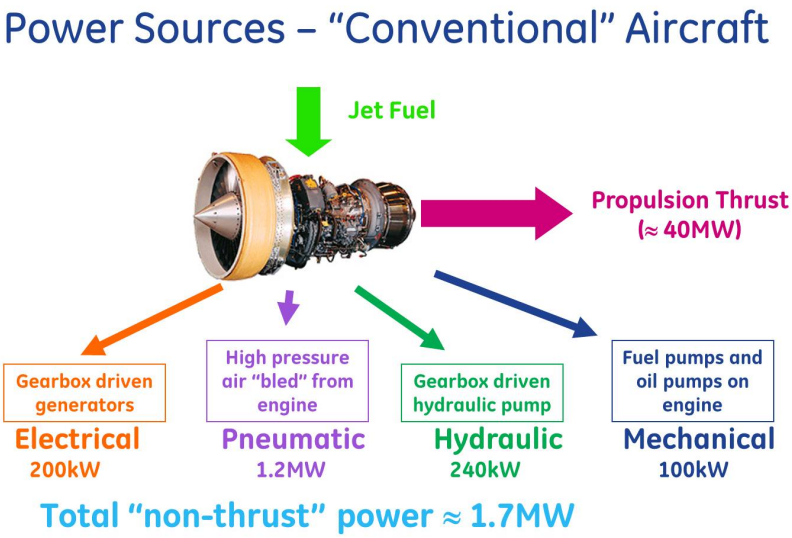

Figure 2.7: Conventional Electrical Power System

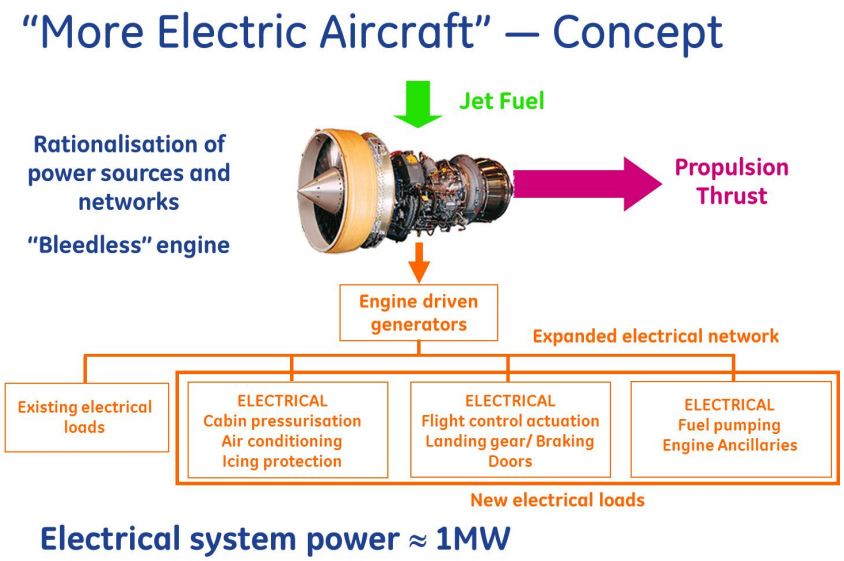

Figure 2.8: A More Electric Aircraft Concept

Courtesy of The University of Nottingham.

The above figure shows the next potential step of migrating what is currently done by the hydraulic systems to their electrical equivalent, however, this is only a concept. Although it appears clear that distributing power electrically makes good economic and engineering sense, power conversion on the other hand certainly comes with its own set of challenges as pneumatic and hydraulic power conversion offer unrivaled power density and power level. Hydraulic more so than pneumatic. It is expected that there will be a few more leaps in technology before the All Electric Aircraft (AEA) will be able to be realised, however, judging by previous trends a high(er) voltage architecture will be necessary for its inception.

2.2.1 Derating Requirements for Aerospace

When a new aircraft is being conceived, equipment that is ultimately to be put on the aircraft is not considered. In fact, the aircraft is discussed and debated in terms of functions that must operate and to what Design Assurance Level (DAL). For example the functions 'essential' for flight are;

- Thrust
- Steering
- Landing Gear
- Electrical System

The above aviation functions would then be given an appropriate DAL level, as the above are essential for flight they would be attributed DAL A categorisation. This classification is then attributed a probability of failure figure for that function. A probability of failure for a DAL A function could be 1×10^{-9}. There are other functions that are required for safe commercial flight or passenger comfort, however, these will not be considered as part of this thesis.

Systems will now be considered for the aircraft for the above functions of thrust, steering, landing gear and the electrical system. Each system will comprise invariably of smaller sub-systems interconnected to form the main system. In order to achieve the main function probability of failure, each system considered will have to have a certain amount of redundancy, sometimes this will mean duplicating the whole system and in others the whole system is triplicated. Which means that multiple failures would need to

occur to result in the loss of a given function.

In order to meet the overall function probability of failure, each individual piece of equipment that makes up that system will be assigned a probability of failure figure which it must be designed to meet, for the system as a whole to achieve certification by the aviation authorities. These probability of failure figures are derived by applying a fault tree analysis to the system.

Following the hazard analysis as described above, the specific interconnections and design performance required by each of the sub-systems is compiled, so too is the environmental considerations for each box as its position on the aircraft is better understood. Once the functional requirements are complete, the environmental considerations are applied in terms of altitude, temperature range, Electro Magnetic Compatibility (EMC), then the probabilities of failure are assigned, then, an individual piece of equipment can begin to be designed.

Each piece of equipment will be further sub-divided into sub-sub-systems and real hardware will be engineered to realise the design. This design will now be analysed by what is know as a Failure Mode Effect and Criticality Analysis (FMECA). A FMECA is essentially a fault tree analysis as described previously, coupled with a probability of failure for every single component that the equipment comprises of. These probability of failure figures that are provided for every component are laid out in MIL-HDBK-217 [23].

The figures laid out in MIL-HDBK-217 assumes that appropriate de-rating has been applied to all components, to make sure that they are not being stressed under normal

operation. For example, the voltage rating of a MOSFET would be expected to be derated by 50%. This means that to use a MOSFET in a 100V environment the minimum of a 200V MOSFET must be used.

When applying derating to clearance distances or dielectric withstand gaps, particularly in air, things are a little less clear, however, still very conservative. For example, if an aircraft is to normally operate at 10000m (30000ft), a requirement of 20000m (60000ft) may be applied. If we also consider its maximum operating voltage of 300V, for example, then if derating is applied, the gaps incorporated in the design to tolerate 600V (50% derating) will be required. The question is, has derating been applied twice? Is qualifying the design to 20000m (65000ft) already applying derating? If a 1mm air gap is applied throughout the design (1mm for the purposes of illustration) then the area of operation can be seen below in figure 2.9.

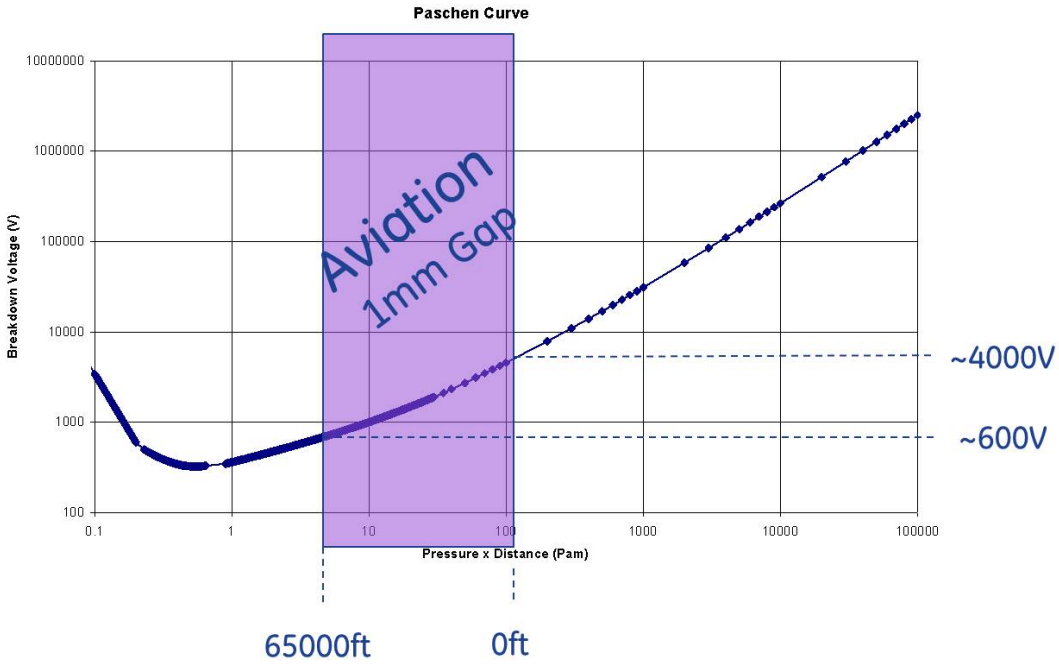

Figure 2.9: The safe operating area for a 1mm air gap from sea level to 65000ft

From the above figure for a 1mm air gap to be able to operate at 600V at 20000m (65000ft) then at see level (0m) the design is capable of withstanding approximately 4kV!.

To ensure the cost competitiveness of commercial aviation many variables are being challenged, 'flight altitude' in certain flight paths offers advantages if it is raised higher than current altitudes. Weight is always being challenged to reduce, which in turn raises system voltage levels. Currently ±270V, but analysing historical trends, this may be raised further in the future, possibly even to ±600V. Applying subsequent de-rating to both altitude and operating voltage for a given volume, then a natural limit for both operating voltage and altitude will be reached. If the current method of designing for high voltage is based on graphical interpretation by applying standards in the form of

tables, then there appears no alternative than to be overly conservative. A fundamental understanding of the mechanisms behind electrical discharge is required to challenge or modify the current methods of design and design practice for aerospace applications.

2.2.2 Electro-Magnetic Interference (EMI)

In aviation, as one would expect, equipment are designed to have no noticeable impact to its functionality when exposed to natural phenomenon such as Electro-Magnetic Interference (EMI). EMI may be derived from many sources, some of which are man-made such as radio frequency communications, others are natural albeit undesirable such as lightning.

Radio Frequency communication is the main stay of everyday life. Satellite communication is used for navigational aids such as Sat-Nav, television and other entertainment is also routed via satellites, mobile phone's are also dependent on satellites to enable communication. This radio frequency based infrastructure that most people use has meant that electronic equipment can become susceptible to interference. Other equipment that is not intended to emit Radio Frequency (RF) waves, such a desktop PC's or arc welders can emit RF waves that can interfere with other electronic goods. This has led to legislation, restricting the amount of RF that any equipment can emit and also how resilient equipment should be when exposed to RF. This in turn has led to standards on Electro-Magnetic Compatibility (EMC). For everyday equipment to be traded in Europe,Certificate of Europe (CE) marking is required. CE marking imposes standards for EMC that all equipment must satisfy. Aircraft and the equipment installed on it also have to meet EMC requirements in order to obtain certification. The EMC requirements

for civil aircraft are detailed in RTCA-DO-160F [5].

The EMC requirements for aviation are more stringent than those required for home and offices and a broader set of tests are required for equipment destined for aviation applications. The reason for this is because aviation experience a broader range of electromagnetic phenomenon. Satellite communication can have high levels of intensity and although this is not directed at people an aircraft may pass through the wave path from the ground station to the satellite. It is for this purpose that High Intensity Radiated Field (HIRF) testing is mandated on aviation equipment.

Other electromagnetic phenomenon that aircraft can and will experience is that of lightning and not only should aircraft be resilient to such events, the aircrafts various functions should not be effected during such an event either. A deeper understanding of lighting in aviation will be the subject of the next section.

2.2.2.1 Direct Lightning Strike

Aircraft are designed to withstand the impacts of a direct lightning strike, whereby the electrical discharge between cloud and ground can pass through the body of the aircraft. As shown below;

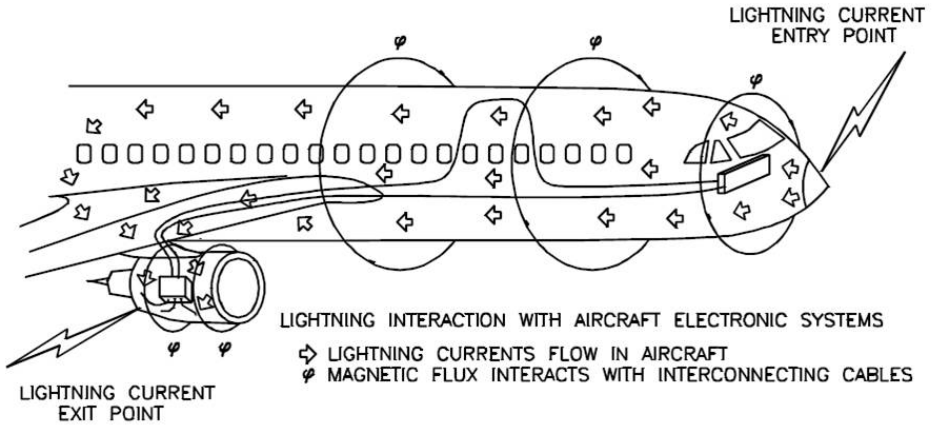

Figure 2.10: Lightning Interaction with Aircraft [4]

A direct lightning strike can reach currents of approximately 200kA and the above figure shows the lightning attaching to the nose of the aircraft and exiting from the tail of the engine. Once the lightning has attached itself to the body of the aircraft, the current density is kept as low as possible by allowing the current to spread though the skin of the aircraft. To aid the spread of the current, the bonding requirements are kept very low, it is not uncommon for the resistance of the aircraft from nose to tail to be approximately 3mΩ. But even with such a low resistance if the aircraft experiences a direct lightning strike of 200kA, then any equipment that is connected together at each end of the aircraft will experience a potential difference of 600V between them! So for example if a piece of equipment located in the nose of the plane is making a measurement of a sensor in the tail of the aircraft, then whatever signal is being measured differentially, this signal will now be subject to an additional common mode voltage of 600V. Electronic equipment on aircraft are not normally subjected to the threat of a direct lightning strike, but are subject to the indirect effects of the lightning current passing through the fuselage of the

aircraft. [24]

2.2.2.2 Indirect Lightning Strike

The lightning strike requirements for electrical equipment are mainly from indirect effects. Referring again to 2.10, it can be seen that the direct lightning strike passes the full 200kA through the fuselage of the aircraft, this current sets up a large and varying magnetic field, this time varying magnetic field will induce currents and voltages into the wiring systems which couple with the magnetic field and it is this induced current/voltage that is referred to as an indirect lightning strike. A Typical waveform of an indirect lightning strike is shown below.

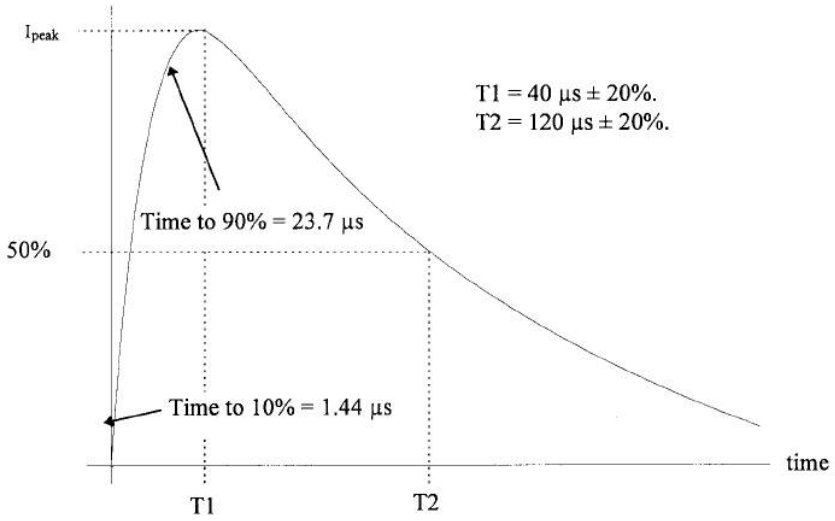

Figure 2.11: Lightning Interaction with Aircraft [5]

The above waveform is one of many that aviation equipment are subjected to as part of their acceptance criteria for aviation deployment. This waveform, (Waveform 5A), is

the highest energy pulse from the lightning strike tests. It is a double exponential curve, which one would expect due to the transformer action of an indirect lightning strike [5].

The coupling mechanism for an indirect lightning strike is similar to that of a current transformer whereby the current and/or voltage induced in the secondary winding of the current transformer (i.e. the aircraft wiring in this example) will depend on what is connected to the end of the aircraft wiring. Should the wire be connected to some circuitry that has a low impedance to ground then a high current will be experienced by this circuit, however, should the impedance be high then a high voltage will result and the circuit should be capable of withstanding such voltages.

2.2.2.3 Attachment Zones

Direct lightning strike is more likely to attach where the E-field will be at its highest. This is usually where objects have the smallest bend radius, (e.g. aircraft nose or wing tip). Aircraft are broken down into lightning strike attachment zones, as shown below.

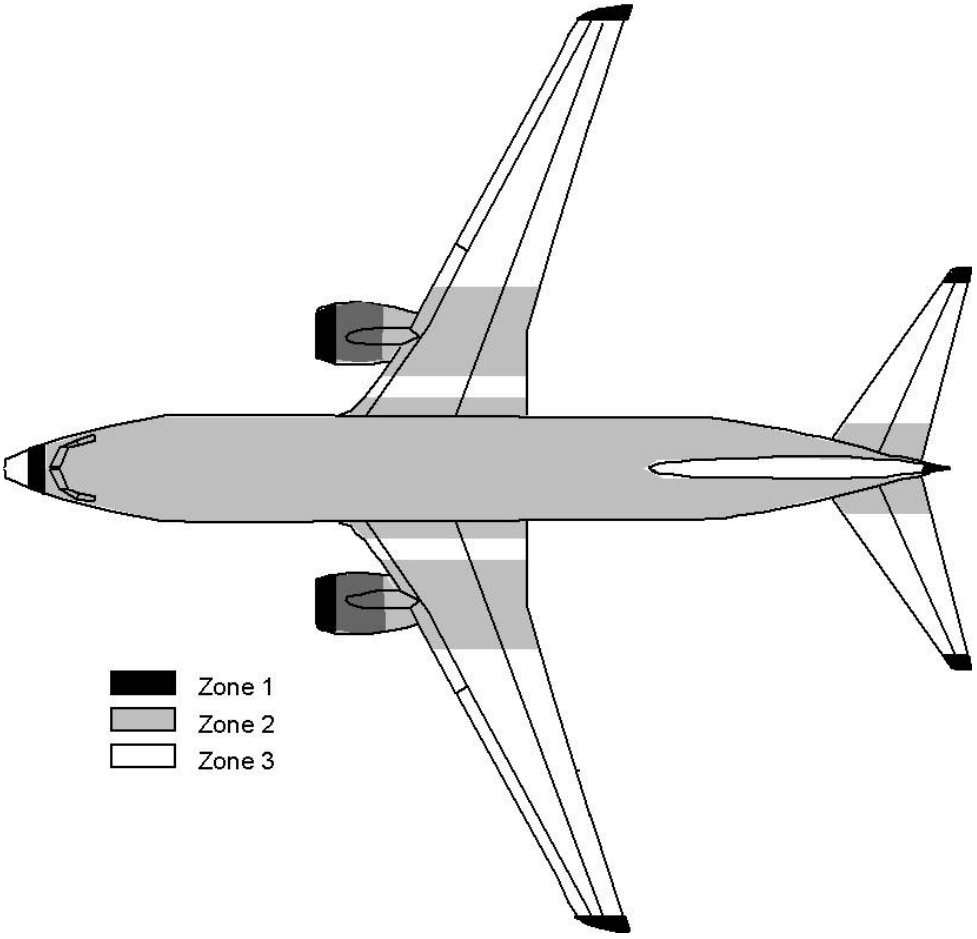

Figure 2.12: Lightning Strike Attachment Zoning on Aircraft [6]

From the above figure it can be seen that the aircraft has been broken down into three zones, zone 1 has the highest probability of initial attachment, zone 2 has the highest probability for swept attachment and zone 3 is most likely to conduct the lightning current with the lowest probability of attachment.

One such incident occurred on a Schleicher ASK-21 Glider, as shown below.

Figure 2.13: Schleicher ASK-21 Glider [7]

On the 17^th April 1999 a Schleicher ASK-21 Glider was struck by lightning whilst passing beneath a cloud, the glider broke apart. The pilot and student managed to parachute to safety.

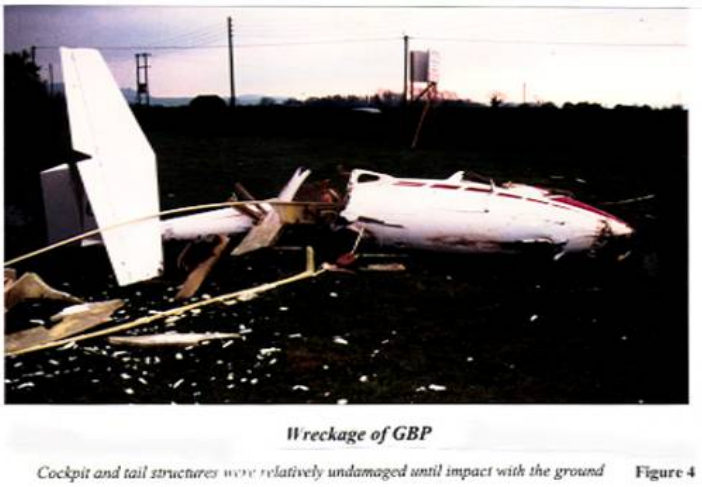

Figure 2.14: Schleicher ASK-21 Glider post lightning strike [7]

The above wreckage was investigated by UK Air Accidents Investigation Branch, Bulletin No. 12/99. The accident details are given below;

- Lightning attached to both wings
- Explosive arcing in wing and fuselage caused structural failure of wing and fuselage
- Significant lightning arc welding on control rod brackets.
- Significant magnetic deformation of control rod tubes.

As to why this happened, the Schleicher ASK-21 has no inherent or designed lightning protection as gliders are not required to have lightning protection. Lightweight fiberglass and foam structure is not tolerant of explosive arcs within the structure, further images of the damaged caused are shown below.

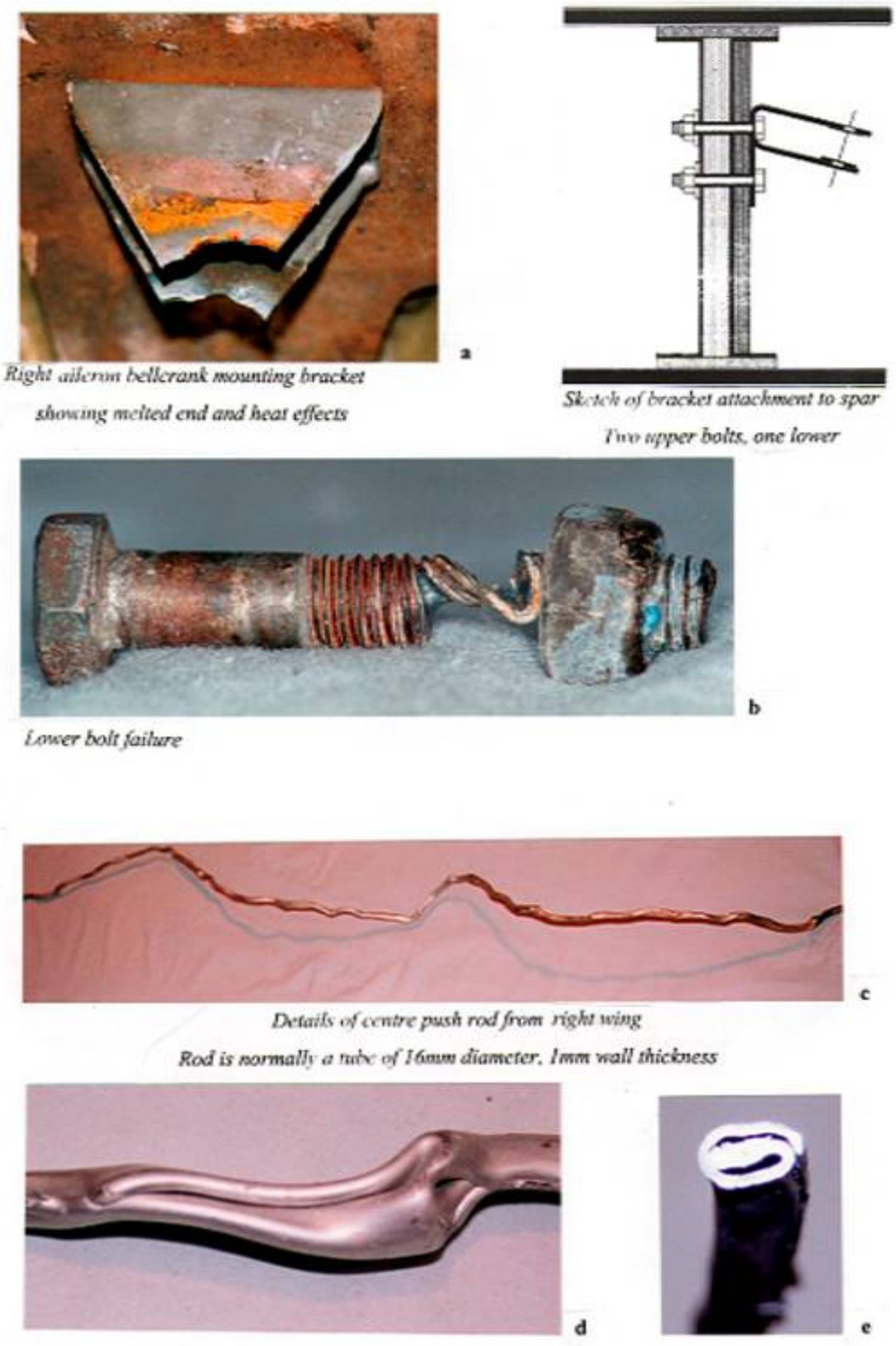

Figure 2.15: Schleicher ASK-21 Glider Internal damage due to lightning strike [7]

As it can be seen from above figures, lightning can be very destructive when designs have not taken it into account, a civil aircraft would be expected to have continued uninterrupted flight and incur no damage to the aircraft or any of the systems that are functioning on it.

2.2.2.4 Lightning Strike Waveforms

When an aircraft is struck by lightning, many secondary indirect effects can be observed by on-board equipment. The highest energy indirect pulse is waveform 5A shown in 2.11 and this waveform is formed by the primary lightning current passing through the fuselage and coupling into the aircraft wiring. If the primary attachment pulse is thought of as the start of a traveling wave, when this pulse reaches the end of the aircraft, (i.e. end of the transmission line) then this pulse will be reflected due to the discontinuity of the transmission line of the aircraft. This reflected pulse will now travel back towards the nose of the aircraft where it will be reflected yet again, this constant reflection of the lightning pulse will continue until the lightning energy has been dissipated. This reflective phenomenon gives rise to multiple burst requirements, as shown below.

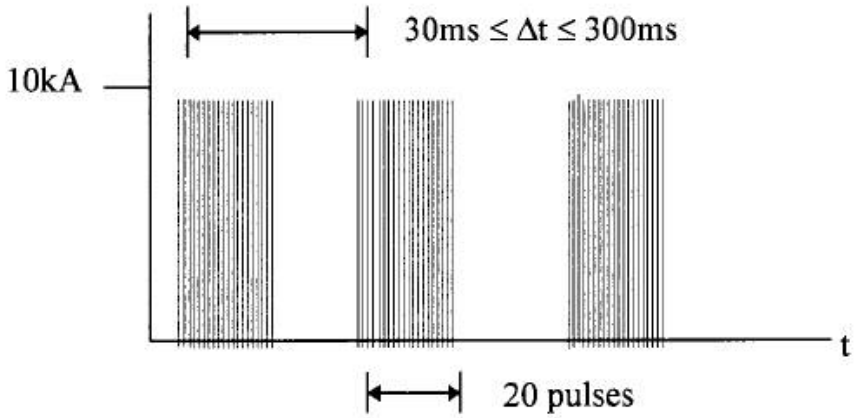

FIGURE 11 - Multiple Burst Waveform Set

Figure 2.16: Multiple Burst caused by lightning reflections in the fuselage [4]

The frequency of the burst is very structure dependent, therefore, it would be reasonable to suggest that the frequency of the burst will be higher for a small regional jet compared to that of a large passenger jet.

Once lighting has attached and the aircraft continues to fly, lightning can become unattached only to re-connect to the aircraft at some further point down the aircraft body. This effect can happen many times during a lightning event and gives rise to a multiple stroke requirement, as shown below.

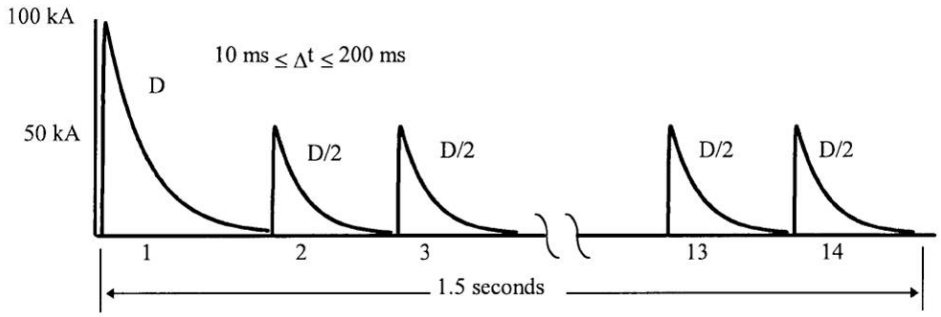

Figure 2.17: Multiple Stroke caused by lighting breaking and re-attaching during flight [4]

From the above figure it can be seen that the frequency is much lower than that of the multiple burst, but one key feature about all of these waveforms is that they can all happen simultaneously. It is only the testing of these waveforms that is done individually to help form the case that the equipment supplied to the aircraft is of appropriate ruggedness.

2.2.2.5 Lightning Requirements

From the previous sections it can be seen how lightning strike can couple into on board equipment and the type of waveforms that equipment are likely to experience and must cater for. However, the levels of current/voltage are to be discussed here.

Primary lightning strike is a current induced threat, however, dependent on what circuitry is connected to a given wire will determine how the threat will manifest itself at the equipment under threat, this is a secondary effect. If, for example the circuitry connected to a given wire has high impedance, then the waveform will be that of voltage not current, i.e. voltage transformer. Obviously if the circuitry is of low impedance then a current

waveform will be expected, i.e. current transformer.

Also consideration must be given to the location of the equipment in the aircraft in respect to the attachment zone where any given equipment is located. With all of these factors being considered various lightning strike levels and waveforms will be attributed to different equipment within the aircraft and design and test criteria will have to be met in order to demonstrate compliance.

TABLE 5 - Individual Conductor TCL, ETDL or Test Levels
Due to Current Component A

Level	Waveform 3 V/I	Waveform 4 V/I	Waveform 5 V/I
1	100/4	50/10	50/50
2	250/10	125/25	125/125
3	600/24	300/60	300/300
4	1500/60	750/150	750/750
5	3200/128	1600/320	1600/1600

Figure 2.18: Lightning test waveforms and levels [5]

From the above figure it can be seen that two figures are given for any test. The figure on the left is for that of Voltage and that on the right is for Current. These two numbers are to take account of whether a circuit has high impedance (Voltage test) versus a low impedance (Current test). If a circuit has high impedance then the whole design needs to be able to cope with the voltage waveform, this means that a design that is to operate at 28V, will have to have components selected and connectors appropriate for the voltage

lightning strike design. So for example, a design that must meet Waveform 3, level 4. The 28V circuit must be rated to 1500V which may be an overkill or just simply not possible, in which case the 28V circuit may be protected by a Transient Voltage Suppressor (TVS) which would clamp the voltage to a much lower level such that 1500V parts are not required, but this now means that incorporating a TVS the PCB tracks and the connectors must be able to withstand a pulse of 60A at the appropriate waveform.

This thesis is concerned with voltage threats and the design considerations required to withstand voltage based threats.

2.2.3 Design Standards

Currently there are no design standards only guidelines that have been widely adopted. The most commonly referenced in aerospace is IPC-2221A [8]. There are other guideline documents, such as EN-60664 [25], however, IPC-2221A makes reference to altitude and breakdown voltage in a single table, whereas EN-60664 only accounts for altitudes up to 2000m in a single table and altitude corrections must be sought in another. This minor extra work effort may explain why IPC-2221A is adopted for aerospace guidance. IPC-2221A on the other hand gives air gap isolation requirements to any elevation, as shown below.

Table 6-1 Electrical Conductor Spacing

Voltage Between Conductors (DC or AC Peaks)	Minimum Spacing						
	Bare Board				Assembly		
	B1	B2	B3	B4	A5	A6	A7
0-15	0.05 mm [0.00197 in]	0.1 mm [0.0039 in]	0.1 mm [0.0039 in]	0.05 mm [0.00197 in]	0.13 mm [0.00512 in]	0.13 mm [0.00512 in]	0.13 mm [0.00512 in]
16-30	0.05 mm [0.00197 in]	0.1 mm [0.0039 in]	0.1 mm [0.0039 in]	0.05 mm [0.00197 in]	0.13 mm [0.00512 in]	0.25 mm [0.00984 in]	0.13 mm [0.00512 in]
31-50	0.1 mm [0.0039 in]	0.6 mm [0.024 in]	0.6 mm [0.024 in]	0.13 mm [0.00512 in]	0.13 mm [0.00512 in]	0.4 mm [0.016 in]	0.13 mm [0.00512 in]
51-100	0.1 mm [0.0039 in]	0.6 mm [0.024 in]	1.5 mm [0.0591 in]	0.13 mm [0.00512 in]	0.13 mm [0.00512 in]	0.5 mm [0.020 in]	0.13 mm [0.00512 in]
101-150	0.2 mm [0.0079 in]	0.6 mm [0.024 in]	3.2 mm [0.126 in]	0.4 mm [0.016 in]	0.4 mm [0.016 in]	0.8 mm [0.031 in]	0.4 mm [0.016 in]
151-170	0.2 mm [0.0079 in]	1.25 mm [0.0492 in]	3.2 mm [0.126 in]	0.4 mm [0.016 in]	0.4 mm [0.016 in]	0.8 mm [0.031 in]	0.4 mm [0.016 in]
171-250	0.2 mm [0.0079 in]	1.25 mm [0.0492 in]	6.4 mm [0.252 in]	0.4 mm [0.016 in]	0.4 mm [0.016 in]	0.8 mm [0.031 in]	0.4 mm [0.016 in]
251-300	0.2 mm [0.0079 in]	1.25 mm [0.0492 in]	12.5 mm [0.4921 in]	0.4 mm [0.016 in]	0.4 mm [0.016 in]	0.8 mm [0.031 in]	0.8 mm [0.031 in]
301-500	0.25 mm [0.00984 in]	2.5 mm [0.0984 in]	12.5 mm [0.4921 in]	0.8 mm [0.031 in]	0.8 mm [0.031 in]	1.5 mm [0.0591 in]	0.8 mm [0.031 in]
> 500 See para. 6.3 for calc.	0.0025 mm /volt	0.005 mm /volt	0.025 mm /volt	0.00305 mm /volt	0.00305 mm /volt	0.00305 mm /volt	0.00305 mm /volt

B1 - Internal Conductors
B2 - External Conductors, uncoated, sea level to 3050 m [10,007 feet]
B3 - External Conductors, uncoated, over 3050 m [10,007 feet]
B4 - External Conductors, with permanent polymer coating (any elevation)
A5 - External Conductors, with conformal coating over assembly (any elevation)
A6 - External Component lead/termination, uncoated, sea level to 3050 m [10,007 feet]
A7 - External Component lead termination, with conformal coating (any elevation)

Figure 2.19: Electrical conductor spacing requirements for voltage withstand [8]

The above table is broken down into two sections; namely, Bare board (B1 - B4) and Assembly (A5 - A7). The bare board refers to the Printed Circuit Board (PCB) and the assembly refers to the collection of PCB's orientated and connected together with wires and connectors to form the assemble product or equipment.

Column B1 refers to the distances required on inner layer tracks within the PCB and although these distances are extremely conservative compared to the dielectric withstand properties of PCB material, solid insulation is not being treated as part of this thesis is in considered beyond scope.

Columns B2 provide spacing guidance to uncoated external layers of PCB up to 3050m and column B3 provides spacing consideration above 3050m, unfortunately no upper limit is given. For aerospace applications columns B2 and B3 are virtually never used as all PCB's are invariably coated.

Column B4 provides the spacing guidance necessary to prevent electric breakdown from occurring on the surface layers of a coated PCB. The guidance to prevent electric breakdown from occurring claims to be good at any elevation, however, this is not given as a distance so is impossible to interpret. This column is the most commonly used one for PCB's in aerospace.

Column A5 and A7 gives spacing requirements for external conductors or components with conformal coating, stating it is for any elevation, again no actual distance is provided. These two columns are also mainly used for aerospace guidelines.

As would be expected columns B4, A5 and A7 have the same data, so only the rationale behind the choice of column may vary. But the spacing requirement will remain the same.

Electric breakdown cannot occur at voltages as low as 15V, however, the above table mandates requirements for spacing. The only conclusion that can be drawn is that the table is taking account for other failure mechanisms in addition to electric breakdown, such as moisture and impurities allowing tracking to occur, which is also undesirable. From this table it is impossible to extract exactly the gaps required for electric breakdown, however, for voltages above 200V it is assumed that this is the most likely cause.

2.2.4 Temperature Effects on Partial Discharge

Both IPC-2221A and EN-60664 take no reference for temperature effects on partial discharge. However, it appears reasonable to expect that there be some form of relationship between partial discharge and temperature as the gases mean free path (λ) feature in some of the previous arguments in relation to effects of altitude on partial discharge in section 1.3.4.2 and as the gases mean free path (λ) is directly related to temperature by the following relationship.

$$\lambda = \frac{kT}{\sigma p} \tag{2.1}$$

Where;

k is Boltzmann's Constant,

T is Absolute temperature (K),

p is pressure (Pa),

σ is the collision cross sectional area of the gas molecule (m^2)

From the ideal gas law [26].

This thesis will detail the fundamental connection between the voltage responsible for partial discharge and temperature.

2.2.5 Density of Wiring and Electrical Equipment on Aircraft

With the trend to replace existing functions on the aircraft with their electrical equivalents, which is the trend for the More Electric Aircraft (MEA), the quantity of wires must increase and as with all technologies related to aviation, the density of the wiring system must also rise. To minimise the wiring weight, the benefits of employing higher voltages may be realised and taken advantage of. Increased wiring density and higher voltage requirements become mutually exclusive, as higher voltages will mandate greater separation distances in air. It is true that cable insulation provides much greater dielectric withstand capability, however, aircraft are designed for 25 year or more in service operability. Therefore insulation cracking over the life of the aircraft should be expected and catered for. This may negate the dielectric strength improvement offered by the insulation material if it is expected for the insulation to crack, however, if this is not an acceptable philosophy, due to space restrictions, maintenance schedules will be mandated so that the wiring systems have routine visual inspections.

Whichever method is adopted, maintenance schedules versus 'fit and forget' options, one thing is true for both, wiring density will increase in the future.

2.2.6 Chapter Summary

The requirement for increasing system voltage and density of wiring have led to mutually exclusive design constraints. On the one hand the increase in system voltage necessitates larger and larger spacing requirements. However, the demand for increased wiring density requires spacing to reduce.

There also appears to be a variance between the Paschen curve and the guidelines provided by both IPC 2221-A and EN 60664. The spacing requirements are quite inconsistent. The guidelines, being extremely conservative in nature make the design of much aerospace equipment prohibitively difficult.

If moisture and impurities could be removed as fault propagation mechanisms, as is the case with current state of the art coating technologies, such as parylene, leaving only electric breakdown as the only mechanism of failure. Then greater reliance could be attributed to the Pachen curve over the guidelines of IPC 2221A. But this can only be done, should a fundamental theoretical understanding be provided for such curve. If such a fundamental understanding could be gained, then greater density could be realised as the overtly conservative guidelines may be replaced with fundamental minimum. This fundamental minimum is the topic for future chapters.

Chapter

3 Currently Accepted Theory of Electric Breakdown

In classical electromagnetism, André-Marie Ampere in 1826 proved a relationship between the integrated magnetic field around a closed loop of an electrical conductor to that of the current passing through the conductor. This became later known as Ampere's Law and is shown below.

$$\oint_C B \cdot dl = \mu_o I \tag{3.1}$$

The above equation became the accepted theory and has been applied to physics and electrical engineering for the last 150 years or so.

James-Clerk Maxwell noticed an inconsistency with the above equation when expressing current in terms of current density (J).

$$\oint_C B \cdot dl = \mu_o \int \int_S J \cdot dS \tag{3.2}$$

The term $\int \int_S$ denotes an integral over the surface S enclosed by the curve C. This

is of particular interest when considering an electric circuit including a capacitor, formed by two metallic plates separated by an air gap, as shown below.

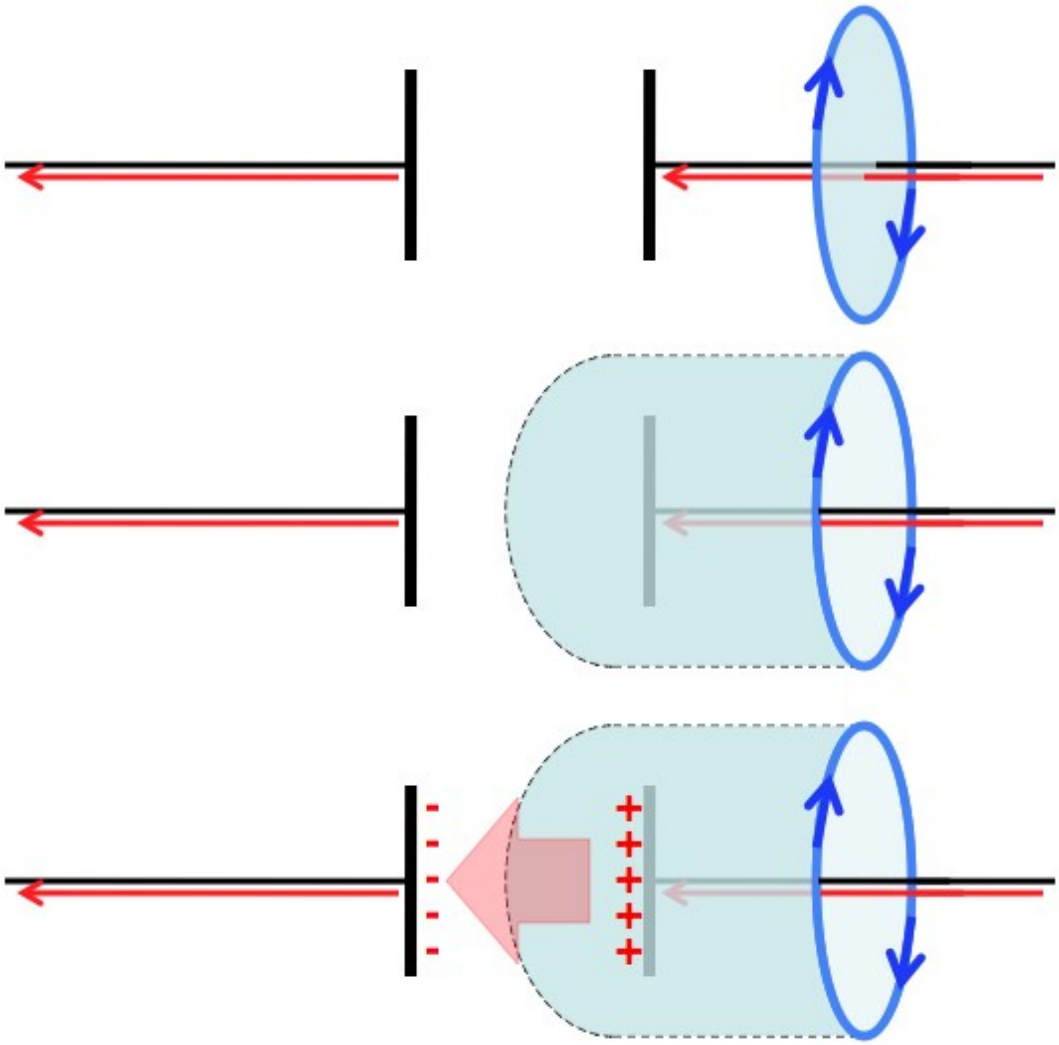

Figure 3.1: Visual representation of Integral form of Ampere's Law

As it can be seen from Figure 3.1 the path integral (C) closes around the electrical conductor, however, the surface integral (S), which is a three dimensional surface, connects to the path integral (C) but the surface passes between the plates of the capacitor. This

surface is passing through the air gap of the capacitor, before 1826 would have appeared inconsistent as current should not pass through air (which is an insulator).

Maxwell resolved this inconsistency by the inclusion of the D-Field (Displacement-Field), which comprises of the original E-field but with the addition of a new Polarisation-Field (P), related as follows.

$$D = \epsilon_o E + P \tag{3.3}$$

This new D-Field removes any discontinuities across boundary layers and in turn removes the inconsistencies of Ampere's law. In the above example, over the length of the wire the $\boldsymbol{D}$-Field is equal to the $\boldsymbol{E}$-Field whereby $\boldsymbol{P}$ is equal to zero as the wire is a conductor. Within the air gap the $\boldsymbol{E}$-Field is reduced to zero and in the insulator there are no free electrons. The introduction of the $\boldsymbol{P}$-Field means an equal but opposite field has been introduced, which is equal in magnitude, but opposite in sign to that of the original $\boldsymbol{E}$-Field. In this air gap it is the $\boldsymbol{P}$-Field that provides all of the forces on any atoms contained within it. The introduction of the $\boldsymbol{D}$-Field has provided a continuous field across discontinuous boundary layers between conductors and insulators.

The introduction of equation 3.3 modifies equation 3.2 in the following way;

$$\mathbf{J} = \epsilon_o \frac{\partial \mathbf{E}}{\partial t} + \frac{\partial \mathbf{P}}{\partial t} \tag{3.4}$$

Replacing the current density term $\boldsymbol{J}$ with the partial derivative was one of the nec-

essary steps allowing Maxwell to form his equations.

Experimental evidence was also growing in this arena, however, Maxwell's adjustment to Ampere's law was only true for time varying E-fields, but evidence was also becoming apparent for DC steady state currents in air gaps and this will be discussed in the next section.

3.1 Current Through a Uniform-Field Air Gap

J.S. Townsend observed that the current through a uniform-field air gap at first increases proportionately with applied voltage in the region (0 - V_1), then remains nearly constant at a plateau value I_o as shown in figure 3.2. The current I_o corresponds to the photoelectric current produced at the cathode by external radiation. At voltages higher than V_2, the current rises above I_{o1} at a much higher rate with increasing voltage until a spark results. Further increases to the power available result is a further rise to I_o, but the voltage V across the gap will remain unaltered. The increase of current in the region V_2 - V_3 is attributed to ionization by electron impact. As the electric field increases, electrons leaving the cathode are accelerated between collisions, until they gain enough energy to cause ionization on collision with gas molecules or atoms. The secondary process accounts for the sharp increase of the current in the region V_3-V_S and the eventual spark breakdown of the gap [27].

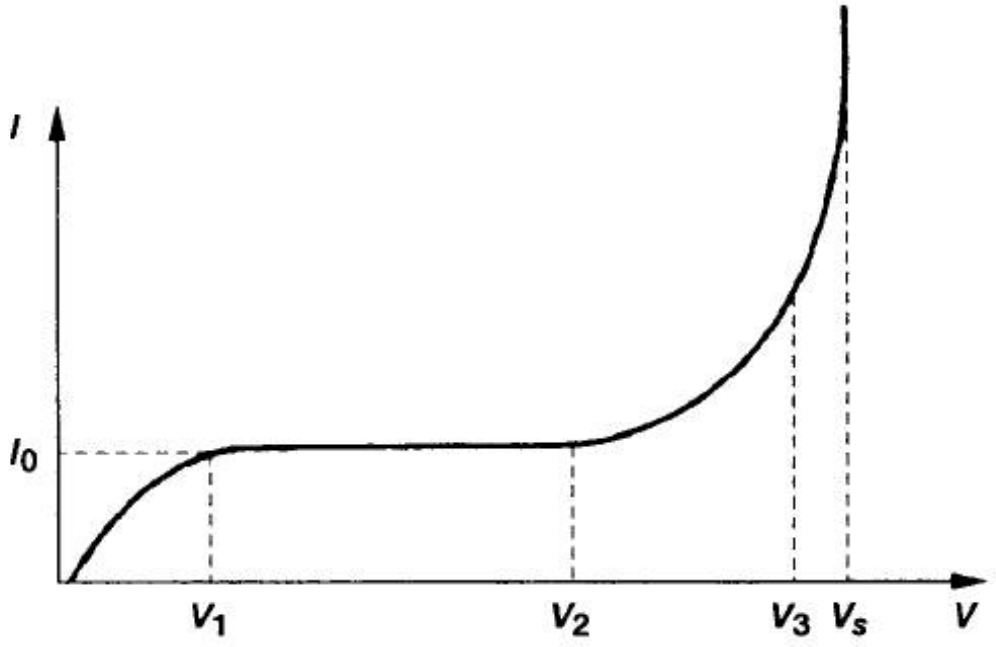

Figure 3.2: I-V curves related to Air Gap's [9]

3.2 Townsend Primary Ionization

In order to explain the change in behavior over regions V_3-V_S in figure 3.2 above, Townsend introduced the quantity α, known as the Townsend primary ionisation coefficient. It is defined as the number of additional electrons generated by an electron per unit length in the path of the Electric-field. If n is the number of electrons per second reaching a distance x from the cathode in the field direction, the increase dn in an additional distance dx is given as

$$dn = \alpha n dx \tag{3.5}$$

Integrating the above equation over a distance d between the cathode and the anode results in

$$n_a = n_o e^{\alpha d} \tag{3.6}$$

From the above equation, n_o is the number of primary electrons generated per second at the cathode and n_a is the number of electrons reaching the anode per second. In terms of current, if we assume that the current leaving the cathode is I_o, equation 3.6 becomes.

$$I = I_o e^{\alpha d} \tag{3.7}$$

The term $e^{\alpha d}$ is referred to as the electron avalanche term, which represents the number of electrons produced by a single electron whilst traversing from the cathode to the anode.

In addition to electrons being produced from collisions, electrons can be lost due to re-combination, if we attribute a re-combination coefficient (η) which has the opposite effect to the ionisation coefficient (α), the the amount of current lost due to recombination may be shown as.

$$dI = -\eta I dx \tag{3.8}$$

Applying the same method as before, with current I_o at the cathode, the current at the anode, a distance (d) away, can be shown to be.

$$I = I_o e^{-\eta d} \tag{3.9}$$

If the electrons produced by collisions and the electrons lost due to recombination

operate simultaneously, then the resulting number of free electrons is given as

$$dn = n(\alpha - \eta)dx \tag{3.10}$$

It therefore follows that the number of electrons at a distance x from the cathode, in line with the field lines of the E-field that traverse the cathode and anode gap, where $x = 0$ at the cathode and with n_0 electrons starting from the cathode, the result is shown below.

$$n = n_o e^{(\alpha-\eta)d} \tag{3.11}$$

According to equation 3.7, a graph of lnI against the gap length d should give a straight line of slope α, assuming variables such as the E-field (E) and air pressure (p) are kept constant. Measurements of current between parallel plate electrodes showed that, at higher voltages, the current I increased more rapidly than that predicted by equation 3.7, the results of which are shown below [9].

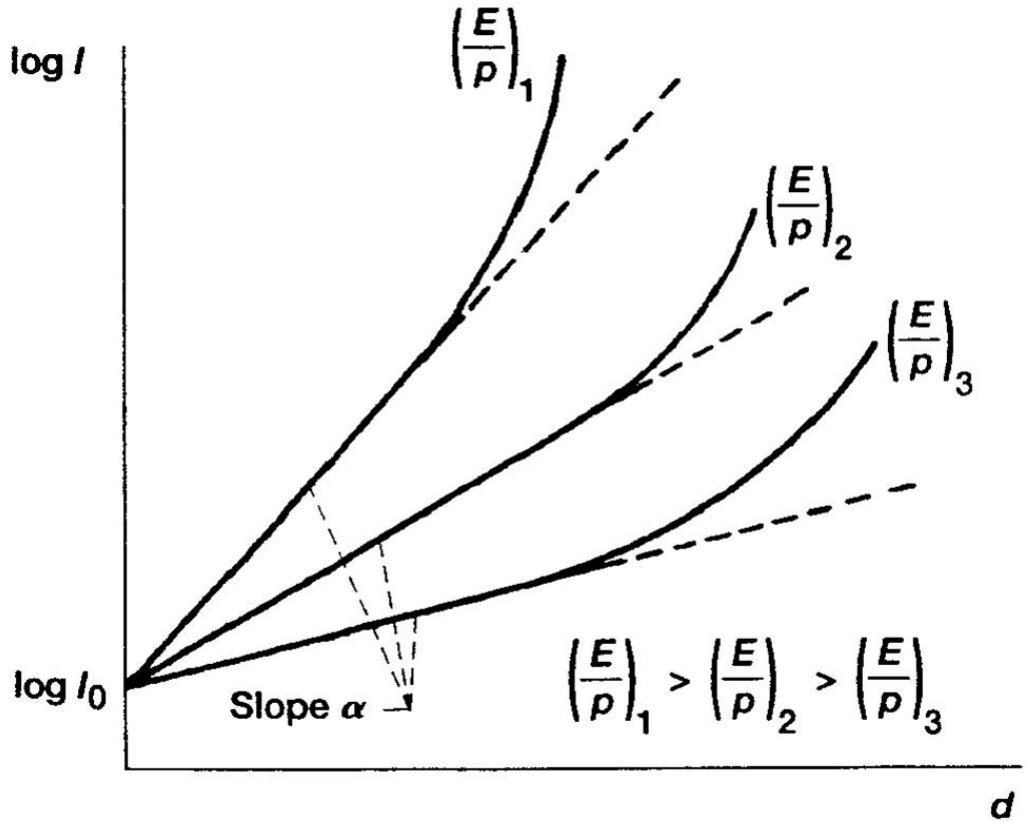

Figure 3.3: Theoretical and experimental currents in air gap plotted against distance [9]

Theses results led Townsend to postulate further in that this effect is due to another mechanism which he termed the secondary ionisation method, which will be described in the following section.

3.3 Townsend Secondary Ionization

Townsend argued that in addition to the primary ionisation, whereby accelerating electrons could produce further electrons by dislodging them from their neutral gaseous molecules, further electrons could be liberated from the cathode electrode by the bombardment of positive ions with the cathode. The positive ions where created when its electrons became dislodged during the initial collision.

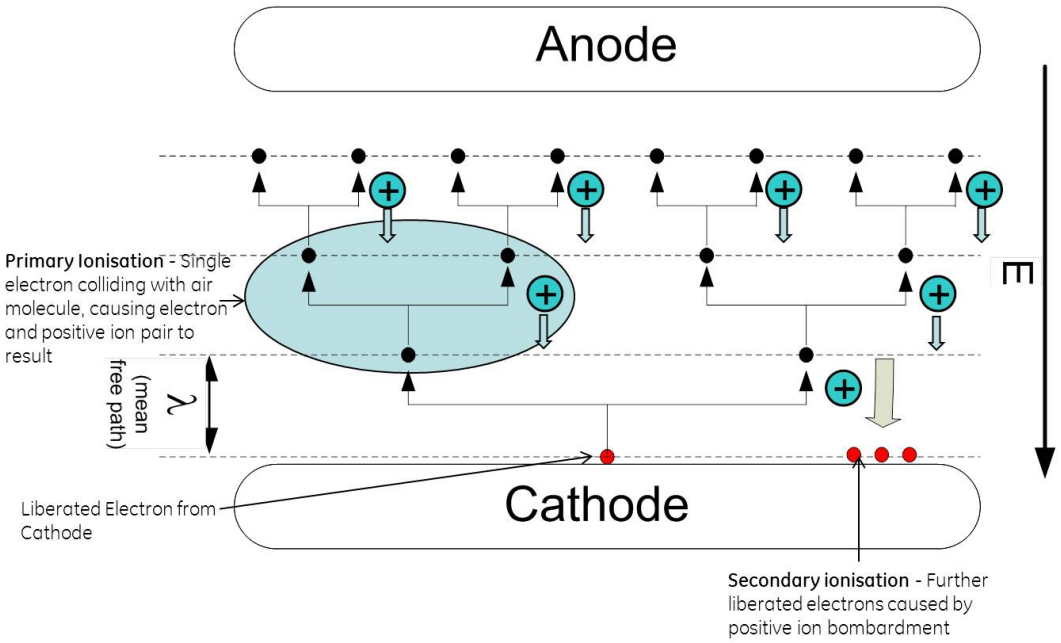

Figure 3.4: Image showing Primary and Secondary Ionisation collisions [10]

From the above figure it can be seen that the electrons will accelerate to the Anode, colliding with gas molecules along the way and positive ions will accelerate back towards the cathode. Should the positive ion make it to the cathode without being recombined with free electrons, the positive ion might dislodge an electron from the cathode surface,

which in turn will start the process again.

So with one accelerating electron, two electrons will form after a collision with a gas molecule and in addition a positive ion. The positive ion will produce another electron when/if it collides with the cathode, so now there are three electrons. Thus the secondary process will produce more electrons than the primary process alone.

Let n_a be the number of electrons reaching the anode per second, n_0 the number of electrons emitted from the cathode, n_+ the number of electrons released from the cathode by positive ion bombardment and γ the number of electrons released from the cathode as a proportion of the free electrons within the air gap.

$$n_a = (n_o + n_+)e^{\alpha d} \tag{3.12}$$

and

$$n_+ = \gamma[n_a - (n_0 + n_+)] \tag{3.13}$$

Eliminating n_+ leads to

$$n_a = \frac{n_0 e^{\alpha d}}{1 - \gamma(e^{\alpha d} - 1)} \tag{3.14}$$

The expression for steady-state current follows as

$$I = \frac{I_0 e^{\alpha d}}{1 - \gamma(e^{\alpha d} - 1)} \tag{3.15}$$

It has been experimentally confirmed that the ionisation coefficient α, the gas pressure

p and the electric field intensity E are related as follows.

$$\frac{\alpha}{p} = f\left(\frac{E}{p}\right) \tag{3.16}$$

where f is an arbitrary function. Now by introducing the above equation and $E = V/d$ with equation 3.15 we get.

$$I = I_0 \frac{e^{pd} \cdot f(\frac{V}{pd})}{1 - \gamma[e^{pd} \cdot f(\frac{V}{pd}) - 1]} \tag{3.17}$$

As Voltage (V) increases a point is reached when there is a transition from steady current I_0 to a self sustaining discharge. At this point I becomes indeterminate as the denominator approaches zero.

$$\gamma(e^{\alpha d} - 1) = 1 \tag{3.18}$$

If electron recombination is also taken into account then equation 3.18 becomes.

$$\frac{\gamma\alpha}{\alpha - \eta}[e^{(\alpha-\eta)d} - 1] = 1 \tag{3.19}$$

With the above condition being met, the process is now self sustaining and the original current I_0 is no longer required, this breakdown phenomenon has effectively latched.

Equation 3.19, defines the condition for spark onset, this is referred to as the Townsend's breakdown criterion. For $\gamma(e^{\alpha d} - 1 = 1)$, the discharge due to the ionisation process is self-sustaining and can continue in the absence of I_0 (i.e. latched), therefore the criterion $\gamma(e^{\alpha d} - 1 = 1)$ defines the sparking threshold.

For Townsend phenomenon to occur, with both primary and secondary ionisation, collisions with gas molecules are required to free up other electrons and cause an avalanche condition and thus breakdown. Therefore if the air gap is shorter than the mean free path of the gas (λ) then no (or less) collisions will occur and breakdown will be less probable and will explain why the paschen curve rises for small (pd) product.

3.4 Summary

The mechanism's for electric breakdown, according to the accepted Townsend theory of primary and secondary ionisation may be illustrated by the following figure.

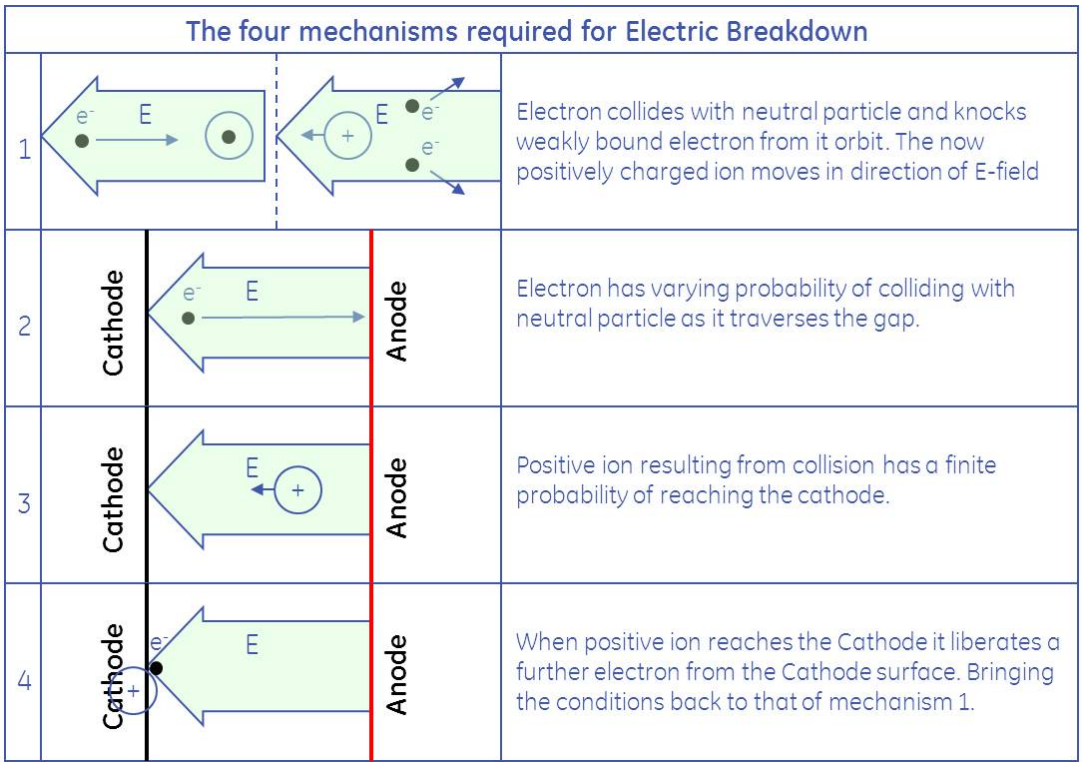

Figure 3.5: Image showing the four mechanisms for Townsend electric breakdown

Referring to figure 3.5 Paschen demonstrated electrical discharge is linked to the (pd) product, however, the derivation above did not show this link until much work was carried out proving that the quantities, E, p and α are related, as detailed in equation 3.16 [28].

The Paschen curve was formed by raising the voltage across an air gap until a current could be measured and then the experiment was terminated and a new (pd) product would be set up and the whole experiment repeated. The accepted theory as detailed above predicts a self sustaining electric breakdown, although the experimental validation did not test for this, due to the termination of the experiment once current was detected. The theory presented above is correct and is applied to avalanche phenomenon in semiconductor theory. However, The theory to be detailed in this thesis assumes the Paschen curve to be that of a partial discharge curve, which is non-sustaining and is expected to be at a lower energy level to that of Townsend breakdown. It must be again repeated here, that the term partial discharge refers to the proposed definition provided in section 1.3.4.1 in Chapter 1, whereby a non-sustaining discharge (PD) is a transitory discharge mechanism that can occur in voids in dielectric material or between the conductors across the dielectric material which provide electric field stress between these two conductors. The theory to be proposed allows voids to grow under certain conditions until the void extends the whole distance between the conductors. The theory also details mechanisms whereby voids can extend from the surface of the dielectric material and then protrude across the entire gap between the conductors, however, the 'void' appears an incorrect term when it begins from the surface of the dielectric, therefore this mechanism is referred to as dielectric erosion.

It must again be repeated and stressed that the current accepted theory detailed in

this chapter is not deemed incorrect, but occurs at much higher energy levels than that proposed in this thesis. The energy levels required in the current accepted theory allow for electrons to collide with other atoms or molecules and dislodge more weakly bound electrons from them, this proposed theory does not require these mechanisms and can occur at much lower energy levels. It is for this reason that the current accepted theory cannot predict the minimum voltage required for breakdown and the proposed theory can provide such a minima. The following citations provide the same treatment to the current accepted theory. [29] [30] [31] [32] [33] [34] [35] [36] [37] [38] [39] [40] [41] [42] [43] [44] [45]

Chapter

4 Plasma Formation and its Effect on Polarisation

Plasmas have been observed for many years, and are simply a concentration of charge carriers that can be found outside the boundaries of an electrical conductor. Physicists and engineers have made use of them in many applications, such as valves, Cathode Ray Tube (CRT) televisions and arc welders, all of which have been instrumental in our technological development. Other, less desirable plasmas may be observed in lightning, between the opening contacts of a relay or contactor and partial discharge.

Not all plasmas are visible and are mostly observed when they interact with other systems or particles. Corona is a plasma interaction that can be both visible and non-visible alike. Corona is usually found near areas of high electric field concentration, such as sharp edges or points in an electrical system. If the electric field is sufficient to ionise the surrounding air molecules, by either electron bombardment, or by dislodging weakly bound electrons from their orbits then this can usually be observed as a distinct glow in and around the area of high electric field concentration.

If on the other hand the electric field is insufficient to cause ionisation of the surrounding gas molecules but still causes a concentration of charge carriers then this is still a plasma. If the charge concentration is able to bridge the gap between the Anode and Cathode then this could result in a short temporary un-sustained conduction path which can be referred to as partial discharge. In instances such as partial discharge this may be of greater concern due to it going undetected for long periods of time and only when the plasma forms a long enough length, enough to form a circuit that was not there previously can the plasma be observed.

4.1 The Electric Field

An electron or positive ion will move under the influence of a surrounding electric field (E-field). The force (F) experienced by a single electron is given by the equation $F = eE$, where e is the charge of the electron and E is the electric field strength. The electric field is formed by applying a potential difference between two electrodes. The convention is to show the electric field direction from anode to cathode and as an electron is negatively charge it will experience a force in the opposite direction from cathode to anode, as shown below.

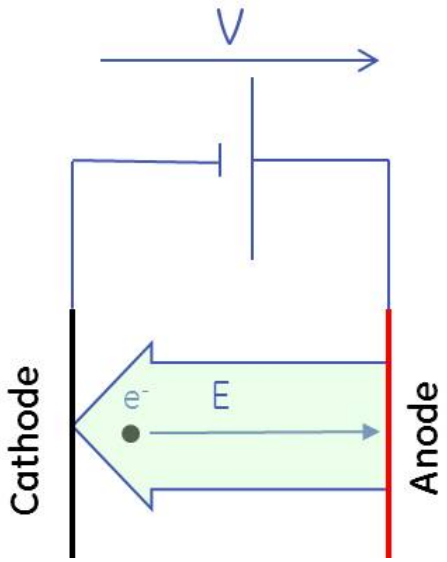

Figure 4.1: Electric Field Convention and forces experienced by electron

4.1.1 Lines of Flux

An electric field is usually discontinuous, in that it is created at the anode and is continuous along its path until it terminates at the cathode and is bound between these two points. The individual lines of flux are not easily observable, however, they are similar in nature to the lines of magnetic flux around a bar magnet which are observed by sprinkling iron fillings on and around the paper where the bar magnet is resting.

Each electric field line operates in exactly the same way in that they are ordered, non-turbulent and do not cross. The flux line is created by the presence of a positively charged particle and is terminated by a corresponding negatively charged equivalent. The quantity of charged particles forming a given flux line provides a measure of the electric field strength. The charged particles may be realised by the use of a battery, or may build

up over time as in the case of clouds prior to an electrical storm.

It is the treatment of individual flux lines and how they operate collectively that will form the basis of explaining partial discharge in this thesis.

4.1.2 Surface Charge

As explained previously it is the collection of oppositely charged particles that form electric field flux lines. Within an electrical conductor electrons experience an extremely high degree of mobility, however, in the case shown in figure 4.1 the two facing surfaces of the electrodes that form the anode and the cathode is where the charge particles will congregate. The reason for this is because the electrons and positive ions are attracted to one another and due to the high mobility for these charged particles within the electrical conductor, it is at the surface of the conductor where they will come to rest.

Surface charges will be present at either end of each E-field flux line and the quantity will depend on the electric field strength and thus the voltage across the two surfaces, in this example as shown below.

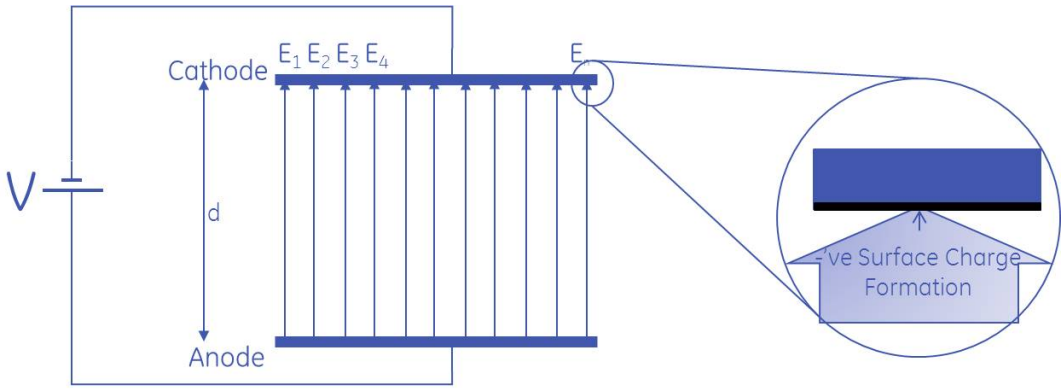

Figure 4.2: An image of individual flux lines forming an electric field showing surface charge

4.2 Dielectrics and Polarisation

Dielectrics and other insulative materials are often employed in electrical equipment for a wide variety of reasons. These may be used for cable insulation to allow cables to be safely routed avoiding fear of electrification. Other dielectrics have other properties that can be exploited, such as those used in the construction of capacitors, whereby materials are sourced that have high permittivity (ϵ) to allow higher values of capacitance to be realised in a given volume.

Dielectrics have a neutral charge as the atomic bonds are complete, however, they can be polarised and form an electrostatic dipole. As a dipole has equal but opposite charge at either of its end, at a macroscopic level it still retains a neutral charge, although near each end of the dipole an electric field can form attachments.

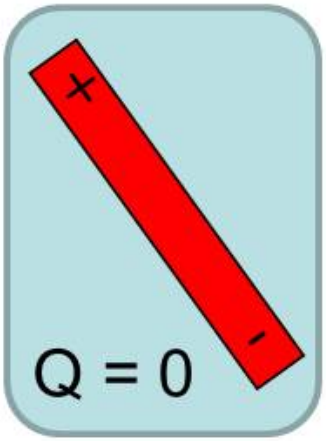

Figure 4.3: Image of Dipole

From the above figure it can be seen that the total charge (Q) enclosed by the boundary box is equal to zero, meaning that it is neutral in charge.

4.2.1 Solid Dielectric

If a solid dielectric material is now placed between two parallel plates, electric flux lines will still traverse the total original gap (d) when a voltage is applied across these plates, however, other flux lines will now form new attachments with the now polarised dielectric.

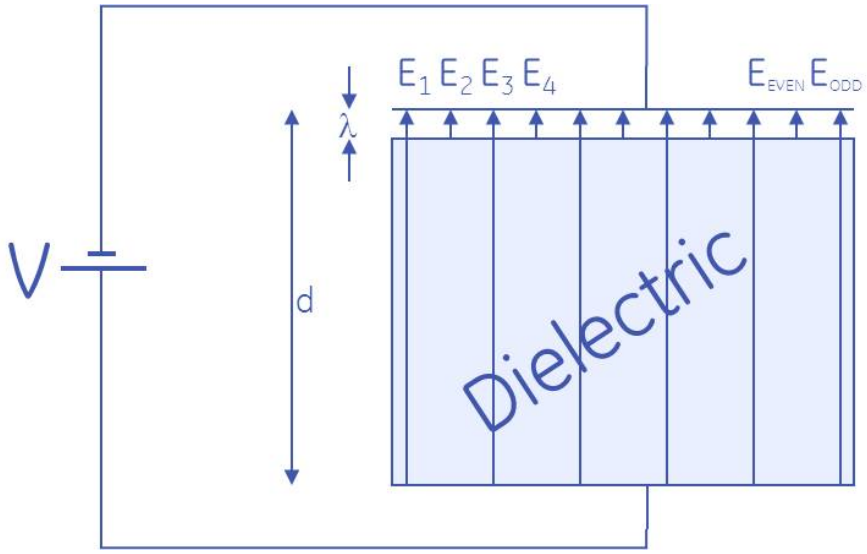

Figure 4.4: E-Field Flux line formation when a dielectric material is introduced between two plates

For the purposes of illustration the above figure 4.4 shows the situation when the dielectric material does not perfectly fill the gap between the two plates and leaves a small air gap of distance (λ). This figure shows flux lines passing uninterrupted between the two plates and others terminating at the surface of the dielectric material.

Dielectrics are usually characterised by their permittivity (ϵ). This is a dimensionless quantity and is a measure of how polarisable a given material is. Materials are usually characterised relative to the permittivity of air (ϵ_0) and are expressed by their relative permittivity (ϵ_r). The total permittivity is therefore expressed as $\epsilon = \epsilon_0\epsilon_r$

If every flux line emitted from the cathode was to form attachments to the dielectric material, thereby preventing any electric field to be present in the dielectric material, this would be said to have infinite permittivity. Whereas if no flux attachments were made

and all flux lines passed between the two plates, then the permittivity would only be that of air, thus its relative permittivity $\epsilon_r = 1$.

It must be noted, however, that the relative permittivity of a material is given at a macroscopic level, thereby taking a more averaged out view over a multitude of flux lines. But for an individual flux line that does attach a flux line at its polarising surface, it does indeed have an infinite permittivity on that flux line.

4.2.2 Gaseous Dielectric

When the dielectric is a gas, many of the features detailed in the previous section still apply, what is less likely is the uniformity and structure that a solid dielectric brings.

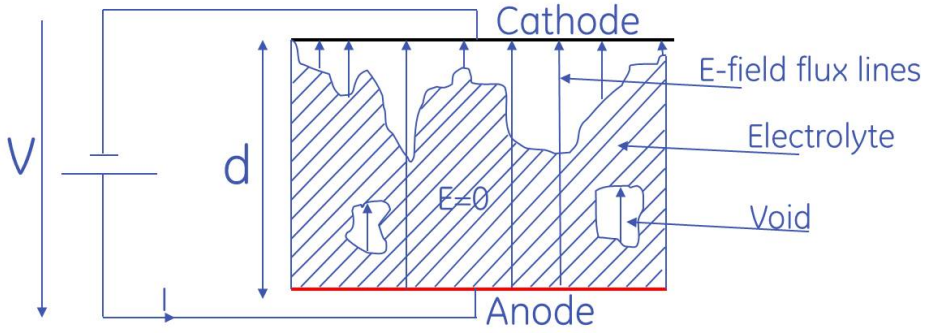

Figure 4.5: E-Field flux line formation when a gas dielectric is introduced between two plates

From the above figure 4.5 it can be seen that there are still areas of infinite permittivity, where flux lines have terminated to the dielectric material and the E-field is reduced to zero, as shown above. In a gaseous dielectric the individual molecules experience the

forces exerted by an individual flux line and each one of these will become polarised and form subsequent field line attachments, as shown below. [46]

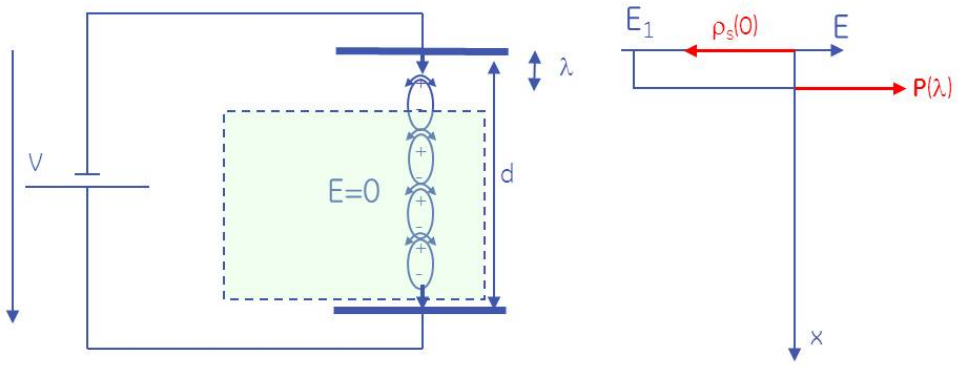

Figure 4.6: Image of gas molecule polarisation over the whole gap d for a particular flux line

From figure 4.6 an $\mathbf{E} - Field$ is formed from a surface charge density of electrons located on the metallic surface of the cathode, these surface charges located at a distance 0m from the cathode surface are expressed by $\rho(0)$. The $\mathbf{E} - Field$ remains present until it is terminated at the dielectric boundary, where the $\mathbf{E} - Field$ is reduced to zero by an equal yet opposite polarisation field $\mathbf{P}$ in this example this occurs at a distance λ away from the cathode surface, the $\mathbf{P} - Field$ at this point is expressed as $\mathbf{P}(\lambda)$.It can be seen that polarisation occurs through the entire region and gas molecules will become polarised should they fall onto a flux line, these polarised molecules will produce further flux line attachments and form effectively a polarisation chain, but again the E-Field will remain zero within this area of polarisation, as shown.

On the right hand side of figure 4.6 the surface charge density is shown and the E-field that is generated from the charges. When the E-Field reaches the first polarisation charge,

which is of equal magnitude but opposite polarity, the E-Field reduced to zero ($E = 0$) within the polarised gas on that particular flux line.

4.3 Gauss' Law in One Dimension

As explained previously, each of the individual E-field flux lines may be irregular and vary in magnitude from flux line to flux line, but all of them will satisfy Gauss' law.

$$\nabla \cdot \mathbf{D} = \rho_f \tag{4.1}$$

Where $\mathbf{D}$ is the Displacement vector field, introduced in equation 3.3. The use of the $\mathbf{D}$-field is important as we are dealing with discontinuities in the field lines, this is accommodated for by the $\mathbf{D}$-field by the inclusion of the Polarisation vector field $\mathbf{P}$. Therefore in terms of the $\mathbf{D}$-Field the flux lines are continuous from cathode to anode.

Referring back to figure 4.6, at the intersection of the E-Field with the polarised gas molecule, although the E-Field is reduced to zero, the P-Field becomes established at this interface and allows the D-Field to remain constant over the various boundaries between the two plates.

As we are applying Gauss' law to an individual flux line as shown in figure 4.6 that has infinite permittivity, $\mathbf{D} = 0$ as $\epsilon\mathbf{E} = \mathbf{P}$. Also only a collection of individual flux lines are being treated here, this means that Gauss' law need only be considered in one dimension. The $\mathbf{E} - Fields$ that do not terminate in the dielectric and are able to span the entire gap between the electrodes have a non-zero $\mathbf{D} - Field$

Therefore from equation 4.1 we get.

$$\frac{d\mathbf{D}}{dx} = \frac{d}{dx}(\epsilon_0\mathbf{E} + \mathbf{P}) = \rho_f \tag{4.2}$$

$$\epsilon_0\mathbf{E} + \mathbf{P} = \int \rho_f dx \tag{4.3}$$

In its integral form, equation 4.3, Gauss' law is often stated as 'The net electric flux across (leaving) any closed surface is equal to the charge enclosed by that surface'.

4.4 Plasma Formation

Electrons may be liberated from the surface of metals via several different mechanisms. In 1905 Einstein explained the photo-electric effect by introducing the 'work-function' concept, whereby if light energy exceeding the work function of the metal was shone on to the metal, electrons would be released from the metallic surface. Thermal agitation has also been used to explain electron release from metals, in fact this is how electrons and electron plasma are formed in cathode ray tubes. Electricity is passed through a coil of wire, heating it up until enough energy is injected allowing the release of electrons from the coil itself. Another electric field is then applied to the electron plasma in order to accelerate the plasma toward a phosphorous screen to allow images to be projected. Electron Emissions from metal was first proposed by the Fowler-Nordheim theory, [47]. Lower energy mechanisms have been also proposed providing and alternate theory to that of Fowler-Nordheim, [48]. Lower still energy levels for electron emission from metals based on the surface roughness of the metal itself have been also proposed, [20].

Surface charges formed by the application of a voltage across two conductors or plates also experience a force due to the electric field that are formed by the charges themselves. This thesis makes the assumption that the electric field is strong enough to liberate electrons at a sporadic rate, randomly sourced from the electrodes where the surface charges have accumulated.

The theory here is that these random emission of electrons from the surface of the metallic plates, will, under certain conditions form plasma that will effectively extrude from the metallic cathode and track the electric field flux line towards the anodic plate. Many plasmas over many electric flux lines will attempt extrusion over a given flux line, all with equally low probability of successfully traversing the air gap over which the electric field flux line suspends.

The theory presented here explains the conditions that need to be met to allow plasma to form and extrude from the cathode to the anode metallic conductors, tracking an electric field flux line and resulting in partial discharge. In the next chapter a treatment of the minimum charge distribution over this traversing plasma will be given that would cause partial discharge. With an understanding of the charge distribution required for partial discharge, the electric field distribution may be analysed and thus the minimum voltage capable of partial discharge may be calculated.

To understand plasma formation a treatment of electron mobility under the conditions stated previously must be given. This is the topic of the next section.

4.4.1 Electron Mobility and Surface Charge Recombination

As explained previously, when a voltage is applied across two parallel plates a uniform electric field will be established. This electric field will comprise of many electric field flux lines joining the two plates, as we are considering here two uniform parallel plates it may be fair to assume that the lines of flux will also be parallel and uniform. However, should the electrode be non-uniform, so too will be the electric field between the electrodes. The electric field flux lines will no longer be equally spaced over the air gap and will be much closer together where the electric field is higher, which will be near to where the surface area of the electrode is smallest (e.g. sharp points or edges). But even with this non-uniform electric field all of the conditions presented in this thesis will apply and provide an explanation for partial discharge.

Each electric field line will be established by a collection of surface charges on both of the metallic plates. The strength of the electric field flux lines is inversely proportional to the length over which the flux line traverses, as per Gauss' law. As the electric plates form an equi-potential surface the voltage across any point on the plates will be the same, as one would expect. But as the electric field flux lines are of varying lengths, each varying flux line must also have a varying field strength and with shorter flux lines it necessarily follows that the field strength must be higher.

In order to support the varying field strength of the multitude of flux lines, varying surface charge densities at the end of each flux line must be present. Referring back to figure 4.4 where a solid uniform dielectric is depicted, there are two lengths of electric field flux line, this is obviously for illustrative purposes. All of the odd electric field flux lines

are shown with length λ and all of the even field flux lines are of length d. It therefore follows that the charge density of electrons at the surface of the cathode electrode, where the electric field flux line is λ will have a much higher concentration than those where the electric field flux line length is d.

The above explanation was given for a uniform solid dielectric, however, the explanation equally translates to that of a gaseous dielectric, the primary difference is that the varying length of the electric field flux lines will be much more varied, as too the variation in electron surface charge density distribution at the cathode electrode. What is important to note, is that once these flux lines are established the forces exerted by the electric field will be such that subsequent variation of the flux lines will be resisted and polarisation force field will help to retain the charge balance.

The electric field strength of the shortest flux line will be the highest, requiring the greatest quantity of surface electrons to support it. The forces exerted on these electrons will also be the greatest. So it seems reasonable to expect that should an electron be liberated from the surface of the cathode, that it will be more probable that the electron be from the area of highest concentration. There is still a finite probability that an electron could be liberated from the surface electrode of the lowest concentration, where the electric field flux line extends between both electrodes. This method of electron movement may go some way to explaining the plateau current I_0 shown in 3.2.

What is being presented here is more substantial discharge, greater than that of many 'single' electrons passing between electrodes, but by no means great enough to be considered as electric breakdown and effectively connect the two electrodes by a very intense

plasma, as explained in Chapter 3. Here the build up of plasma on a single flux line is being considered, that has been able to build up and traverse the gap between the electrodes to cause a discharge.

Once a surface charge electron has been liberated from the surface of the electrode it will accelerate under the influence of electric field in which it resides. The path of its trajectory will be that of the electric field flux line, which in the case of two uniform parallel plates will be a straight line. The electron will accelerate until it either collides with the anode electrode, or it collides with a polarised molecule.

Once an electron is emitted from the cathode electrode, Gauss' law must still apply and if the electron remains on its original electric field flux line then this is satisfied. If, however, the accelerating electron collides with a polarised gas molecule and is not recombined, then its resultant trajectory will be unknown. This electron is no longer in it original electric field flux line, but is still under the influence of the electric field and it seems reasonable to expect that the electron will attach itself to another flux line as this will provide the strongest attraction to a free electron. In this situation, however, Gauss' law is no longer satisfied!

If a given electric field flux line looses an electron, then the voltage across that flux line must reduce. Whereas the flux line that increases its electron count must also have a higher voltage across it. The fact that both of these flux line are connected to the same cathode electrode, which is an equi-potential surface, means that this situation cannot remain.

Gauss' law can remain consistent if surface charge re-distribution takes place. The mobility of the charge carriers in the metallic cathode electrode is extremely high, which will allow the surplus electron from the one flux line to migrate to the flux line that is currently in deficit. This may be shown below in figure 4.7.

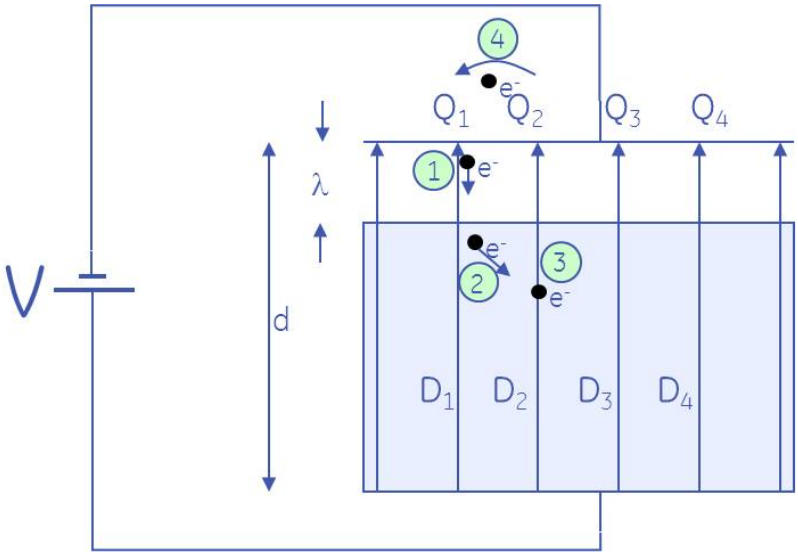

Figure 4.7: Motion of liberated charge collisions and surface re-distribution for charge balance.

The above figure shows the motion of an electron colliding with polarised molecules and the processes required to bring stability to the charge balance equilibrium, prior to the collision. The motion has been broken down into four activities, which will be described below.

1. An electron is liberated from the cathode electrode by the electric field and is accelerated under the influence of this electric field along its electric field flux line until it collides with a molecule as the polarisation boundary layer.

2. After the collision at the polarisation boundary layer the trajectory is undefined,

but will be attracted to an adjacent electric field flux line.

3. After an undefined period of time the electron will converge on a flux line that is not the original, causing an charge unbalance and temporarily violating Gauss' law.

4. Surface charge re-distribution will take place, in order to restore balance to the electric field flux lines as too Gauss' Law.

From the above it can be seen that if a liberated electron remains on it own flux line then no re-distribution of surface charge carriers is required, however, if it does not and falls into another flux line, then surface charge re-distribution will restore the charge density of the original flux line to its original condition, permitting the whole event to be repeated.

With the restoration of surface charges replacing ones that have been lost due to collisions at polarisation boundaries. It follows that electrons that have been liberated from the cathode electrode may remain free but confined to its electric field flux line. Over time, as this process is repeated a greater charge density of free electrons will be created, allowing a plasma to result, as shown below.

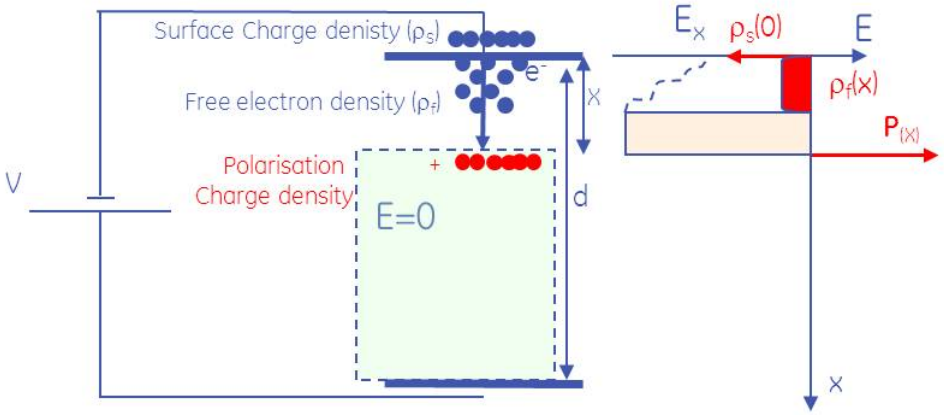

Figure 4.8: Plasma formation due to collisions and surface charge re-distribution in 1-D.

On the right hand side of figure 4.8 the $\mathbf{E} - Field$ is shown. The surface charge is still given by $\rho_{(0)}$, however, there is less surface charge density here compared to 4.6. This reduction is due to liberated electrons from the electrode surface being now present between the cathode and the dielectric boundary. These now free electrons are represented by ρ_f. Over the distance where these free electron density are present the $E - field$ will rise due to the accumulation of surface and free charges. x is the variable distance quantity between the the two electrode plates, therefore the $E - Field$ at any point from the cathode is E_x. At the point were the free charges cease the $E - Field$ will no longer rise and will remain at this $E - Field$ strength until the $E - Field$ attaches at the dielectric boundary at a distance x. At x there will be a polarisation field P_x which will have equal but opposite magnitude to the original $E - Field$ at this point the $E - Field$ will reduce to zero.

4.4.2 Dielectric Penetration

The previous section describes what will happen should an electron fall into another electric field flux line, however, no account has been given to the situation where an electron penetrates into the dielectric material after a collision has taken place. Electrons are not confined to field lines of electric field alone, within the dielectric material the electric field (**E**) is zero, however, the polarisation field (**P**) is present and together they form the Displacement vector field (**D**) and it is permissible for electrons to be present over the whole **D**-Field.

The electric field distribution brought about by the plasma formation will now vary as it is no longer formed solely by the collection of surface charges but rather by surface charges and plasma distribution, as shown below.

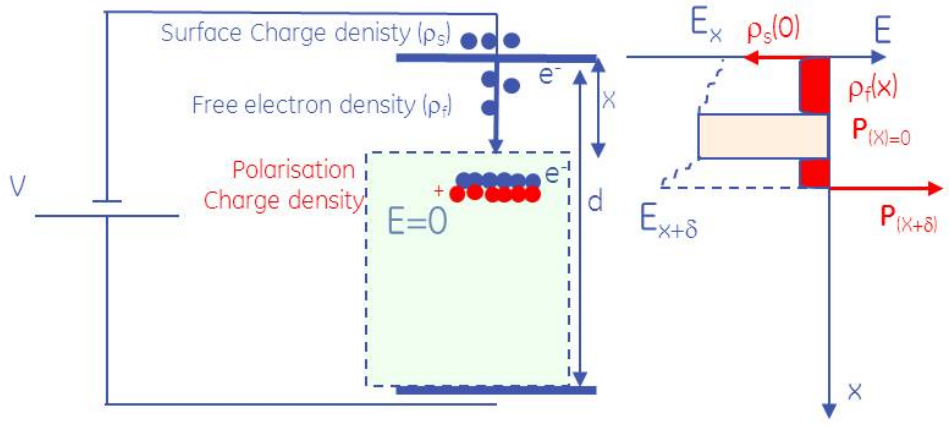

Figure 4.9: E-Field distribution formed by surface charges and plasma

On the right hand side of figure 5.2 the $\mathbf{E}-Field$ is shown. The surface charge is still given by $\rho_{(0)}$, however, there is less surface charge density here compared to 4.6. This

reduction is due to liberated electrons from the electrode surface being now present between the cathode and the dielectric boundary. These now free electrons are represented by ρ_f. Over the distance where these free electron density are present the $E - field$ will rise due to the accumulation of surface and free charges. This figure is illustrating that the charge density of free electrons ρ_f is discontinuous and non-uniform, it also shows electrons being present within the dielectric material. Therefore over the distances where free electrons are present the $E - Field\ E_x$ rises due to the accumulation of these free charges, however, over the small gap prior to the dielectric boundary X no free electrons have been shown, it is over this distance where the $E - Field$ remains constant. As free charges are now present within the dielectric material where $X \leq x \leq X + \delta$, the E-Field will rise further over this distance to $\mathbf{E}_{X+\delta}$, but will be reduced to zero when the flux line encounters a $P - Field$ of equal but opposite magnitude $\mathbf{P}_{X+\delta}$.

But as stated previously, it is permissible for the plasma to penetrate the dielectric and if only a small percentage of the overall charge distribution (i.e. surface + plasma) were to penetrate the dielectric, multiple electric field distributions may result due to the distributed polarisation field and charge distribution, as shown below in figure 5.1.

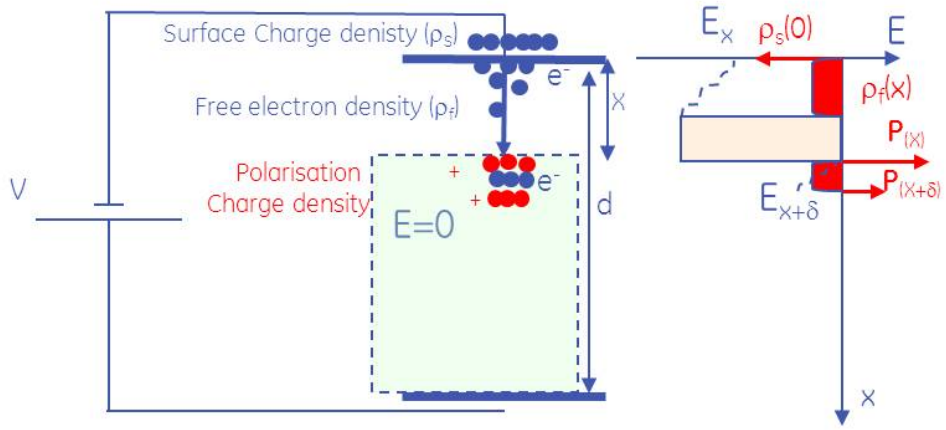

Figure 4.10: E-Field distribution with plasma penetrating into the dielectric

The above figure shows that with the plasma penetrated into the dielectric material, the quantity of charge nearest the cathode is now reduced, therefore the magnitude of the polarisation field at the initial polarisation boundary is also reduced. The plasma that is now within the dielectric material begins to form a new electric field from the penetrated charge distribution, however, this will only be neutralised by the a subsequent polarisation field further into the dielectric material.

On the right hand side of figure 5.1 the $\mathbf{E} - Field$ is shown. The surface charge is still given by $\rho_s(0)$, however, there is less surface charge density here compared to 4.6 as explained previously. The free electrons ρ_f now appear in both the vacuous space between the cathode and the dielectric boundary and also further penetrated within the dielectric material. Therefore over the distance $0 \leq x \leq X$, E_x can be seen to rise over the distances that free electrons are present, however $E_X = 0$ due to the $P - Field$ at the boundary of the dielectric. Due to the penetrated electrons within the dielectric material the $E - Field$ will begin to rise again over the distance $X \leq x \leq X + \delta$ until the $E - Field$

is again reduced to zero by the polarisation field $\mathbf{P}_{(X+\delta)}$. The $E-Field$ over the distance $0 \leq x \leq X+\delta$ can now be seen as discontinuous as it is reduced to zero twice of this distance.

It is one of the topics of the next chapter to explain how this plasma may continue to form and erode the dielectric material away over a given electric field flux line allowing partial discharge to result.

Chapter

5 Proposed Theory of Partial Discharge

5.1 Plasma Formation

When a voltage is applied across two electrodes, it is understood that an electric field will become established between them. This $E-field$ will apply a force to the various molecules forming the dielectric, causing polarisation. The strength of the polarisation force will depend on the distance over which the $E-field$ sub-tends to a particular point on the dielectric boundary, as shown in figure 4.5. If the polarisation force is sufficient to polarise the dielectric molecule such that a dipole is formed, $E-Field$ flux line attachment may be achieved. It is in the areas of high $E-Field$ strength that the polarisation force will be sufficient to form dipoles permitting attachment. The areas of the highest $E-Field$ strength are were the flux lines are of the shortest distance. It is in these areas only, where this thesis will concentrate as these are the areas were the most forces will be experienced by both the electrons that happen to be present in this area and the dielectric.

In other words, what is trying to be described here is that of the whole surface area

of the electrodes, where on average the $E-Field$ across the gap is of moderate value polarising the dielectric material to a lesser extent, providing a positive non-zero $D-Field$. Small areas of high electric field strength will exist providing enough force to polarise the dielectric molecules allowing dipoles to form. This is actually a simultaneous event as it is the presence of a dipole near to the electrode that forms an $E-Field$ of greater intensity. These areas of high $E-Field$ strength may only be small in number compared to the total area over which the $E-Field$ is present, however, these concentrated areas will act as the thoroughfares through which packets of electrons will pass between electrodes causing partial discharge, as will be described in the rest of this chapter. As the polarisation force is equal but opposite to the electric field strength, the $D-Field$ will equal zero over these areas, as $\mathbf{D} = \epsilon_0\mathbf{E} + \mathbf{P}$. It is these small quantities of $D-Field$ flux lines of which $\mathbf{D} = 0$ that figure 4.7 is illustrating and it is over these few $D-Field$ flux lines which have the highest $E\&D-Field$ strength where electrons will experience the most force.

As explained in chapter 4 if an **E**-field of sufficient strength is formed between two electrodes, electrons may be liberated from the cathode electrode and accelerated towards the anode following the direction of whichever **E**-field flux line the electron was liberated from. If, however, this electron collides with a polarised particle, such as an air molecule and as a result of the collision the electron veers off onto another flux line, surface recombination will effectively reset the event allowing the whole event to occur again. If on the other hand the electron remains on its original flux line post collision, then just a redistribution of the E-field will take place, this can be better shown when considering many of these events occurring in a short space of time, or even concurrently, as shown in figure 4.8. It is also feasible that figure 4.8 could also be as a result of dispersive collisions

from neighboring flux lines converging on the flux line shown here.

Non-dispersive collisions will result in electrons penetrating the dielectric and will thus provide a discontinuous non-linear **E**-field distribution, provided again here for completeness.

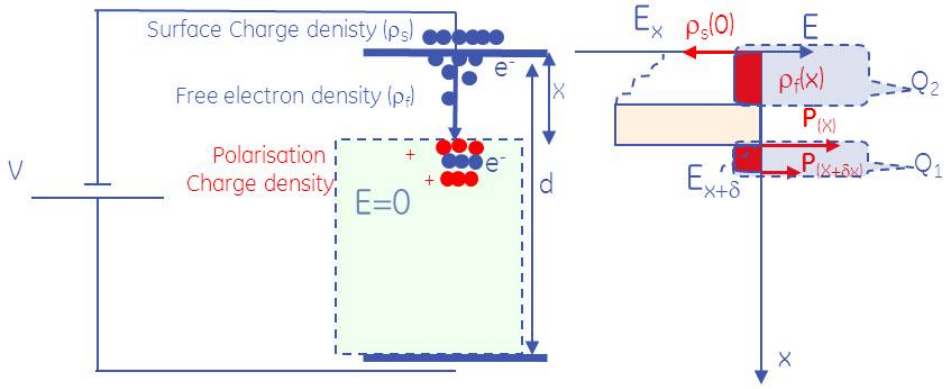

Figure 5.1: E-Field distribution with plasma penetrating into the dielectric

The discontinuous **E**-field distribution is brought about because the polarisation charges at the surface of the dielectric will provide equal yet opposite charge polarity and reduce the E-field to zero. Only the electrons that have penetrated the dielectric material will allow the E-field to rise again, but only until further polarised molecules bring the E-field back to zero, for the remainder of the **D**-Field. Investigating further how the charge distribution can transition the **E**-field from discontinuous to continuous and effectively erode the dielectric away is the subject for the next section.

5.2 Dielectric Erosion due to Plasma Formation

Referring to figure 5.1, the reason why any polarisation field is present is because a charge distribution (in this case formed by electrons) is greater one side of the electrolyte than the other, this in turn produces an E-field which will cause the electrolyte to become polarised and generate an equal but opposite P-field. Referring again to figure 5.1 if the charge between $Q_1 = \int_X^{X+\delta x} \rho(x)dx$ be equal or greater to the charge between $Q_2 = \int_0^X \rho(x)dx$, then there is no **E**-field difference at X to allow polarisation, then the polarisation field at X, P(X) will equate to zero or no longer contribute to the E-field distribution and allow it to be considered continuous across the original boundary as shown in figure 5.2. In the case of $Q_1 > Q_2$ the polarisation at X will be in the opposite direction to that previously described, however, in this direction no $E - field$ attachement will be possible making a continuous, un-interrupted $E - field$ formation again as shown in figure 5.2

It is by this mechanism that the dielectric will become eroded. Therefore, should enough electrons penetrate a dielectric boundary, such that the total charge within the dielectric material is equal to or greater than the total charge between the dielectric and the cathode electrode, then the original dielectric boundary will be altered as shown below in figure 5.2.

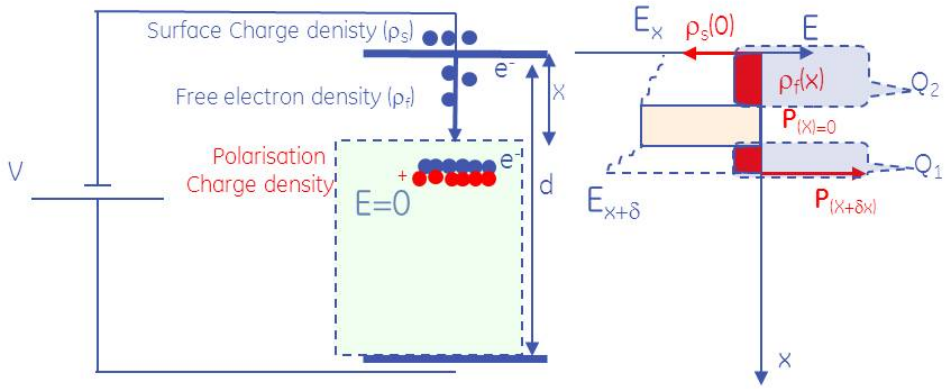

Figure 5.2: E-Field distribution with plasma penetrating into the dielectric

The above figure shows that the original dielectric boundary (shown by the dotted lines) has effectively been moved by a distance δ due to the charge distribution within the dielectric, neutralising the dielectric boundary layer polarisation charge and forming a new boundary layer a distance δ further in. It must also be noted that the E-field is now continuous due to this charge distribution.

5.2.1 Charge Distribution Criteria

The polarisation field may be neutralised by a given charge distribution provided a key criteria is met and that is; at any point in the electron charge distribution the total electron charge furthest away from the cathode must be equal to or greater than the total electron charge distribution nearest the cathode, in short $Q_1 \geq Q_2$ no matter where x_1 is located, as shown in figure 5.3 below.

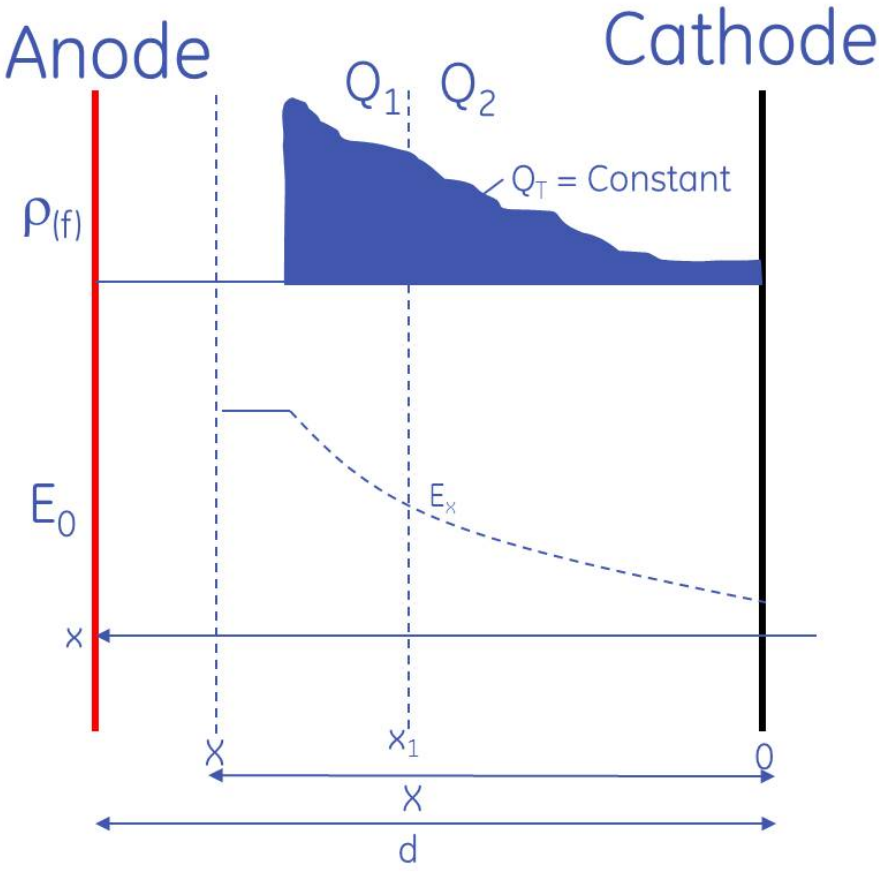

Figure 5.3: Charge distribution penetrating the dielectric whilst maintaining $\mathbf{P} = 0$

The above figure is a 1-D plot taken on a particular cut through what has previously been described in 2-D. The actual scenarios depicted are in reality 3-D as we are discussing areas of high $E - Field$ where $\mathbf{D} = 0$, however, the analysis is able to be performed in one dimension, due to the symmetry of cylindrical polar co-ordinates in this case.

From the above figure;

Q_T =Total electric charge

λ =mean free path of air

x =variable distance from cathode

E_x =Electric field strength at any distance x from the cathode

d =total distance between electrodes

X =distance from cathode to boundary layer of dielectric material

x_1 =Arbritary distance within X

$\rho_{(f)}$ =charge density of free electrons

For the Polarisation field **P** to remain zero between the distances 0 to X, (i.e. $0 \leq x_1 \leq X$) the condition $\int_{x_1}^{X} \rho(x) \geq \int_{0}^{x_1} \rho(x)$ must be satisfied, where x_1 is an arbitrary point within the plasma.

The plasma may further migrate towards the Anode provided the above condition is satisfied and all of the previous arguments hold until the charge plasma reaches the anode at which point a conduction path will exist between the Anode and the Cathode and Gauss' law will no longer apply on that flux line. At this point the E-field will collapse, the plasma will begin to disperse and subsequentaly the conduction path will now be broken (I = 0), which will allow the E-field to be re-established and the previous condition of the plasma will be restored. The theory being presented here details the minimum conditions that must have been met just prior to the collapse of the E-field allowing conduction between the Anode and Cathode. As the collapse of the E-field is only temporary but repeatable this may be the mechanism by which partial discharge could be attributed.

5.2.2 Limitation of Plasma Length Formation

The furthest distance that the plasma may traverse the gap between the electrodes without reaching the Anode is shown in Figure 5.4 below.

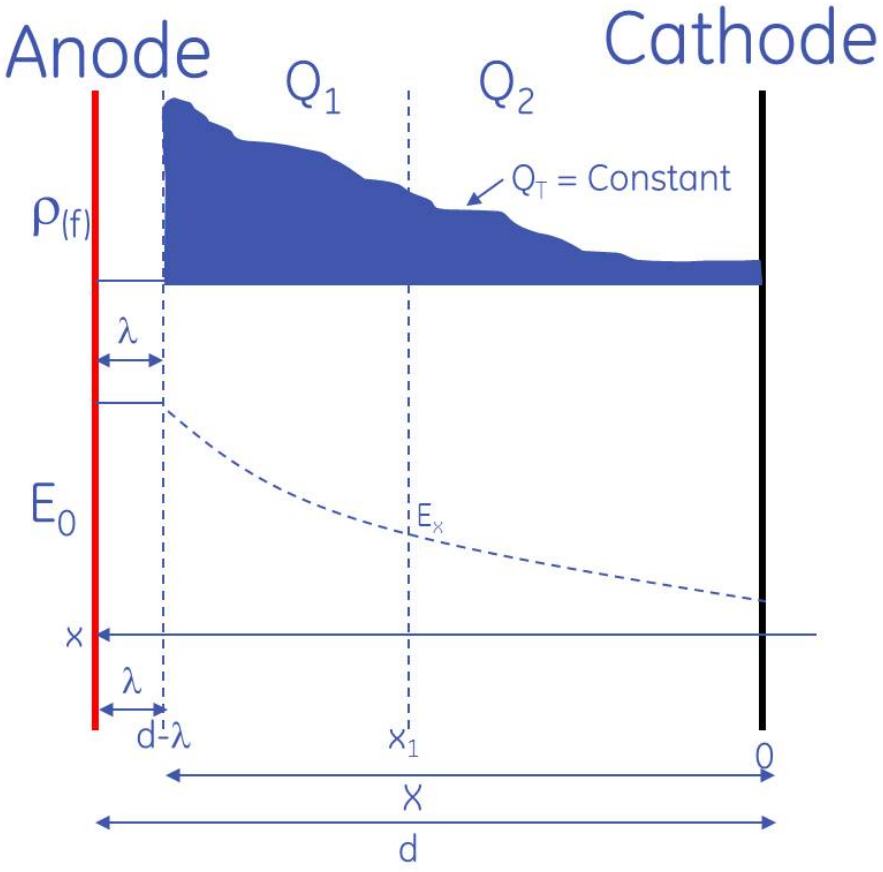

Figure 5.4: Plasma charge distribution immediately prior to partial discharge

The smallest gap that can be realised between the plasma and the Anode is given by 'λ', which is the mean free path that an electron can travel before it will collide with another molecule, for a gas this is given by [49];

$$\lambda = \frac{kT}{p\sigma} \tag{5.1}$$

Which derives from the ideal gas law

Where;

k is Boltzmann's constant

T is Absoulute Temperature kelvin (k)

p is pressure(Pa)

σ is the collision cross sectional area of the gas (m^2)

Therefore the maximum length that the plasma can traverse between the two electrodes is one 'mean free path' (λ) less than the total gap (d)

i.e. Maximum Plasma length = $d - \lambda$, however, the E-field must be calculated over the whole gap d, as the $E - field$ is still present over the vacuous final mean free path λ, as shown in figure 5.17 above.

5.2.3 Atomic Polarisation

Under normal conditions a neutral un-polarised atom is represented by a spherical electron cloud, centered on a proton nucleus, as shown below;

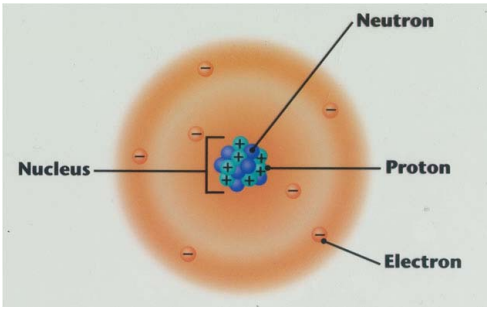

Figure 5.5: Classical representation of neutral atom

When the neutral atom is exposed to an electric field, polarisation is accounted for by applying a shift in position of the positive nucleus, brought about by the force applied to it by the polarising electric field, this can be seen in Figure 5.6 below.

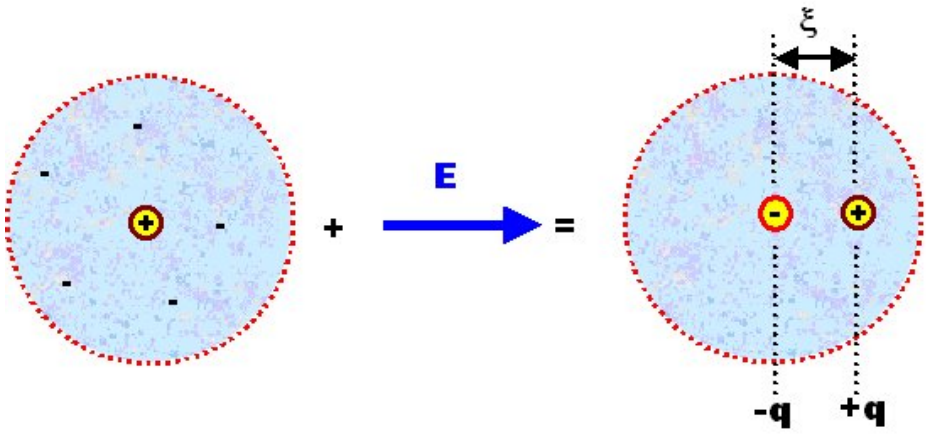

Figure 5.6: Classical representation of atomic polarisation

Figure 5.6 is also used to describe atoms such as hydrogen, which comprises of one electron and one proton. If, however, we consider an electron near the hydrogen atom, the electron will experience a repulsive force brought about by the electron 'cloud' enveloping

the positive nucleus as shown below in figure 5.7.

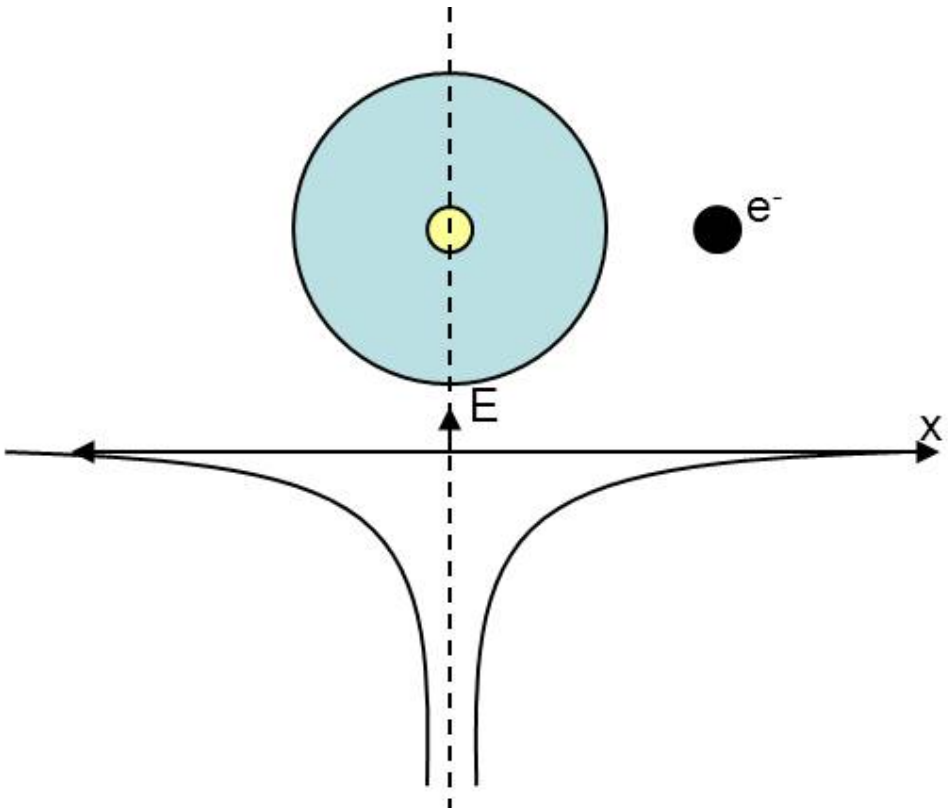

Figure 5.7: Repulsive force experienced by nearby electron.

If we now expose the nearby free electron and the hydrogen atom to an external applied E-field, the electron will be accelerated due to the applied E-field and the hydrogen atom will become polarised, as shown in Figure 5.8.

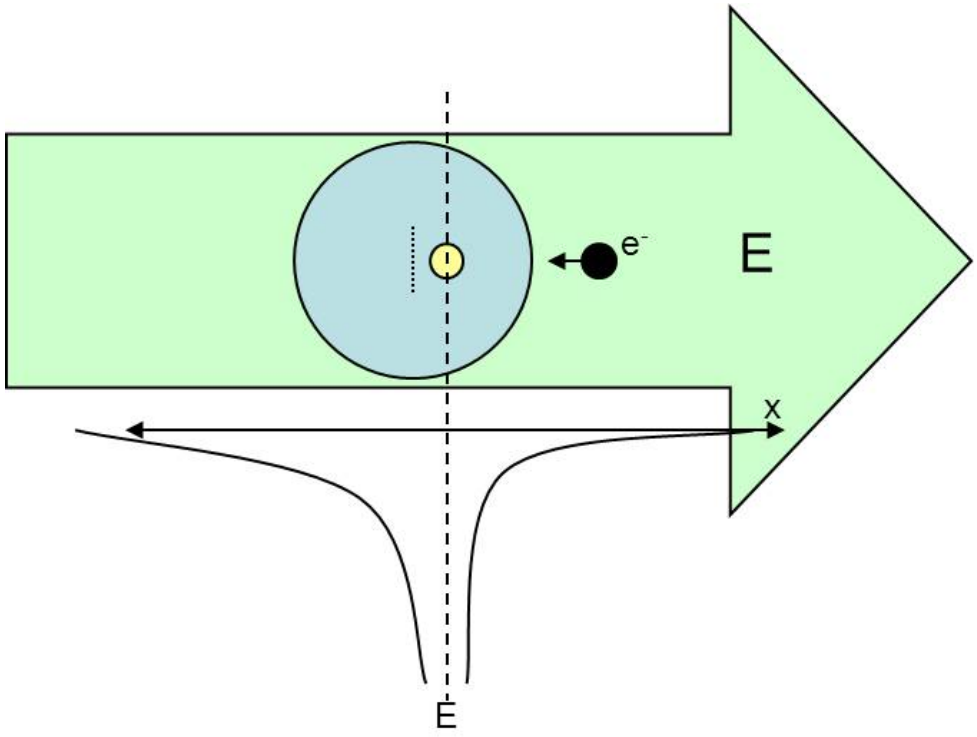

Figure 5.8: Atom and electron exposed to external applied E-field.

From Figure 5.8 it can be seen that the accelerating electron will always experience a repulsive force, but this cannot always be the case as hydrogen only has one electron.

Quantum mechanics predicts that the above is true 'on average', 'over time' and it is from this point that a consistent alternate interpretation may be given.

If we again consider the hydrogen atom, at any instant in time (or event) a dipole moment (μ) will be observed, by the positive nucleus and its negative electron, as shown below in Figure 5.9. $\mu = ql$, where q is charge and l is the distance separating the two charges.

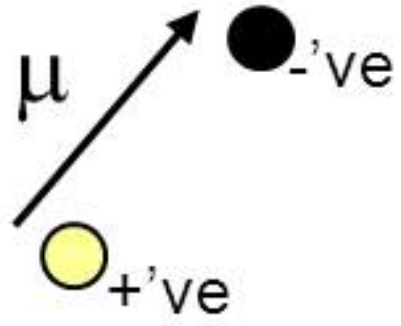

Figure 5.9: Dipole moment event in hydrogen.

At any subsequent event the dipole moment vector will appear random in orientation with an equal probability of occurrence.

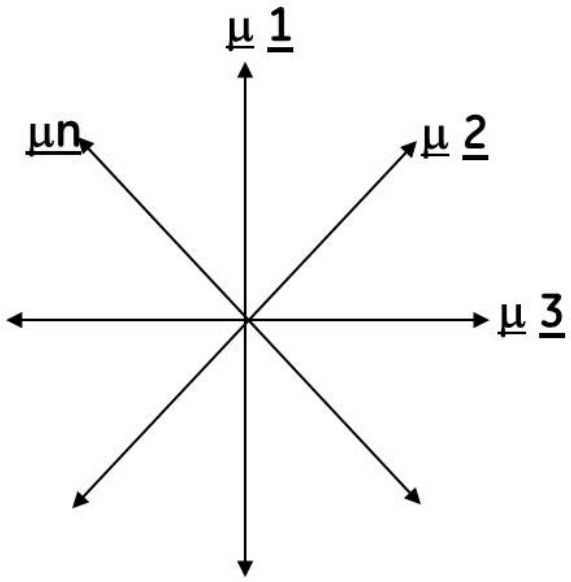

Figure 5.10: Dipole probability distribution of hydrogen atom.

Therefore referring to figure 5.5 and applying the dipole moment as illustrated in 5.10 to that, we arrive at an alternate description and that is the neutral atom must have an equal probability of a dipole moment occurring in all directions, but at any given time or event on one will exist. The dipole moments being of equal magnitude and probability will give rise to a spherical shape, as shown above in Figure 5.10.

If the probability distribution of the hydrogen atom is now considered when an external E-field is applied, then it maybe reasonable to accept that the distribution may be skewed due to the applied E-field, as shown in Figure 5.11.

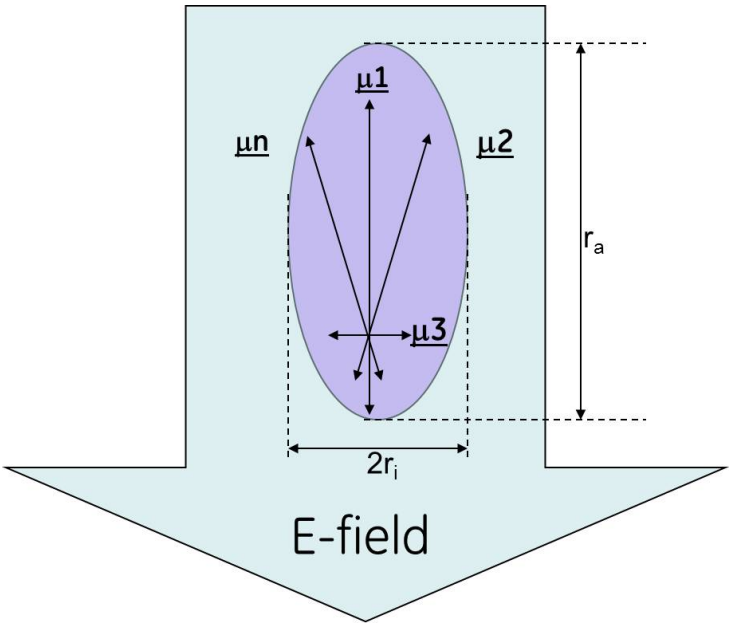

Figure 5.11: Dipole probability distribution of hydrogen atom when an external E-field is applied.

where r_a is the atomic radius, and r_i is the ionic radius

From Figure 5.11 it can be seen that the polarised atom now has a higher dipole moment probability of occurrence in a direction opposite to the applied E-field. Also the

probability of occurrence in a direction orthogonal to the applied E-field is also reduced.

5.2.4 Atomic Polarisation & Torque

The previous interpretation may also be used to explain the dipole moment shown in Figure 5.6. The only difference being that the interpretation here results in a reduction in the radius of the atom in a direction orthogonal to the direction of the applied E-field. In the extreme case the atomic radius (r_a) may reduce to that of the ionic radius (r_i), in the orthogonal direction as shown in Figure 5.12.

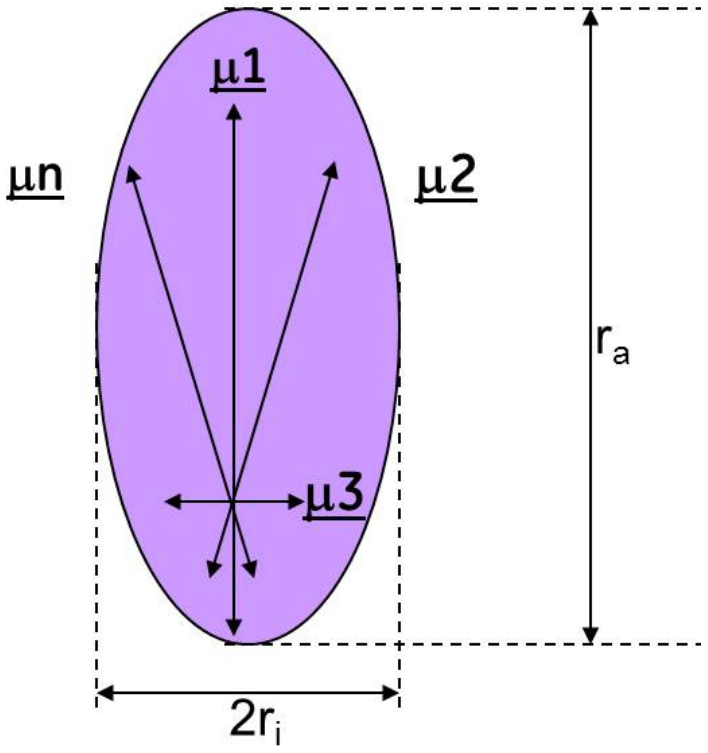

Figure 5.12: Representation of extreme polarised atom.

From Figure 5.12 it must also be noted that the dipole shown will also experience torque between the applied E-field and the dipole moment when the angle between them is greater than 0^o. Also the reason the length of the dipole moment is the atomic radius (r_a) and not $2r_a$ is because the applied E-field has only increased the probability that atoms electrons will occupy a much smaller region of the allowed eigen-distances between the atomic nucleus and its outer electrons.

Another point to note is that if the dipole experiences torque, then the pivot point on the dipole will no longer necessarily be the nucleus. In fact, the nucleus will also experience the torque resulting in the pivot point being at the mid-point, this may be shown in Figure 5.13 below.

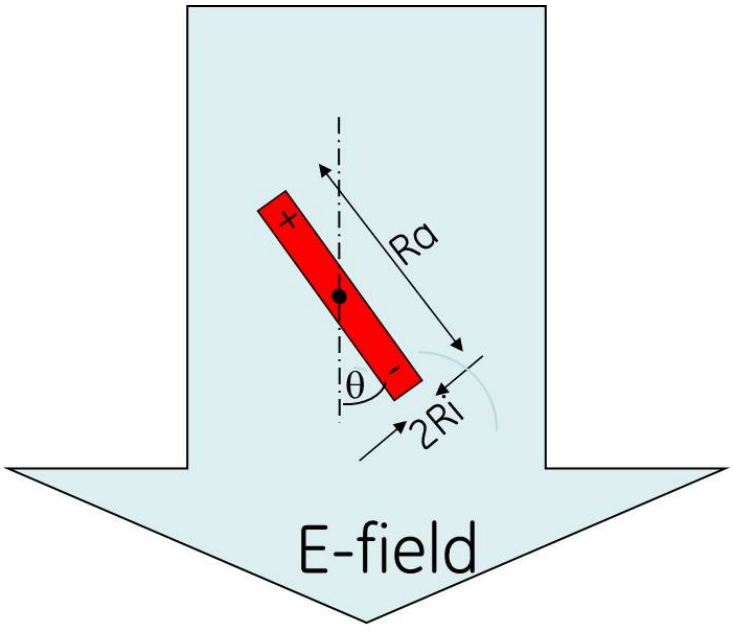

Figure 5.13: Torque moment of polarised atom in applied external E-field.

Where

$$\tau = -\mu \mathbf{E} \sin\theta \tag{5.2}$$

5.2.4.1 Dipole Oscillation

Polarised air molecules will experience torque moments causing it to align with the applied $E - field$, however, due to the inertia of the polarised molecule, an oscillation will occur. Over time however, if this situation remains unchanged it is reasonable to assume that the oscillation will be damped and the oscillation will ultimately cease. As described previously the situation does not remain the same, in fact the plasma formation will provide continuous changes as it propagates from the cathode to the anode.

As the plasma erodes its way through the dielectric, the $E - field$ will cause new dipoles to begin to oscillate and because the magnitude of the $E - field$ over which the dipoles will oscillate does not change, due to charge re-distribution. The frequency of oscillation will be constant.

The reason why the magnitude of the $E - field$ remains unchanged over the distance where the dipoles will oscillate due to charge re-distribution, is as a consequence of electron mobility and surface charge recombination as described in section 4.4.1. In short as the total charge forming the $E - field$ that is being considered by this thesis is finite and constant, it necessarily follows that the $E - field$ itself being emitted from the plasma must also be finite and constant. Provided the charge distribution criteria is met as described in section 5.2.1.

The oscillation of a dipole at any given event as the plasma propagates will be gov-

erned by the following standard equations;

$$I\ddot{\theta} = -\tau\theta \tag{5.3}$$

$$\omega_o^2 = \frac{\tau}{I} \tag{5.4}$$

Where;

I is inertia (kgm^2)

θ is angular momentum (Nms)

τ is torque (Nm)

ω_o is Natural harmonic frequency of the dipole oscillations (Hz)

In order to find the minimum E-field required for the electron to traverse the gap (λ), the maximum time possible must be calculated for the dipole oscillation and this can be shown to be the time it takes for the dipole to oscillate between $\theta = 0$ radians, which in fact is twice the natural harmonic frequency of the dipole, i.e. $4\ddot{\theta} = \frac{\tau}{I}$.

When considering Electric dipoles and fields over the final gap (λ) these further equations must also be taken into consideration.

$$\tau = \mu \times \mathbf{E} \tag{5.5}$$

$$U = -\mu \cdot \mathbf{E} \tag{5.6}$$

Which gives;

$$\tau = \mu E \theta \tag{5.7}$$

$$\tag{5.8}$$

For small θ

The dipole is oscillating in an $E-field$ between the end of the plasma and the Anode, as shown below in figure 5.14.

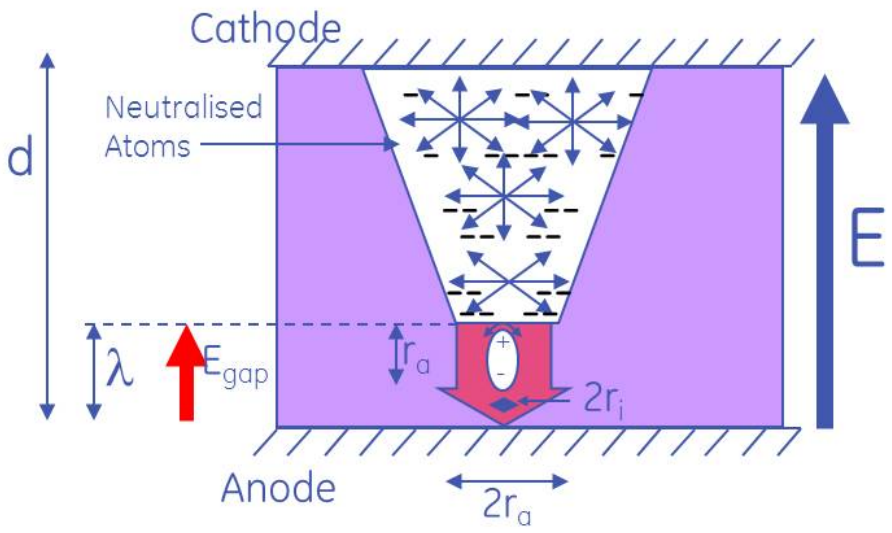

Figure 5.14: Depiction of plasma and final polarised air molecule, where capacitance is formed over the final distance λ from the anode

The energies that are present between the plasma and the anode may be understood relating to figure 5.14. It is therefore reasonable to assume that a capacitance is formed across the final gap λ, the energy U stored in this gap is given by;

$$U = \frac{CV^2}{2} \tag{5.9}$$

Where C is the capacitance of the air gap λ which may be expressed as:

$$C = \frac{\epsilon A}{\lambda} \tag{5.10}$$

The inertia of the dipole of a dipole pivoting about its centre may be expressed in standard form as;

$$I = \frac{m r_a^2}{12} \tag{5.11}$$

Referring again to figure 5.14, the diameter over which the capacitance is formed is given by the diameter $2r_a$, which is the width of the unpolarised molecules which has been realised due to the plasma formation. Therefore the area (A) of this capacitance is given by $A = \pi {r_a}^2$, where r_a is the atomic radius.

The mass m in equation 5.11 may be expressed in terms of the gas density ρ and volume V, $m = \rho V$ where $V = \pi {r_i}^2 \lambda$. Where r_i is the ionic radius of the molecule. Referring again to figure 5.14 as the dipole is formed by that of a polarised molecule, therefore the area that it subtends ($\pi {r_i}^2$)is much reduced when compared to that of an unpolarised gas molecule ($\pi {r_a}^2$)

Where;

μ is the dipole moment (Cm)

V is Voltage (V)

C is Capacitance (F)

I is moment of inertia (Kgm^2)

ρ is the gas density (Kgm3)

m is mass (Kg)

ϵ is permittivity (Fm^{-1})

r_a is Atomic radius (m)

U is potential energy (J)

As we are attempting to find the conditions necessary for an electron to travel a distance λ in the time that it takes a dipole to oscillate between angles of $\theta = 0^o$ relative to the $E - field$, then we must include the fact that the frequency of $\theta = 0^o$ is twice the natural harmonic frequency of oscillation. Applying this to equations 5.3 gives.

$$4{\omega_o}^2 = \frac{\tau}{I} \tag{5.12}$$

Combining equations 5.7, 5.9 gives;

$$\tau = \mu E = \frac{CE^2\lambda^2}{2} \tag{5.13}$$

Therefore continuing from equation 5.12 we get;

$$4{\omega_o}^2 = \frac{\tau}{I} = \frac{1}{2} \times C \times \frac{1}{I} \times E^2\lambda^2 \tag{5.14}$$

$$= \frac{1}{2} \times \frac{\epsilon\pi {r_a}^2}{\lambda} \times \frac{1}{\frac{\rho\pi {r_i}^2 \lambda\pi {r_a}^2}{12}} \times E^2\lambda^2 \tag{5.15}$$

$$\tag{5.16}$$

Which reduces down to

$$\omega_o = \sqrt{\frac{6\epsilon E^2}{4\rho\sigma}} \tag{5.17}$$

Where ρ is the density of air (Kgm^{-3}) and $\sigma = \pi {r_i}^2$ (m^2)

Expressing the above equation in terms of periodic time is provided in equation 5.18 below.

$$t = \frac{1}{E}\sqrt{\frac{8\pi\rho\sigma}{3\epsilon}} \tag{5.18}$$

5.2.4.2 Air Decomposition

Composition of Dry Air

Substance	% by volume
Nitrogen, N_2	78.08
Oxygen, O_2	20.95
Argon, Ar	0.93
Carbon dioxide, CO_2	0.033
Neon, Ne	0.0018
Helium, He	0.00052
Methane, CH_4	0.0002
Krypton, Kr	0.00011
Nitrogen(I) oxide, N_2O	0.00005
Hydrogen, H_2	0.00005
Xenon, Xe	0.0000087
Ozone, O_3	0.000001

Figure 5.15: Composition of Air

From the above table it can be seen that Nitrogen is the most abundant element in air at 78.084 %, therefore for the purposes of analysis details will be taken from this element.

5.2.4.3 Nitrogen

Referring to figure 5.13, when the Nitrogen molecule is polarised, the probability for dipole moment events occurring orthoganol to the E-field is much reduced, in the limit removed. So too is the probability for moment events to occur in line with the E-field.

It is therefore reasonable to suggest that the width of a polarised Nitrogen molecule is reduced to twice it's ionic radius r_i, however, it's length will be that of it's Atomic Radius r_a.

For Nitrogen the Atomic radius (r_a) is 65nm and the Ionic radius (r_i) is 30nm [50]

5.3 Atomic Stresses in an Electric Field - Electron Ballistics

An electron of charge (e) will experience a force in the presence of an external applied E-field. The force experienced by the electron is given by.

$$\mathbf{F} = e\mathbf{E} \tag{5.19}$$

The work exerted on the electron will give rise to acceleration, as described by the

equations below;

$$\mathbf{F} = m_e\ddot{x} \tag{5.20}$$

$$e\mathbf{E} = m_e\ddot{x} \tag{5.21}$$

Thus

$$\ddot{x} = \frac{e\mathbf{E}}{m_e} \tag{5.22}$$

Integrating twice with respect to time and assuming $x_{(0)} = 0$ gives;

$$x = \frac{eEt^2}{2m_e} \tag{5.23}$$

5.4 The Minimum Conditions for Partial Discharge

The minimum conditions that will result in a partial discharge are enough liberated electrons from the cathode electrode to form a plasma. The charge distribution forming the plasma will allow a continuous E-field to result, the criterion for this will be analysed in the next sub-section. The plasma will extend to within one mean free path (λ) of the gap separating the electrodes.

For the minimum conditions to cause partial discharge the resultant E-field strength must be such that an electron accelerating under the influence of this E-field must traverse the final distance (λ) in the maximum amount of time. This time can be calculated as the maximum time to cause non-dispersive collisions.

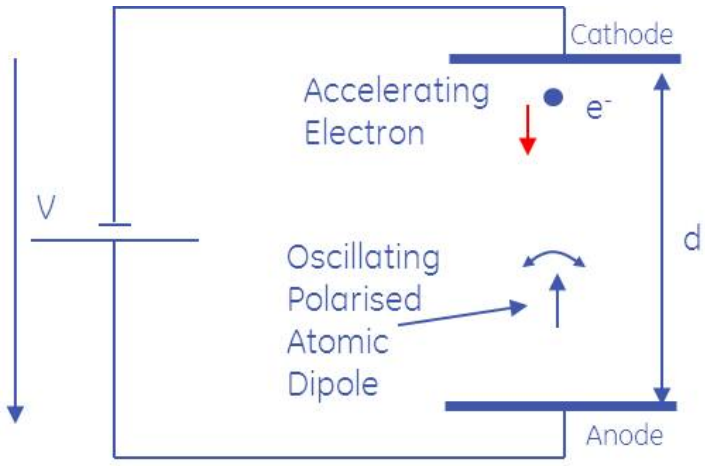

Figure 5.16: Experiment depicting accelerating electron colliding with polarised atomic dipole

The above figure may be used to illustrate this point. If the accelerating electron is to remain within a given $E-field$ strength represented by a flux line that it currently is being influenced by, after it collides with the polarised oscillating molecule, (i.e. non-dispersive collisions), then only collisions when the polarised molecule is in line with the flux line itself will allow non-dispersive collisions to occur. Even under these conditions there is only a small probability that the electron will tunnel through the polarised molecule.

As we are attempting to find the minimum $E - field$ that will accelerate an electron over the distance concerned and thus give the maximum time for an electron to accelerate over one mean free path (λ), between oscillating dipoles. Assuming acceleration begins from standstill, this will be achieved over one period of oscillation between angle of $\theta = 0$ as expressed by equation 5.18.

Therefore combining equations 5.23 and 5.18 will give the following result;

$$E\lambda = \frac{4\pi\rho\sigma e}{3m_e\epsilon} \tag{5.24}$$

where;

$\sigma = \pi r_i^2 \ \ (m^2)$

r_i = Ionic radius of molecule (m)

Here the term $E\lambda$ is a measure of the voltage V across the gap λ and as we are calculating the minimum $E - field$ required to achieve this condition, we are inadvertently deriving the minimum voltage required for partial discharge.

5.4.0.4 Charge Distribution

The above analysis covers the electron interactions over the final distance (λ) which is the mean free path between collisions in a gas. Here the analysis is going to look at the plasma itself that will result in a continuous $E - field$ over the length of the plasma thereby forcing the P-field to be zero within the plasma. The resultant E-field must be the minimum required as described above.

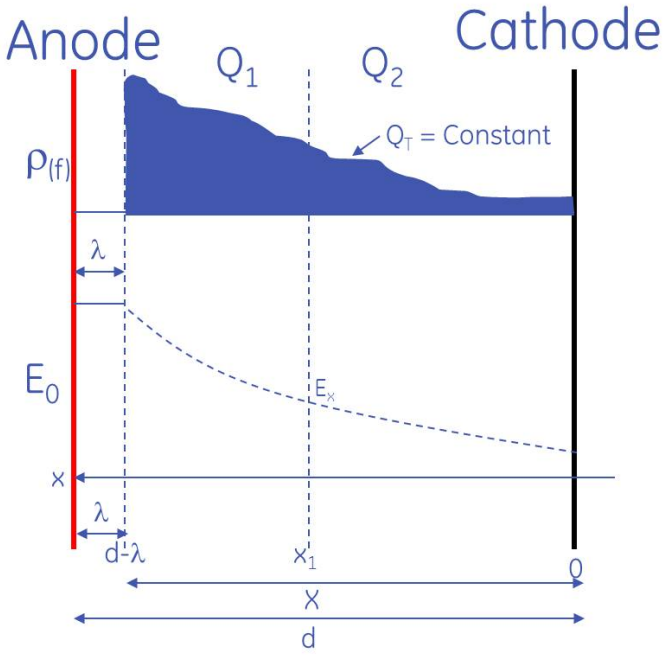

Figure 5.17: Charge distribution capable of ensuring **P**=0 within the plasma

To ensure that the polarisation field **P** is equal to zero within the plasma the below criteria must be satisfied, as decribed previously in section 5.2.1, repeated again here that Q_1 must always be greater than or at least equal to Q_2 no matter where x_1 is located.

$$Q_1 \geq Q_2 \tag{5.25}$$

$$\int_{x_1}^{\lambda} \rho_{(x)} dx \geq \int_{d}^{x_1} \rho_{(x)} dx \tag{5.26}$$

This becomes

$$[Q(x)]_{x_1}^{\lambda} \geq [Q(x)]_{d}^{x_1} \tag{5.27}$$

$$Q(\lambda - Q(x_1) \geq Q(x_1) \tag{5.28}$$

Referring to figure 5.17 the above inequality is easily satisfied for nearly all values of x_1. The limiting case is when $x_1 = 2\lambda$.

Thus the limiting case is when $Q(\lambda) - Q(2\lambda) = Q(2\lambda)$ or when $Q(2\lambda) = Q(\lambda)/2$

There are multiple functions that meet this criterion, three arbitrary functions that satisfy the charge distribution criteria are given below;

$$Q_(x) = \frac{Q_T}{x} \tag{5.29}$$

$$Q_(x) = Q_T e^{-(0.693(x-\lambda))} \tag{5.30}$$

$$Q_(x) = \frac{Q_T}{2^(x-\lambda)} \tag{5.31}$$

It must be noted however, that these three equations are not exhaustive and many such equations can be sought that meet the criteria $Q(2\lambda) = Q(\lambda)/2$.

A normalised graph of the above three equations is given in Figure 5.18 below where x is being represented as multiples of λ(n) (i.e $x = n\lambda$);

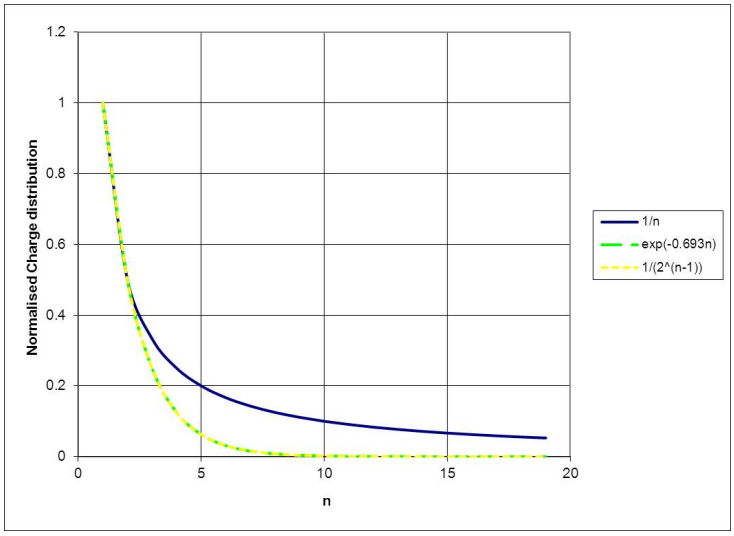

Figure 5.18: Normalised Charge distributions capable of maintaining P=0 within plasma

Therefore applying equation 5.24 The voltage of the plasma can be derived as follows.

$$\frac{Q_T}{\epsilon_0}\int_0^d f(x)dx = \frac{4\pi\rho\sigma e}{3m_e\epsilon\lambda} \tag{5.32}$$

$$E_0\int_0^d f(x)dx = \frac{4\pi\rho\sigma e}{3m_e\epsilon\lambda} \tag{5.33}$$

As $\frac{Q_T}{\epsilon_0} = E_0$

where $f(x)$ is the normalised charge distribution as shown above, transposing equation 5.32 for E_0 gives.

$$E_0 = \frac{4\pi\rho\sigma e}{\int_0^d f(x)dx \cdot 3m_e\epsilon\lambda} \tag{5.34}$$

5.4.0.5 E-Field for Partial Discharge

From the equation 5.32 it can be seen that the largest integral of $f(x)$ will result in the lowest required value for E_0 and thus the minimum voltage required for partial discharge. From the graph in Figure 5.18 it can be seen the equation that would provide the largest integral is $Q(x)_{max} = Q_T/x$. Performing this integral gives;

$$\int_0^d f(x)dx = 1 + ln(\frac{d}{\lambda}) \tag{5.35}$$

Substituting equation 5.35 into equation 5.34 gives;

$$E_0 = \frac{4\pi\rho\sigma e}{\left(1 + ln\left(\frac{d}{\lambda}\right)\right) \cdot 3m_e\epsilon\lambda} \tag{5.36}$$

5.4.0.6 Voltage Required for Partial Discharge Using Two Parallel Plates

Now E_0 is the E-field that would be between the two plates should no electrolyte be present. This is related by the equation $V = E_0 d$. Therefore V(partial discharge) ($V_p d$) is given by;

$$V_{pd} = \frac{4\pi\rho\sigma e d}{3m_e\epsilon\lambda \cdot \left(1 + ln\left(\frac{d}{\lambda}\right)\right)} \tag{5.37}$$

Incorporating equation 5.1 gives an equation for the minimum voltage required for partial discharge;

$$V_{pd} = \frac{4\pi\rho\sigma^2 epd}{3m_e\epsilon kT \cdot \left[\left(1 + ln\left(\frac{kT}{\sigma}\right)\right) + ln(pd)\right]} \tag{5.38}$$

As it can be seen from the above equation there are no curve fitting constants, all of which are natural constants and the only variable pair is 'pd'. Here we have a derivation

theoretically linking the pd product to the voltage of partial discharge.

Applying the constants below

$e = 1.602176487 \times 10^{-19}\ C$

$m_e = 9.10938215 \times 10^{-31}\ Kg$

$k = 1.3086504 \times 10^{-23}$

$\rho = 1.2041\ Kgm^{-3}$

$T = 300\ K$

$\sigma = \pi r_i^2 = 2.82743 \times 10^{-21}\ m^2$

where $r_i = 0.3 \times 10^{-10}\ m$

gives

$$V_{pdmin} = \frac{193.3pd}{0.6182 + ln(pd)} \tag{5.39}$$

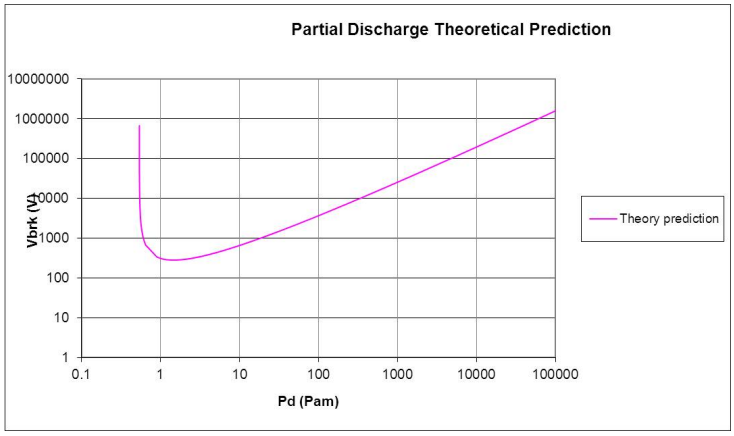

Figure 5.19: Curve showing theoretical partial discharge prediction

The equation 5.38 provides the general equation for the minimum voltage that would result in partial discharge between two electrodes separated by a gaseous dielectric. The variables that correspond to the partial discharge voltage are the *pd* product, Temperature (T), the density of the gas ρ and the ionic radius of the particular gas (i.e. $\sigma = \pi {r_i}^2$). Provided the conditions are stable for a given set up, the only variable will be the *pd* product as experimentally measured by Paschen [18]. The implications of this are that for a given safe operating air gap d at for example sea level (i.e $p \approx 100KPa$), a much larger air gap would be required at 15Km (50,000ft) where $p \approx 10KPa$, to maintain the same safe *pd* product. In this example to maintain the same safe operating parameters the air gap would have to be ten times greater than the original to operate safely at these altitudes.

Applying reasonable parameters for temperature (i.e. 300K), the density of air (i.e. $1.2041Kgm^{-3}$) and applying the parameters for the Nitrogen content in air (i.e. $r_i = 30nm$) then the particular solution to equation 5.38 can be found in equation 5.39, this equation is graphically presented above in figure 5.19. This curve appears to have the characteristics of those experimentally measured by Paschen, i.e. at large values of *pd* product, large voltages would be required to cause partial discharge, however, as the *pd* product is reduced so to does the partial discharge voltage. The partial discharge voltage and *pd* product continue along these lines until a point when the curve begins to rise again for any further reduction in *pd* product and as a result the curve becomes non-monotonic.

A reason for the curve being non-monotonic for low values of *pd* product is that the gap distance d is less than the mean free path λ of the gas. Having the condition $\lambda < d$ may be a reasonable definition for a vacuum, as this will explain why the voltage for

partial discharge rises, trending towards infinity.

In chapter 7 the predicted curve shown above in figure 5.19 will be compared against experimental results.

Chapter 6

Transition from Partial Discharge to Arc

The previous two chapters have detailed a theory of how a plasma is formed, how it is able to progress and migrate from one electrode to the other. The theory, however, only details the plasma formation up to one mean free path (λ) away from the Anode. The reason why the plasma is not considered right up to and including the anode is because the theory would break down at this point. [51] [52]

The theory is still complete as the extra forces to allow the electrons to bridge the final gap (λ) have been accounted for. But once the electrons do bridge the gap and allow a conductive path to form, the forces that are required for the plasma to exist and progress will collapse, the plasma will be broken and the whole cycle will then repeat. This may account for the clicking sounds one hears prior to when an arc establishes. [53]

6.1 The final mean free path λ

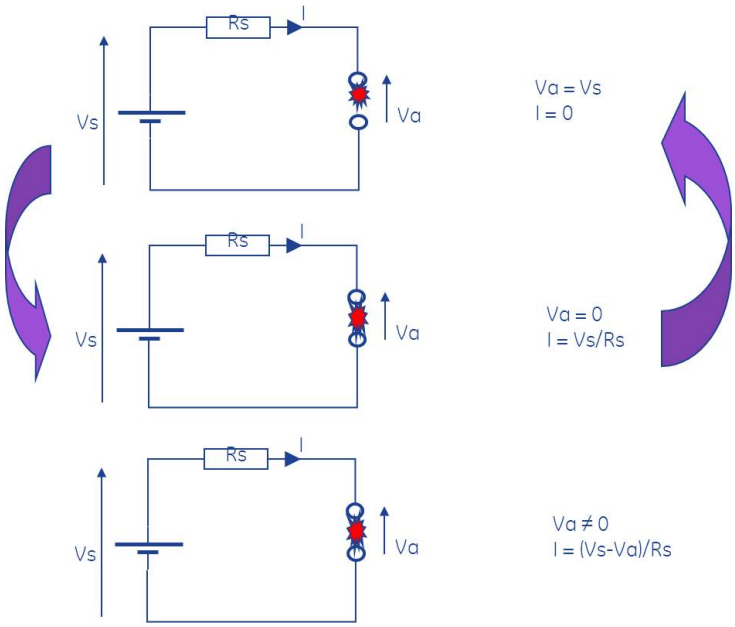

Figure 6.1: A depiction of the formation of an arc

From the above figure the plasma formation can be seen, during this phase the supply voltage is also the voltage across the air gap, with no current flowing. The plasma extends to the anode, at this point the voltage across the gap reduces to zero and the current rises and is only limited by the circuit impedance. With the voltage at zero there will be no E-field to progress the plasma so it will disperse. and the whole cycle will begin again. [54]

The question is what new phenomena may be occurring over this final λ?

Referring to figure 5.19 one way to think about an arbitrary point on the curve is that that voltage is capable of producing a plasma that can extrude over the entire gap separating the cathode and anode electrode. If the distance of gap is considered as multiples

of λ, meaning the gap $d = N\lambda$. Now consider a slightly larger gap by one more mean free path, a slightly higher voltage would be capable of extruding a plasma a slightly further distance may be $(N + 1)\lambda$, as shown below. [55]

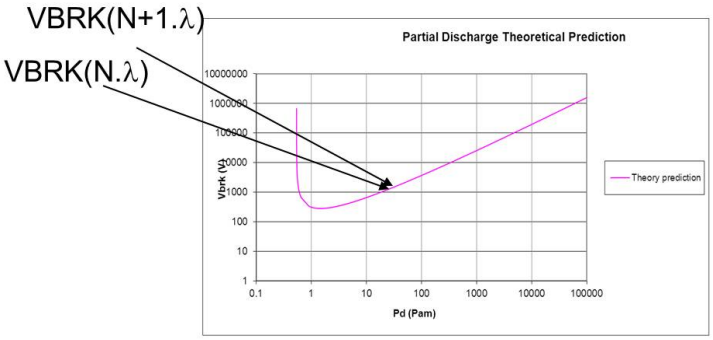

Figure 6.2: General change in discharge voltage with respect to 'pd'

If we therefore differentiate equation 5.38 with respect to 'pd' and then equate d to λ. Then some insight into this region may be gained.

Performing this differentiation as described above yields the following result.

$$\frac{dV_{pd}}{dp\lambda} = 0 \tag{6.1}$$

At first this result was a surprise, however, it need not have been as the plasma formation is effectively akin to an extrusion and if the plasma is broken by a distance λ then one would expect that the plasma fill the gap, thus requiring no change in voltage.

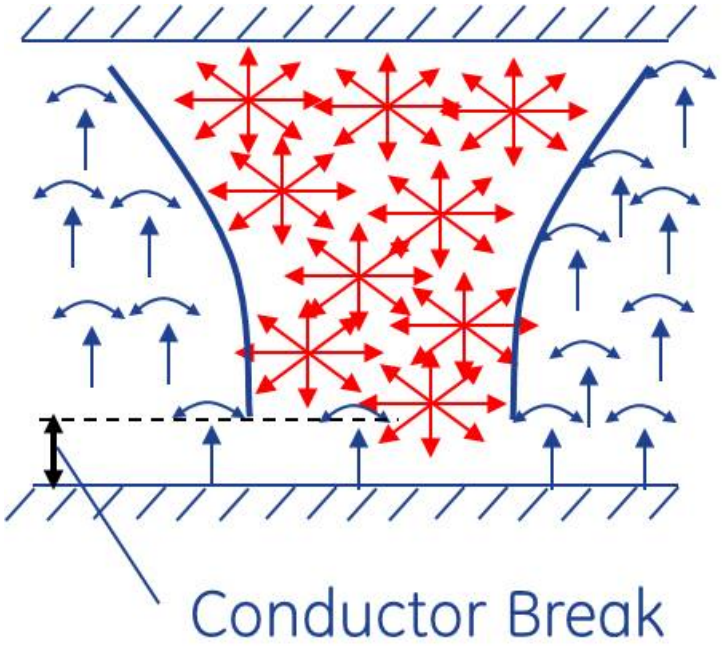

Figure 6.3: A depiction of the plasma with a gap on λ

Referring back again to figure 6.1, the top two captions depict a binary state of partial discharge, whereby either $Vgap = 0$ or $Igap = 0$. However, is there a parameter that could vary that would enable the state where Vgap and Igap are both non-zero? [56] [57]

6.1.1 Variation in λ

A conjecture to try and address the problem is to see if the mean free path over the final gap λ could be different to the mean free paths of the molecules that allowed the plasma formation in the first place. [58]

As mean free path is closely inter-related to temperature (T) then it may be better

stating the situation another way.

Could the temperature closest to the anode be higher than that of the surrounding air? Could it also be possible that this temperature rise give rise to an arc?

6.2 The Arc

In order to analyse the implications of having different temperatures between an arc and the surrounding area, further consideration of how to modify or adapt equation 5.38 must be given. [59] [60]

The whole theory behind equation 5.38 and the formation of the plasma, was with no heat generation, this is because either $I = 0$ or $V = 0$, therefore there is no source for heat to be generated. But over time it could be argued that the plasma could amass enough electron mobility that it be considered a conductor.

If the plasma is considered to be a conductor, then the temperature references in equation 5.38 must be that of ambient air, this must be so because all of the temperature variation will be in the final gap 'd' which in this case is now λ and if this λ is transposed using equation 5.1 in order for it to be expressed in terms of temperature, which will now be the theoretical temperature of the arc, then the equation can be solved. [61]

Differentiating equation 5.38 and applying the above treatment gives.

$$\frac{dV_{pd}}{dp\lambda_{arc}} = \frac{57981ln\left[\frac{T_{arc}}{T_{ambient}}\right]}{T_{ambient}\left[1+ln\left[\frac{T_{arc}}{T_{ambient}}\right]\right]^2} \tag{6.2}$$

The above solution shows the variation in voltage across the final mean free path and it's own variation, (i.e. temperature change). This may be the basis of correlation between arc voltage and temperature. To that end the above equation may be better expressed as;

$$V_{arc} = \frac{57981ln\left[\frac{T_{arc}}{T_{ambient}}\right]}{T_{ambient}\left[1+ln\left[\frac{T_{arc}}{T_{ambient}}\right]\right]^2} \tag{6.3}$$

Plotting the above equation with respect to the temperature gain of $T_{arc}/T_{ambient}$ is shown below.

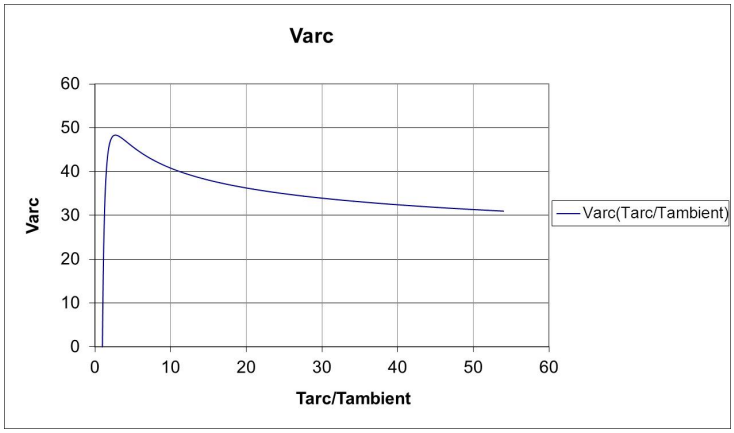

Figure 6.4: A theoretical graph correlating Arc voltage against temperature gain of arc to ambient

For the above graph $T_{ambient} = 300k$ was used.

If a greater range of temperature gain is applied then the above graph may be viewed as shown below.

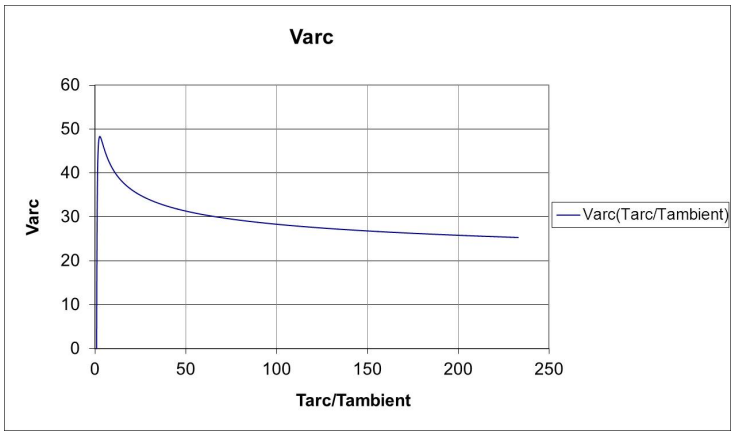

Figure 6.5: A theoretical graph correlating Arc voltage against temperature gain of arc to ambient

From the above graph, applying a greater temperature gain range, it can be seen that the voltage is asymptotically trending towards 20V, however, it has a peak of around 47V.

6.3 Proposed theory for arc formation and extinction

Based on the theory presented previously for plasma formation and referring to figure 6.1 the catalyst for the arc formation appears not to be the making of an electrical connection via a plasma from one electrode to another, but moreover, the subsequent breaking of the plasma connection resulting in a gap. After a period of time of making and breaking this connection, the temperature in the gap will rise considerably and allow the conditions to met to form an arc and establish a voltage nearest the anode in accordance with the curve found in figure 6.5 [62] [63] .

Once an arc is established the actual arc voltage will be determined by a number of factors; current, area, thermal mass and thermal conductivity of the surround area to the arc to name but a few. All of these factors will determine the temperature of the arc and it appears that this is what sets the voltage of the arc.

The above argument holds if a wire breaks or a relay contact opens. If current was passing though the relay contact which is initially under pressure over a certain surface area, but does not have a perfect finish. Should the relay be commanded to open, the pressure on the contacts begins to reduce, the surface area over which current is being conducted will also reduce. This continues until the pressure is at a minimum and the current density is so high, due to all of the current passing through the smallest whisker of metal on the contact. This in turn will cause this metallic whisker to over heat and melt and as the circuit is finally broken the arc is formed, due to a localised heating and the circuit attempting to break. At the initial formation of the arc, the arc voltage may be lower than predicted in figure 6.5, the reason for this will be due to the gas being metallic in composition due to melting of a portion of the contact material. This is to explain why the graph shows a lower and more unpredictable voltage at the initial opening of the contacts. [64] [65]

With the arc voltage effectively reducing the amount of current that can now flow through the circuit, the arc temperature may be forced to reduce. This reduction in temperature will cause the arc voltage to increase, as per figure 8.3. This further increase in arc voltage will cause the current to reduce and so too the arc temperature, this in turn will cause the arc voltage to increase further. This process will continue until the

arc voltage exceeds the available supply voltage whereby the current will fall to zero and so too the temperature available, as proposed in figure 6.6 below. [66] [51] [52] [15] [16] [67]

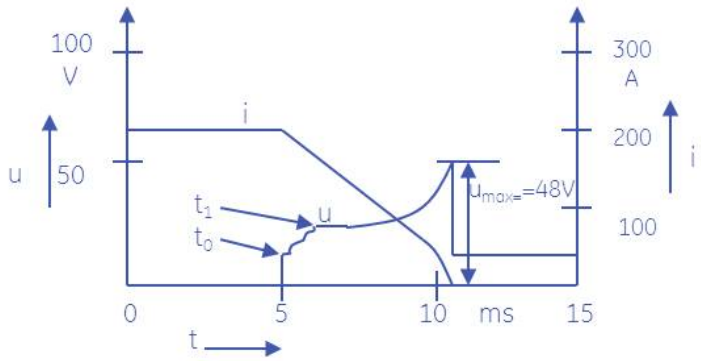

Figure 6.6: A theoretical graph proposing the V & I characteristics of a quenching arc in a 12V system

The above figure proposes that the arc voltage will exceed the supply voltage, the reason for this is due to any inductance in the system. When a circuit is carrying current, energy is stored in the wiring $E = 1/2LI^2$. and this energy will also need to be extinguished in order for the circuit to be broken. [68] [69] [70]

If the system supply voltage exceeds 48V, then the same will apply, however, a drawn arc will be formed and a bigger gap will be required in order to break the circuit. A drawn arc will not be treated in this thesis. [71] [72] [73]

Chapter

7 Experimental Validation

7.1 Breakdown of Air Gaps

Experiments were undertaken to test for breakdown events in air when uniform E-fields were applied. The intention here was to collect raw data under controlled conditions, varying the air gap distance (d) and pressure (p), from which the proposed theory could be validated against. The experiments were conducted by the University of Manchester by Ian Cotton and detailed in a report 'GE270111' [74]. The report details extensive testing on many aspects of breakdown, however, reference to the report is only made for the one section that tested electric breakdown in air.

Gaps of 0.07, 0.165, 0.265 and 0.43mm (2.75, 6.5, 10.4 and 16.9 thou) were tested at varying air pressures resulting in a range of measurements at pressure-distance products of 0.1, 0.25, 0.4, 0.6, 0.8, 1, 2, 5, 10 and 20 Pam. All measurements were carried out at 20^{o}C. The test results have been compared with both proposed theoretical prediction, IEC 60664 and IPC 2221A.

7.1.1 Test Objects

The test objects were two electrodes of brass with a spherical finish which were used to provide a uniform field (their diameter of 12.5mm being much greater than the gap distance being tested). In order to set a precise distance between these electrodes, a calibrated test rig was built as shown in Figure 7.1. This calibrated system consisted of two dummy end spacers with precise dimensions of 43.1546mm (1.699 inch), shown below in Figure 7.1. Smaller dummy spacers were used to fix the test electrodes to the wooden block also shown in Figure 7.1. The method used to specify the gap spacing is given in section 7.1.4.

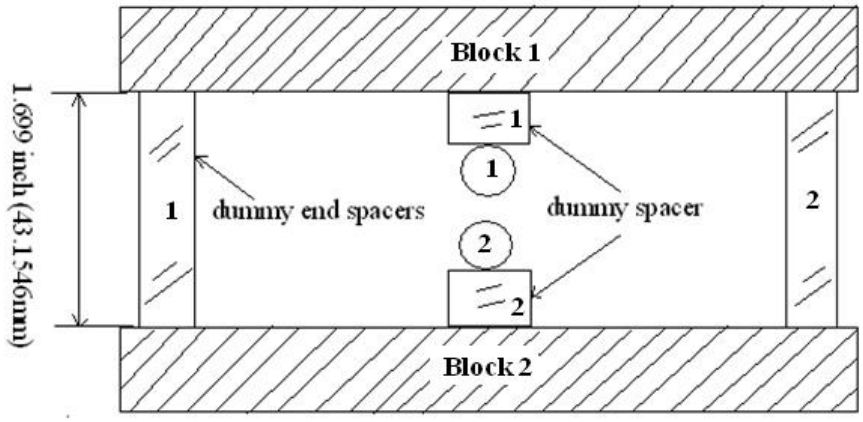

Figure 7.1: Test set up used for breakdown testing in air

7.1.2 Test Equipment

The following equipment was used to carry out the tests. The purpose for including the table here is to detail the calibration records where necessary for any equipment which is being relied upon for validating the experimental data.

Equipment Type	Required Specification	Equipment Identification number	Calibration Certificate	Certificate Date Range
Environmental Chamber	Capable of controlling pressure between 100mBar and 1000mBar absolute and temperatures between -50°C and 20°C	Kasco Thermovac Chamber Model 60/12/2124	Calibration not required	-
Voltage Source	Partial discharge free voltage source with a peak voltage of $3000V_{pk}$.	Matsusada 3kV High Voltage Amplifier Model AMS-3B10-L(203V), serial number 031621L	Calibration not required	-
Temperature Measurement	Capable of measuring temperature to ±2%	Type K Thermocouple and Digitron 2029T Digital Readout – Serial numbers 20543/1 and 4002443	MC31147001 MC31149001	18th Feb 2008 – 18th Feb 2009 13th Feb 2008 – 13th Feb 2009
Pressure Measurement	Capable of measuring pressure to ±2%	Digitron 2025P, serial number 4606113429	MC31146001	12th Feb 2008 – 12th Feb 2009
Voltage Measurement	Capable of measuring applied voltage to ±3%	HVP 15HF 40kV 1000:1 Probe plus TDS1002 Oscilloscope. Serial numbers CN8284 (Calibrators reference) & C05182	4378	7th March 2008 – 6th March 2009
Labview System	Capable of controlling output of HV amplifier through production of an analogue output voltage and reading voltage from HVP 15HF probe.		Calibration not required (voltage measurement verified against calibrated system above)	

Figure 7.2: Test equipment used for breakdown testing in air

All testing undertaken for this section was carried out between the 5th January and 6th February 2009.

7.1.3 Test Circuit

The test circuit used for the measurement of breakdown voltage of the air gaps is shown in Figure 7.3. A HV amplifier with a maximum output voltage of ±3kVpeak was used to

apply high voltage to the air gap. Voltages were measured through a voltage divider with a ratio of 1:1000. A current limiting resistor with a resistance of 100 k was placed before the test gap. The HV amplifier was controlled using a National Instruments LabView program that could ramp the amplifier output at a preset rate and note the voltage at which breakdown occurred (based on the fact that the voltage collapsed across the test object the instant that breakdown occurred allowing a simple peak hold methodology to be used).

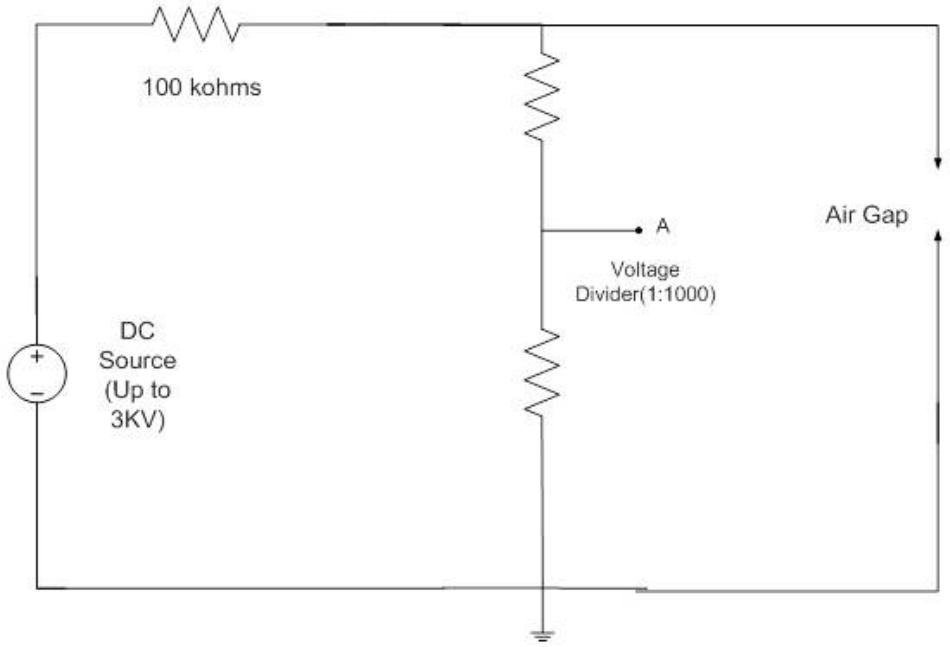

Figure 7.3: Test circuit for air gap breakdown voltage measurements

The LabView with the appropriately developed software and the above test rig formed an automated closed loop control systems for determining and recording the electric discharge of a given test sample. A scaled voltage of V_{AIRGAP} was then continuously monitored by LabView whilst the software controlled the rise of HV amplifier voltage at a rate of 1000V/min. The voltage rise was kept conservatively low in order to increase

the probability of observing the lowest given discharge for an experimental run. Under normal conditions the current through the air gap was 0A, however, if the current rose to $\geq$4 mA, then the experiment halted and the voltage prior to the current measurement was recorded (after applying appropriate scaling to the measured results). This whole experiment was repeated 10 times, in order to produce a spread of results, where the minimum discharge voltage was identified. A list of the actual test procedure is given in the next section for completeness.

7.1.4 Test Procedure

The following test procedure was used:

1. The distance between the two electrodes was set as follows:
    - The heights of the dummy end spacers were measured and checked to be 43.1546mm (1.699 inch).
    - The total height of mid-spacer 1 and electrode 1 were measured to be h1
    - The total height of mid-spacer 2 and electrode 2 were measured to be h2
    - The space between two electrodes is taken to be 1.699-h1-h2 inches.
    - To achieve the gap distance required, additional spacers of a specific height were used
2. The test object was placed in the environmental chamber with the connections being made as shown in Figure 7.3.
3. The environmental chamber was set at the desired pressure and when stable the test pressure was recorded

4. Labview was used to ramp the voltage across the test object at a rate of 1000V/minute
5. The peak voltage the gap withstood was read from the Labview system and noted.
6. The measurement was repeated 10 times at this PD product.
7. For tests using the same gap spacing, the tests were repeated from step '3' using a different pressure. Other tests were repeated from step '1' using a different size gap.

7.1.5 Results

A series of testing was conducted and the results are presented below, showing the various test results with the theoretical prediction as detailed in Chapter 5 superimposed. Therefore for a given 'pd' product ten tests were carried out to determine the minimum discharge voltage and also the spread of discharge voltages. The proposed theoretical prediction is then overlayed over these results, the purpose of which is to see if there are any electrical discharges below the proposed theoretical minimum. The various 'pd' products are arrived at first by setting the distance (d) in the test sample and then adjusting the pressure (p) of the test chamber, in order to achieve a given 'pd' product. The distance 'd' used for each test is given in the caption beneath each figure below.

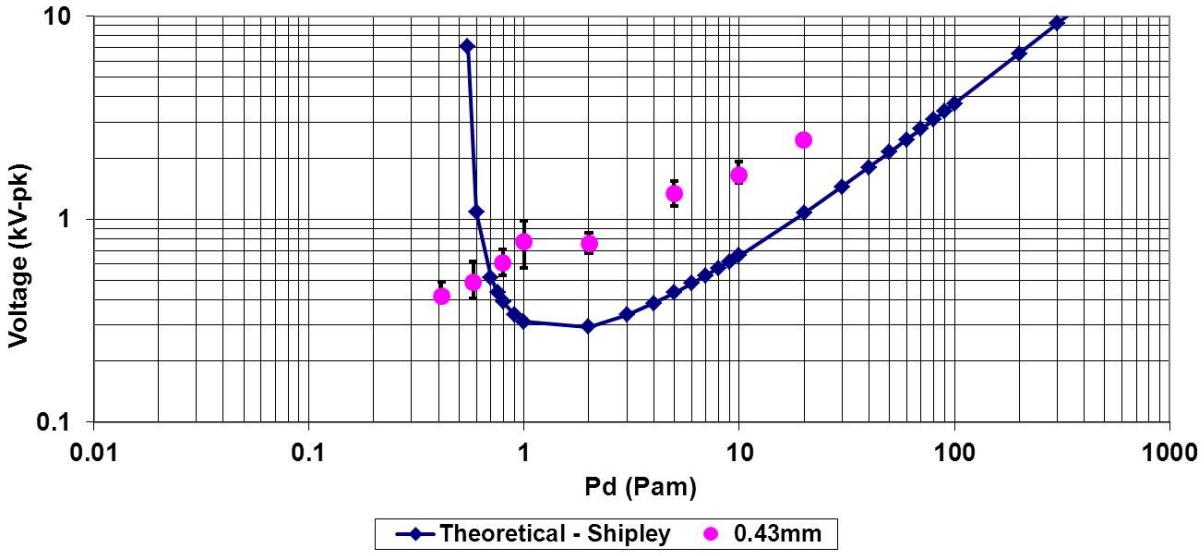

Figure 7.4: Uniform field breakdown test results for 0.43mm (16.9thou) (each data point representing the average of 10 measurements with the error bars stating the maximum and minimum values recorded)

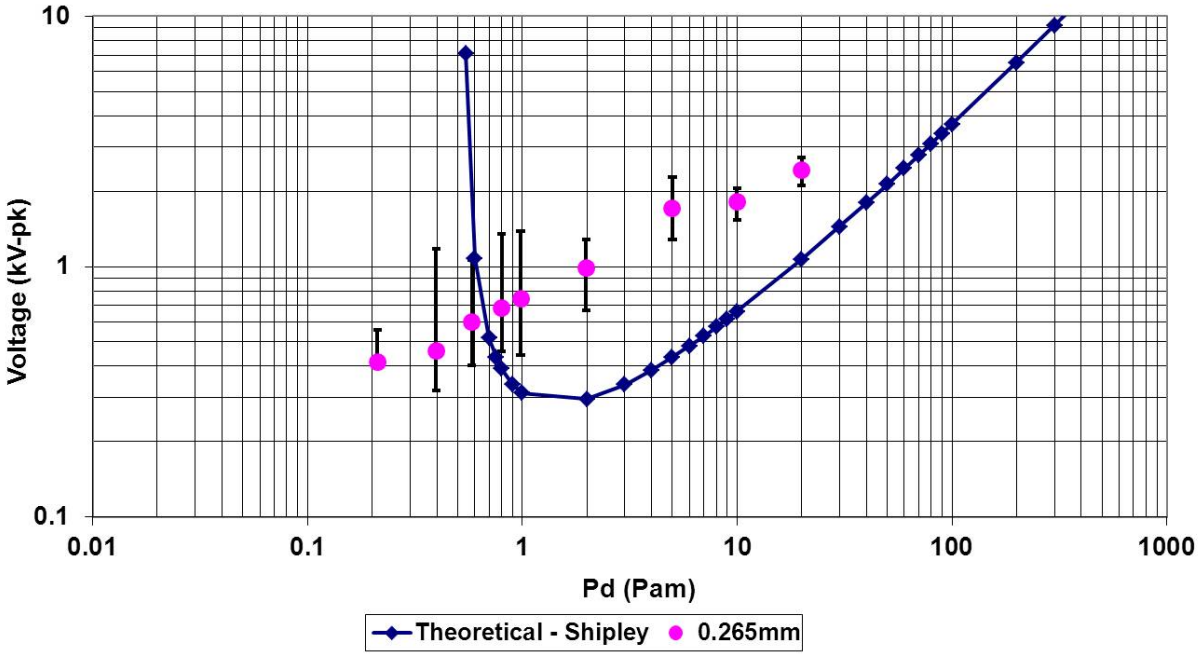

Figure 7.5: Uniform field breakdown test results for 0.265mm (10.4thou) (each data point representing the average of 10 measurements with the error bars stating the maximum and minimum values recorded)

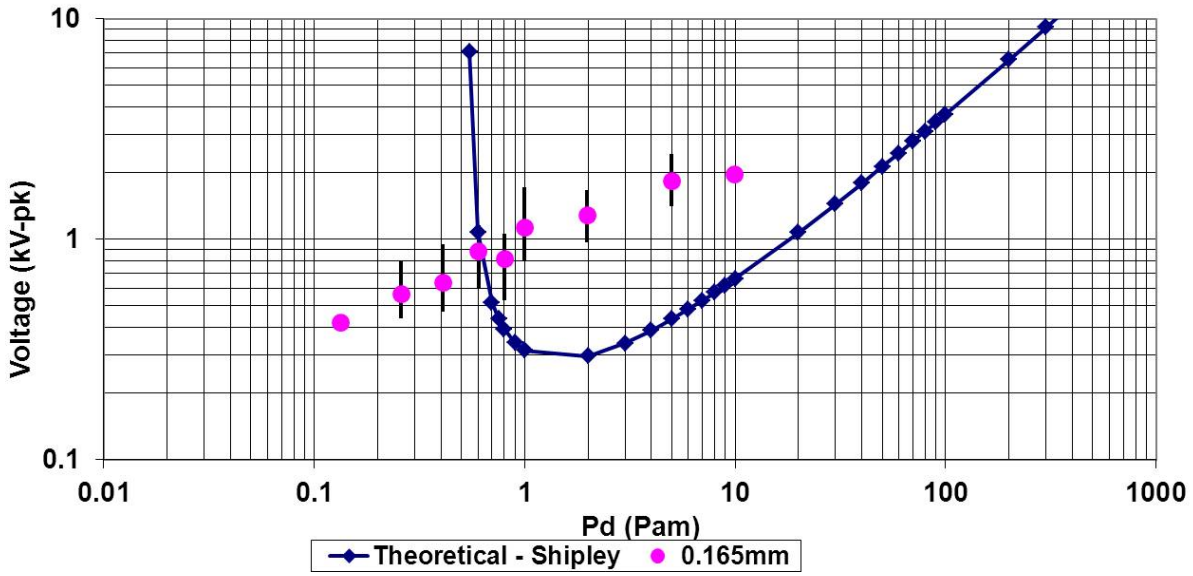

Figure 7.6: Uniform field breakdown test results for 0.165mm (6.5thou) (each data point representing the average of 10 measurements with the error bars stating the maximum and minimum values recorded)

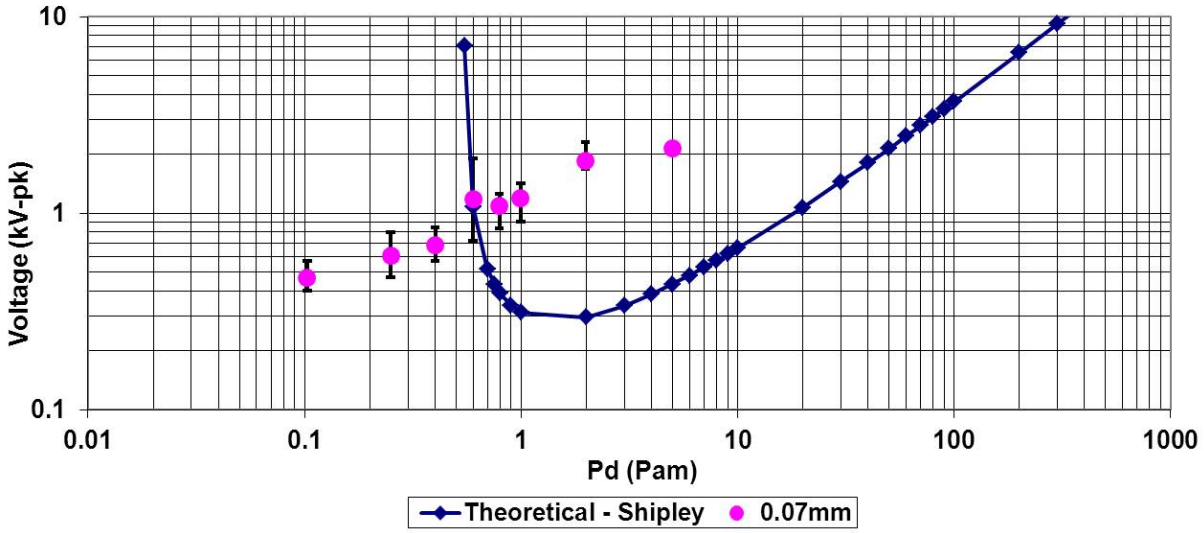

Figure 7.7: Uniform field breakdown test results for 0.07mm (2.75 thou) (each data point representing the average of 10 measurements with the error bars stating the maximum and minimum values recorded)

As discussed in previous chapters, various guidelines are available to allow designers to implement appropriate air gaps for a given application into their designs, (e.g. IPC 2221A and EN 60664). Only IPC2221A provides consideration for altitude variation, however, this guidance comes in the form of gaps required for altitude of up to 3050m or 'any altitude'. The definition of 'any altitude' is not provided by the document. EN60664 offers no air gap guidance above 2000m, however, the guidance in this document can easily be extrapolated to include altitude variation, as distance at 2000m forms a 'pd' product from which 'p' can be varied. The guidance from both of these documents has been translated to a graphical form and provided in the figure 7.8 as shown below. Again the theoretical prediction is also provided on the same figure for the purpose of showing graphically the proposed theoretical minimum discharge voltage and the documented

guidance which is applied to designs. [8] [25]

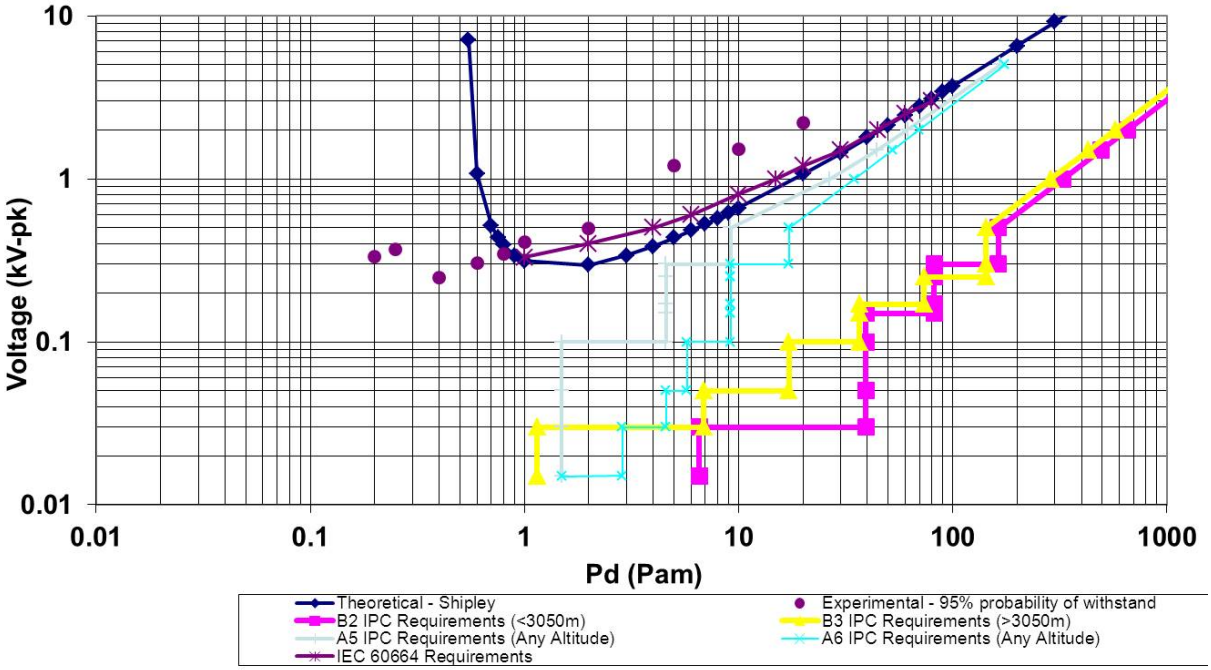

Figure 7.8: Comparison of test results, theoretical curve and standardised requirements

Note: that in the figure 7.8 above, IPC2221A the lowest 'pd' product is 1.14Pam, however, IEC 60664 only uses distance as a variable. The curve that is shown on the has been extrapolated to include pressure variation.

7.2 Tests On Printed Circuit Boards (Uncoated Polyimide and FR4)

The testing conducted in section 7.1 was extremely time consuming ensuring that all distance measurements where accurate and stable. An alternate approach was undertaken,

whereby Printed Circuit Boards (PCBs) where employed and the surface tracks of varying track gap widths were used. This led to a further concern of material variation also (i.e. Polyimide versus FR4), therefore the approach taken was to perform the whole testing twice with both types of PCB construciton material.

Uncoated Polyimide Printed Circuit Boards with gaps of 0.0508, 0.0762, 0.102, 0.152, 0.203, 0.254, 0.508, 0.762, 1.016, 1.27, 1.524, 1.778, 2.032, 2.286 and 2.54mm (2, 3, 4, 6, 8, 10, 20, 30, 40, 50, 60, 70, 80, 90 and 100thou) were tested at pressure-distance products of 0.1, 0.25, 0.4, 0.6, 0.8, 1, 2, 5, 10, 20 and 50 Pam.

Uncoated FR4 Printed Circuit Boards with gaps of 0.0508, 0.0762, 0.102, 0.152, 0.508, 0.762, 1.016, 1.27, 1.524, 1.778, 2.032, 2.286 and 2.54mm (2, 3, 4, 6, 8, 10, 20, 30, 40, 50, 60, 70, 80, 90 and 100thou) were tested at pressure-distance products of 0.1, 0.25, 0.4, 0.6, 0.8, 1, 2, 5, 10, 20 and 50 Pam.

The test results have been plotted and are compared with theoretical prediction, IEC 60664 and IPC 2221-1.

7.2.1 Test Objects

The following figures show the test samples. These were uncoated printed circuit boards made by a supplier to the aerospace industry. As displayed in Figure 7.9, 'V' was connected to high voltage electrode through a wire soldered onto the pad, '0' was connected to the ground in an identical manner. Figure 7.10 shows maximum and minimum size of the test boards received

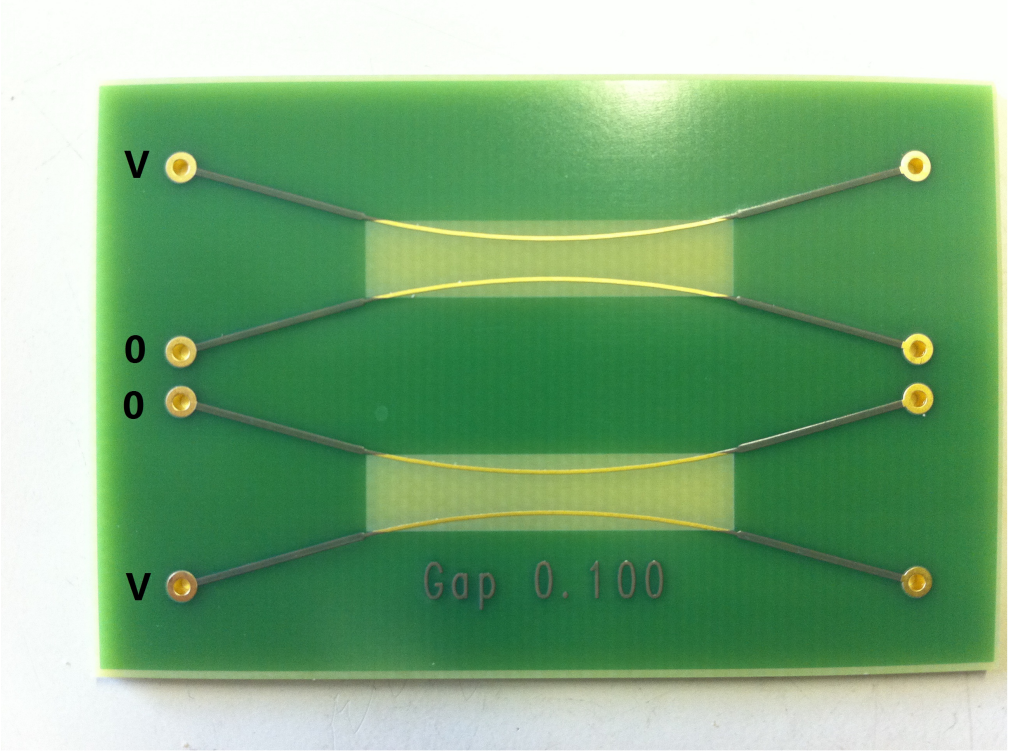

Figure 7.9: Test board sample

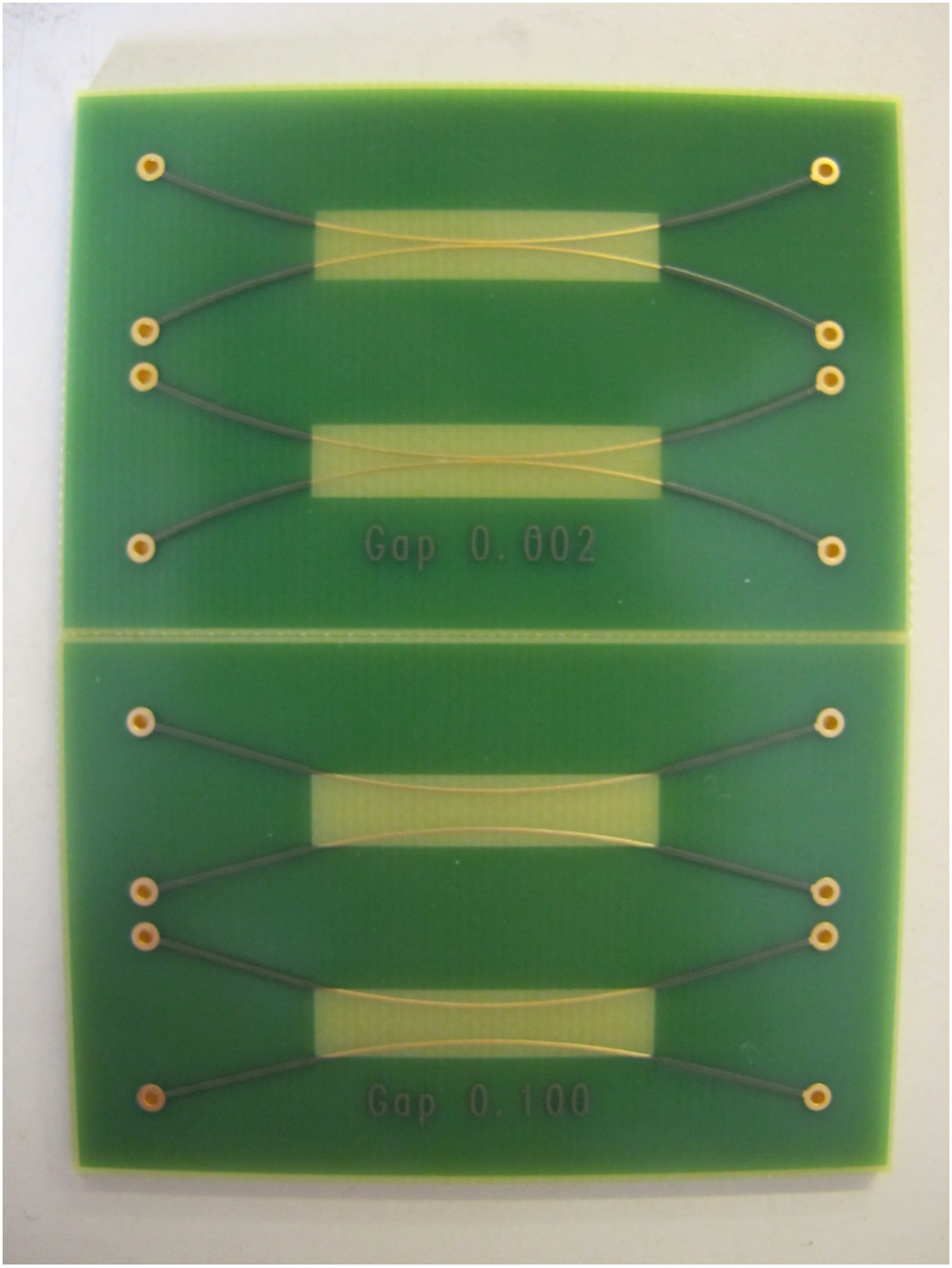

Figure 7.10: Maximum and minimum size of test boards (note that gap sizes are given in inches)

7.2.2 Test Equipment

The following equipment was used to carry out the required tests. The purpose for including the table here is to detail the calibration records where necessary for any equipment which is being relied upon for validating the experimental data.

Equipment Type	Required Specification	Equipment Identification number	Calibration Date / Reference
Environmental Chamber	Capable of keeping pressure between 10mBar and 1000mBar	Island Scientific Chamber Model No.46×305, Serial No.15012009	Calibration not required
Vacuum Controller	Capable of controlling pressure between 10mBar and 1000mBar with ±5% error	THYRCONT Vacuum Controller Model DC1S, serial numbers S130102 & Vacpump Varian Model DS202	Calibration not required
Voltage Source	Partial discharge free voltage source with a maximum DC voltage of 30kV.	Glassman High Voltage Supply Maximum Voltage is DC 30kV, Model PS/MK30P02.5-22, Serial No. M820367-01B2960408	Calibration not required
Video Camera	Recording process of discharge continuously	Digital Video Camcorder, serial number Canon MV 960	Calibration not required
CCTV Monitor	Showing process of discharge continuously	JVC CCTV Monitor, Model TM-A14PN	Calibration not required
Voltage Divider	Capable of measuring voltage up to a peak value of 15kV	Voltage Divider Serial No.20083931	17/03/2010 Narec Ref. CN8382 Certificate No. 4532
Temperature Measurement	Capable of measuring temperature to ±2%	Type K Thermocouple and Digitron 2029T Digital Readout – Serial numbers 20543/1 and 4002443	24/03/2010 Certificate No. MC55707001
Humidity Measurement	Capable of measuring humidity	Rotronic HYGROPALM Serial No. 46659 017	Calibration not required
Pressure Measurement	Capable of measuring pressure to ±2%	Digitron 2025P, serial number 4606113429	19/03/2010 Certificate No. MC55709001
Voltage Measurement	Capable of measuring applied voltage to ±3%	HVP 15HF 40kV 1000:1 Probe plus TDS1002 Oscilloscope. Serial numbers CN8284	17/03/2010 (Calibrators reference C05182)
Connector Block	Capable of connecting PC and circuit to detect the voltage and current	National Instruments Shielded Connector Block serial number BNC-2110	Calibration not required
LabVIEW System	Capable of controlling output of HV amplifier through production of an analogue output voltage and reading voltage from Divider	LabVIEW 2009 LabVIEW Professional Development System, Version 9.0 (32-bit)	Calibration not required

Figure 7.11: Equipment list used to carry out the testing

All measurements were carried out between the dates 15/07/2010 - 25/08/2010.

7.2.3 Test Circuit

The overall layout of the test is as shown in Figure 7.12. The test uses a cylindrical chamber connected to a vacuum pump which could reduce the pressure to a value as low as 10mBar. High voltage and ground connections were available through a bushing. Two insulators were placed in the chamber as a stand for the tested boards to ensure they did not come into contact with the metal chamber. Pressure and temperature measurement sensors were also placed in the chamber. The pressure value was set by a vacuum controller. A LabVIEW system was used to provide high voltage through the control of a DC supply and was also used to record the break down voltage.

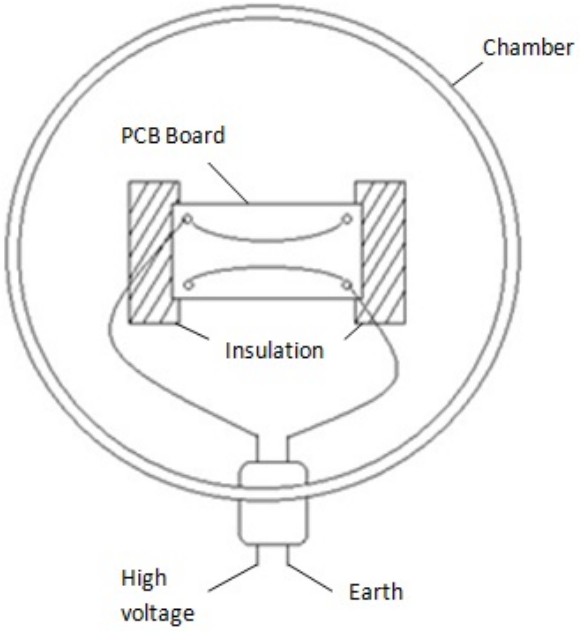

Figure 7.12: Test rig for Printed Circuit Boards

The test circuit used for the measurement of breakdown voltage of the air gaps is shown in Figure 7.13 and uses the same test methodology as previously described in section 7.1. A DC supply with a maximum output voltage of 12.5kVpeak was used to apply high voltage to the test object. Voltages were measured through a voltage divider with a ratio of 1:1000. A current limiting resistor with a resistance of 100 k was placed before the test gap. The DC supply was controlled using a National Instruments LabVIEW programme that could ramp the amplifier output at a preset rate and detect the moment at which breakdown occurred (based on a current threshold set in LabVIEW of 0.2mA). This was a change in circuit to the tests described in section 7.1 but, as will be shown, resulted in measurements with a much smaller standard deviation.

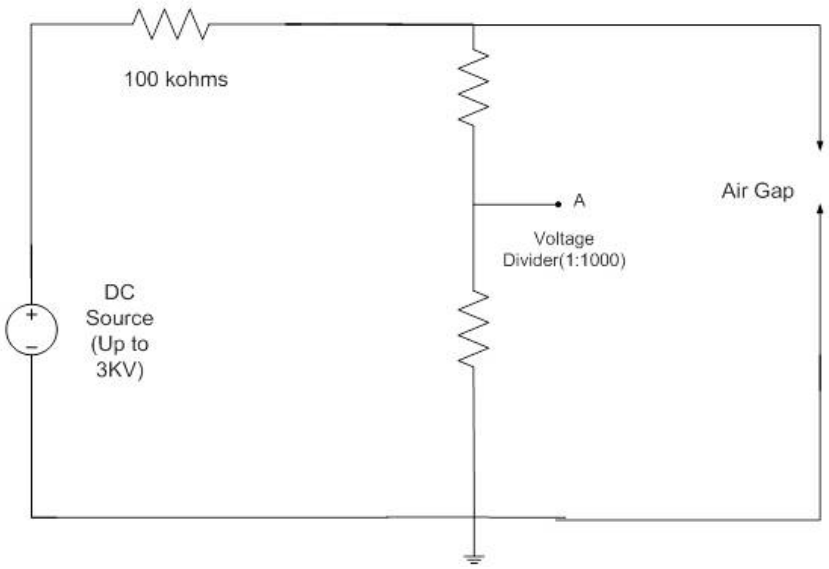

Figure 7.13: Test circuit for PCBs breakdown voltage measurements

7.2.4 Test Procedure

1. The pressures required to achieve the correct PD values for the specific gap distance under test were calculated
2. The sample was connected to the test-circuit in the environmental chamber as shown in Figure 7.13
3. The vacuum chamber was set to the desired pressure and when stable, a record was made of the pressure and temperature.
4. The earth was removed from the circuit
5. The supply voltage on the sample under test was automatically increased by the Labview software at a rate of 1000V / minute until breakdown occurred of the maximum test voltage capability was reached
6. The voltage at which the breakdown took place (and in latter tests the humidity in the chamber when breakdown occurred) were recorded.
7. The test was repeated 10 times
8. The test was repeated at a new pressure from step 2 with a check being made of the circuit board condition and this being replaced should damage be observed.

7.2.5 Results

The results provided in this section will be in the same form as those provided in section 7.1.5, however, this time instead of the discharges occurring exclusively in air, these results will be from the surface tracks of uncoated PCB's, which are free from pollution. The

purpose for including a PCB was to see if there would be any variation in test results with only an air gap, compared to results with the inclusion of a PCB, the type of PCB used can be seen in figure 7.10. Further experimentation would benefit from having improved accuracy and repeatability over the previous tests, which were quite labour intensive. This simple, accurate and repeatable set up allowed the possibility for statistical analysis to be applied to the data, in order to provide the statistical minimum discharge voltage that may have been observed.

Due to the number of boards tested all of the results will not be presented here. What will be given here is a summary of the results on one graph. These data have been further statistically processed by applying a Weibull distribution as this is deemed more likely to provide a reasonable worst case estimate of the data.

Figures 7.14 and 7.15 show the voltage at which at specific probability of breakdown is expected with values given for the 5%, 1%, 0.1% and 0.01% probabilities.

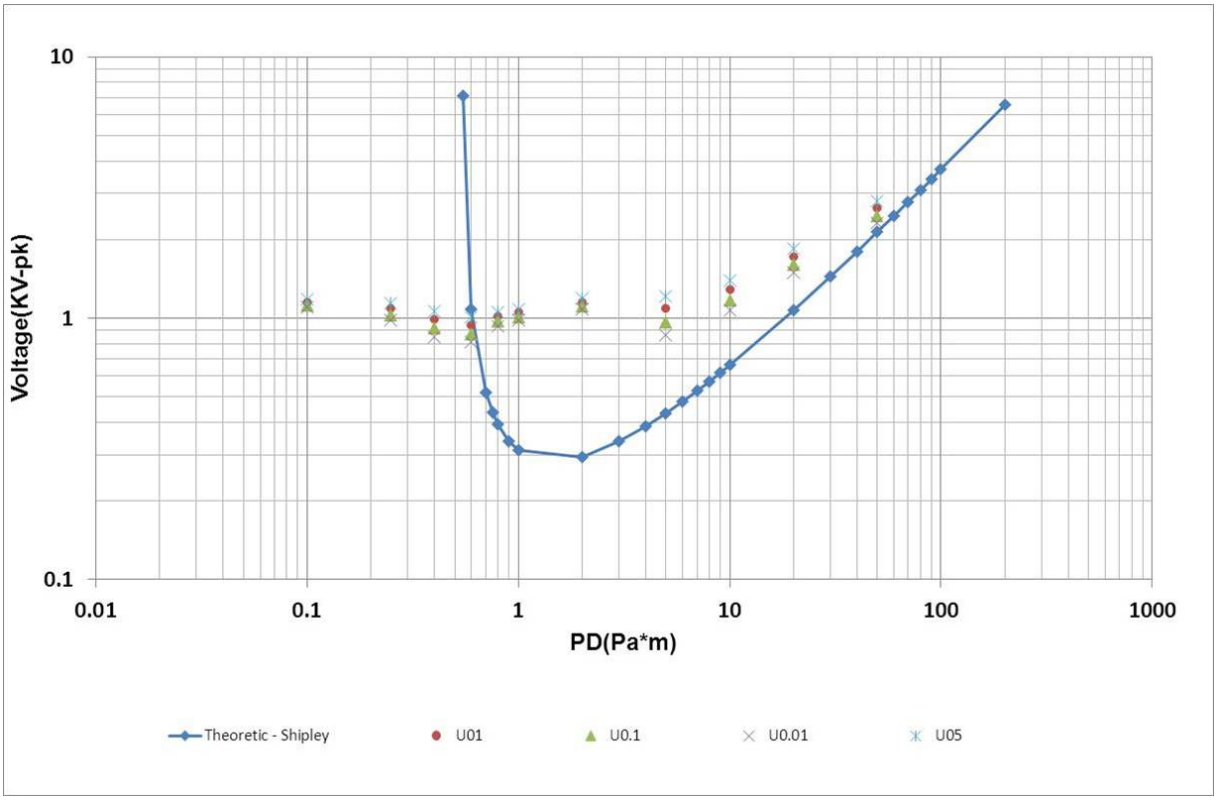

Figure 7.14: Polyimide Results with Theoretical Prediction

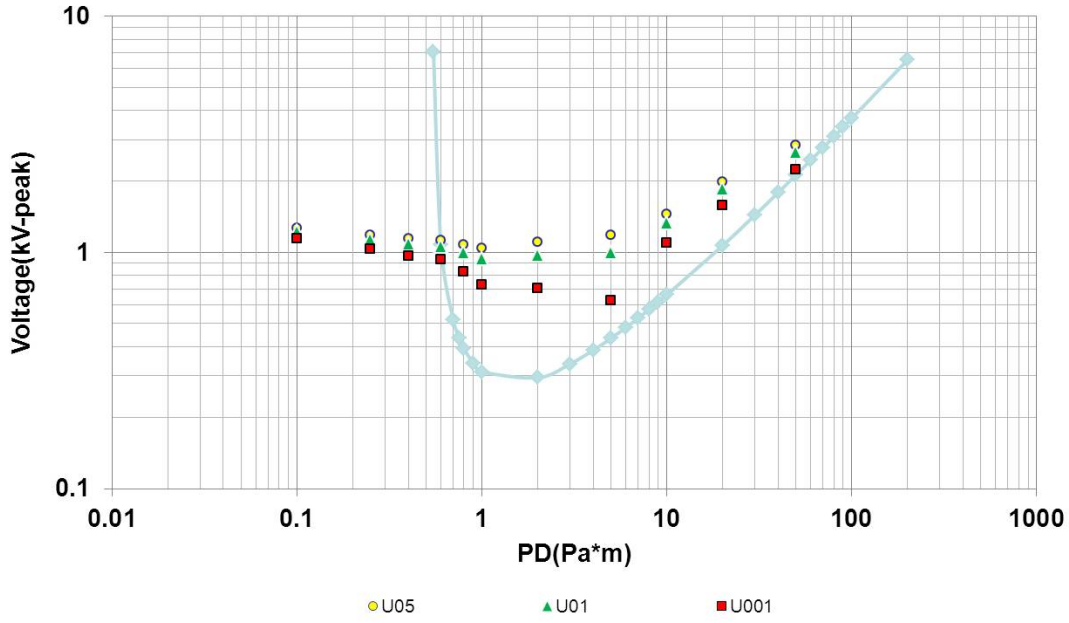

Figure 7.15: FR4 Results with Theoretical Prediction

For completeness the format of the results given in figure 7.8 is repeated here. What figures 7.16 & 7.17 below are showing is a graphical representation of the guidance documents IPC 2221A and EN 60664, the minimum discharge voltages of the various tests (as groups of 10) using both FR4 and Polyimide PCB's against the proposed theoretical minimum discharge curve.

The EN 60664 curve for pollution degree 1 is taken from the creepage distance table in the IEC 60664 standard and is applicable to clean and dry conditions (which is applicable for these tests). The curve for pollution degree 2 is not applicable as it is intended for conditions in which 'Only non-conductive pollution occurs except that occasionally a temporary conductivity caused by condensation is to be expected'.

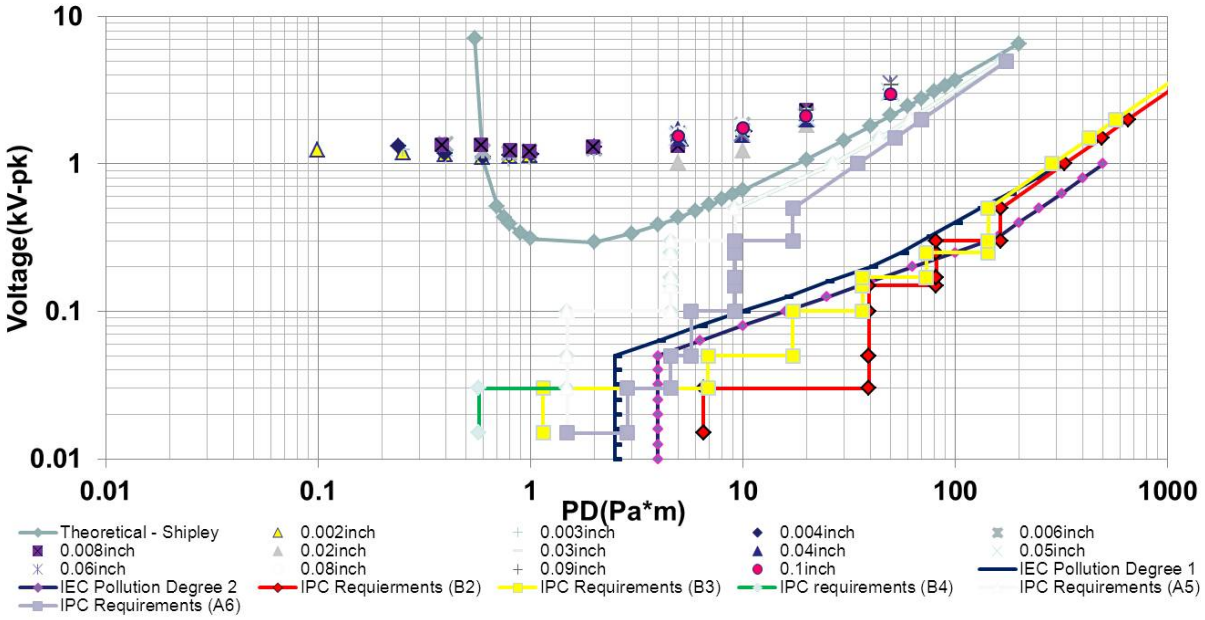

Figure 7.16: Comparison of test results (Polyimide), theoretical curve and standardised requirements

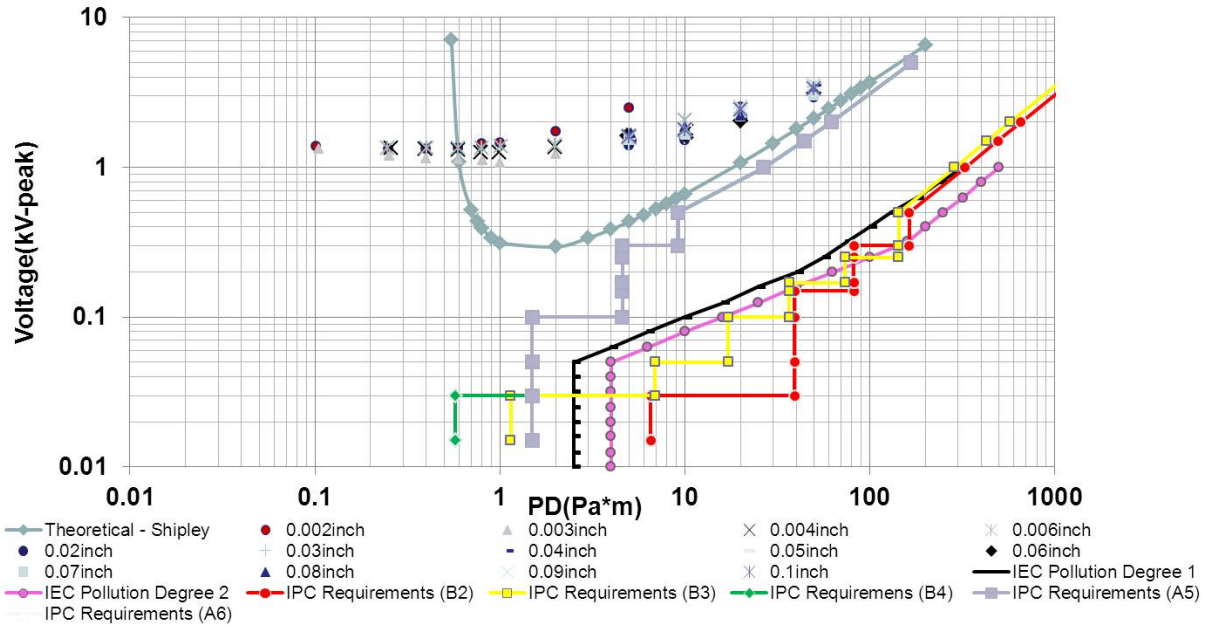

Figure 7.17: Comparison of test results (FR4), theoretical curve and standardised requirements

Again for completeness a comparison between the test results from both FR4 and Polyimide is given below.

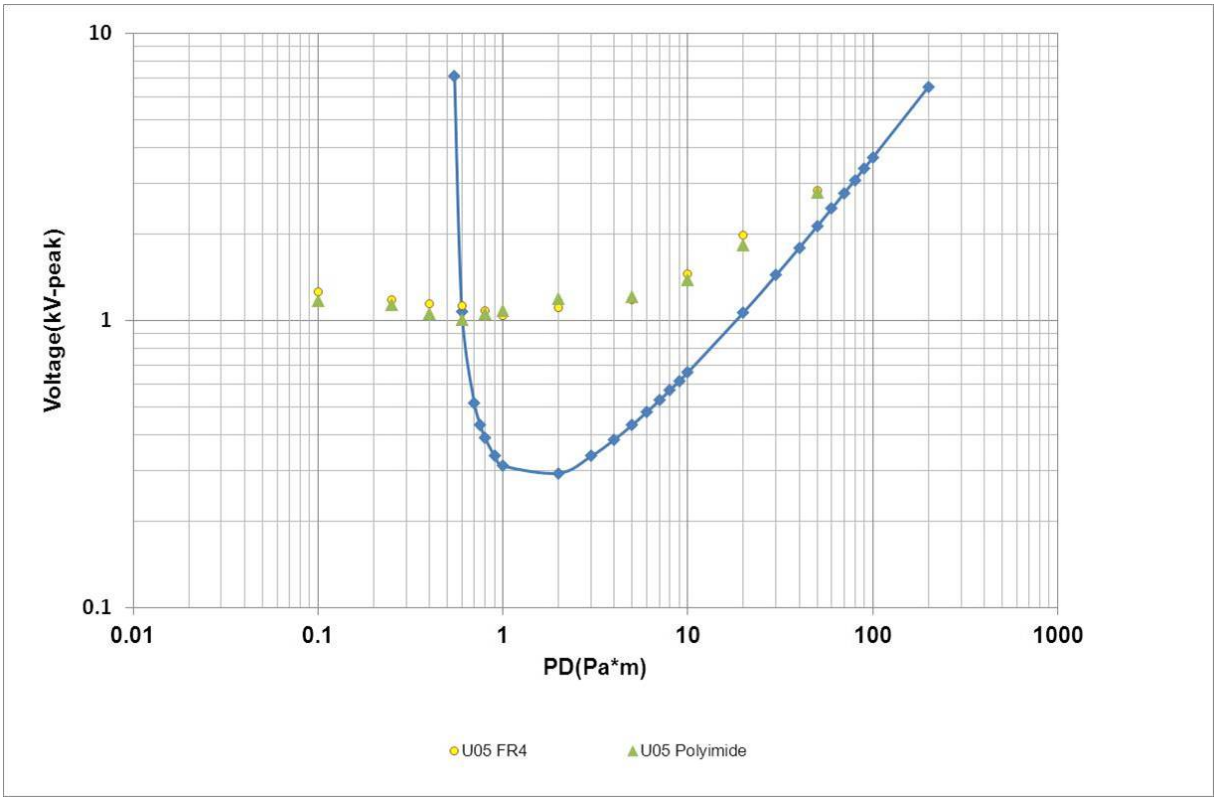

Figure 7.18: Comparison of test results between FR4 and Polyimide

7.3 Arc Voltage test results

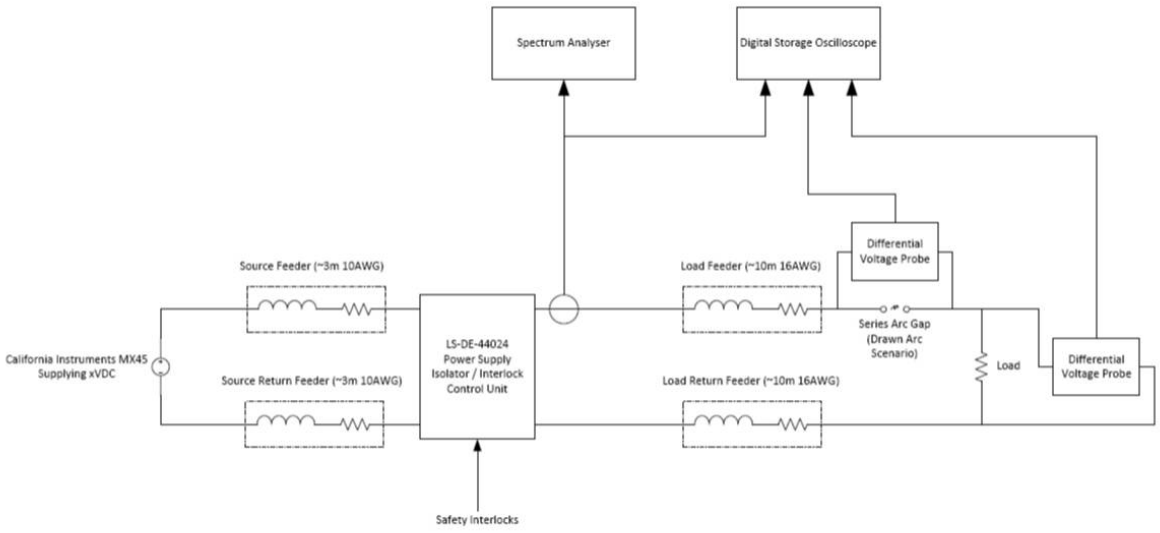

Figure 7.19: Test circuit for creating series arc

The above test set up was used to create series arc. From the above diagram the element labeled 'series arc gap' is actually an array of loose connections residing on a shaker table, as shown below in figure 7.20. This shaker table causes intermittent breaks in a circuit and as explained previously it is the interruption of a circuit that forms arcs. Many tests have been carried out, however, only a few of them will be shown here, as they all show very similar characteristics.

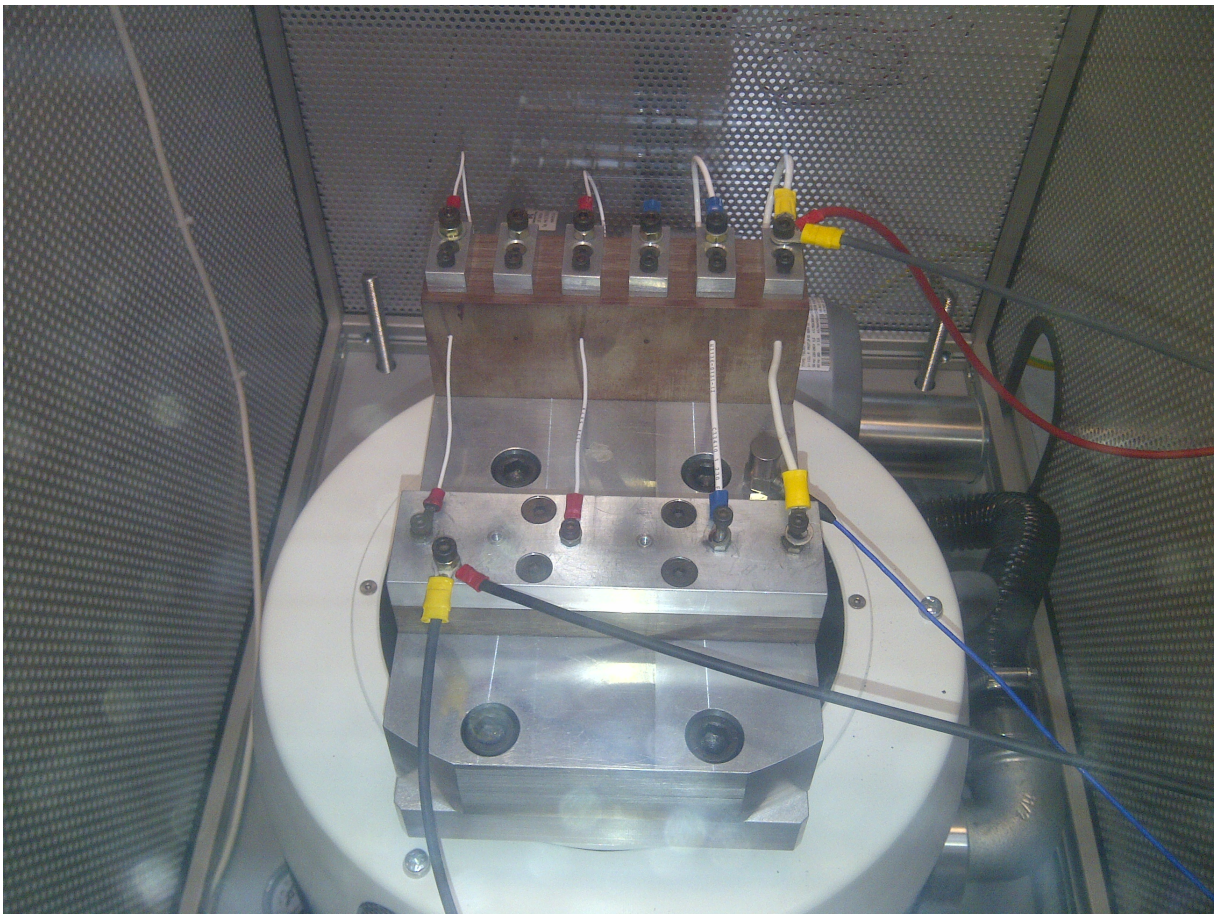

Figure 7.20: Test assembly for creating series arc faults, comprising of an array of loose connections on a shaker table

The supply voltage was derived from a California Instruments MX45 programmable power supply which was set to 270V DC and the load current has been set to 2A. One of the typical results from a shaker table series arc fault experiment is shown below in figure 7.21.

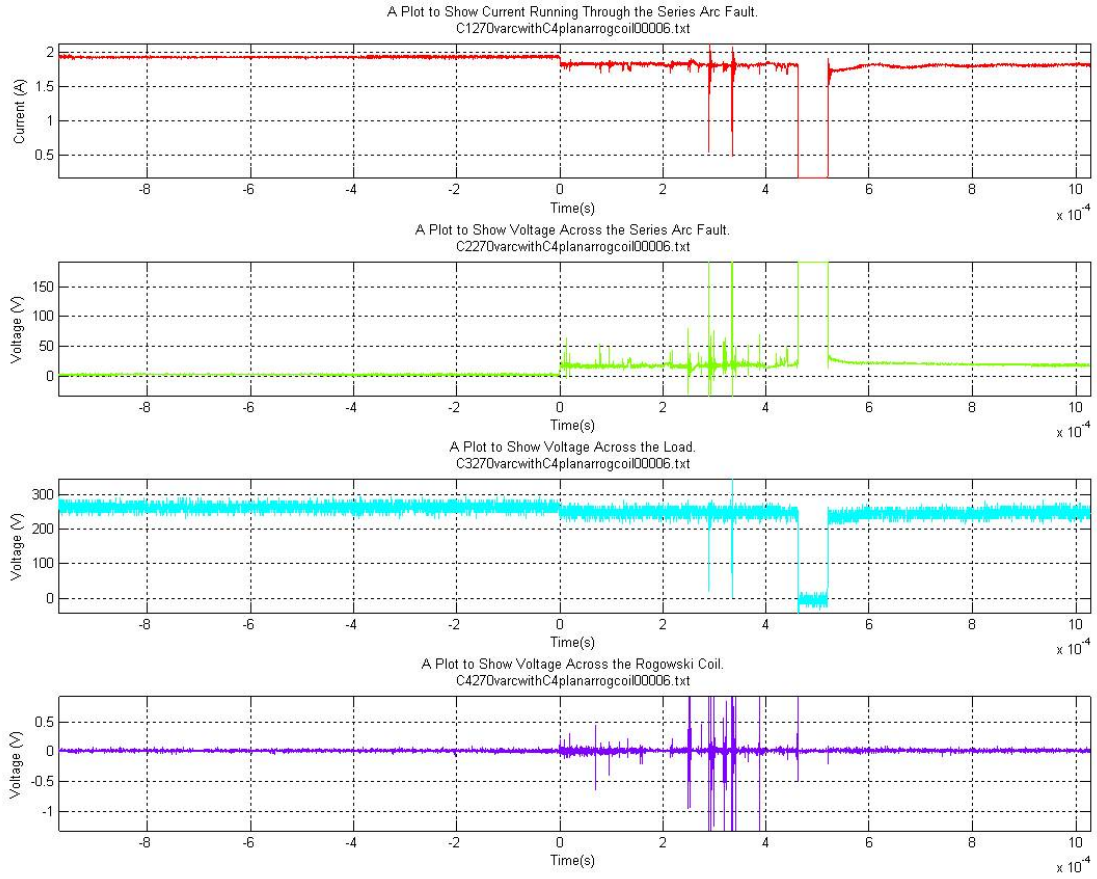

Figure 7.21: One of many results of series arc experiments.

Referring to the top three traces in figure 7.21. What can be seen from zero seconds (Note: all negative time traces are valid, it is just the oscilloscope had it's trigger level set to detect an arc and it sets time to zero at the trigger event). Trace 1 is showing the load current, which is approximately 2A, Trace 2 is showing the voltage across the arc and is measured by a differential probe connected across the shaker table and finally trace 3 is the voltage across the load.

What can be seen is when an arc establishes (trace 2) the load Voltage (trace 3) is reduced by the same amount. As the load is resistive the reduction in load voltage causes a drop in total current (trace1). The arc voltage is approximately 20V and after approximately 430μs the arc is quenched and the load current reduces to 0A and the voltage across the air gap rises to 270V

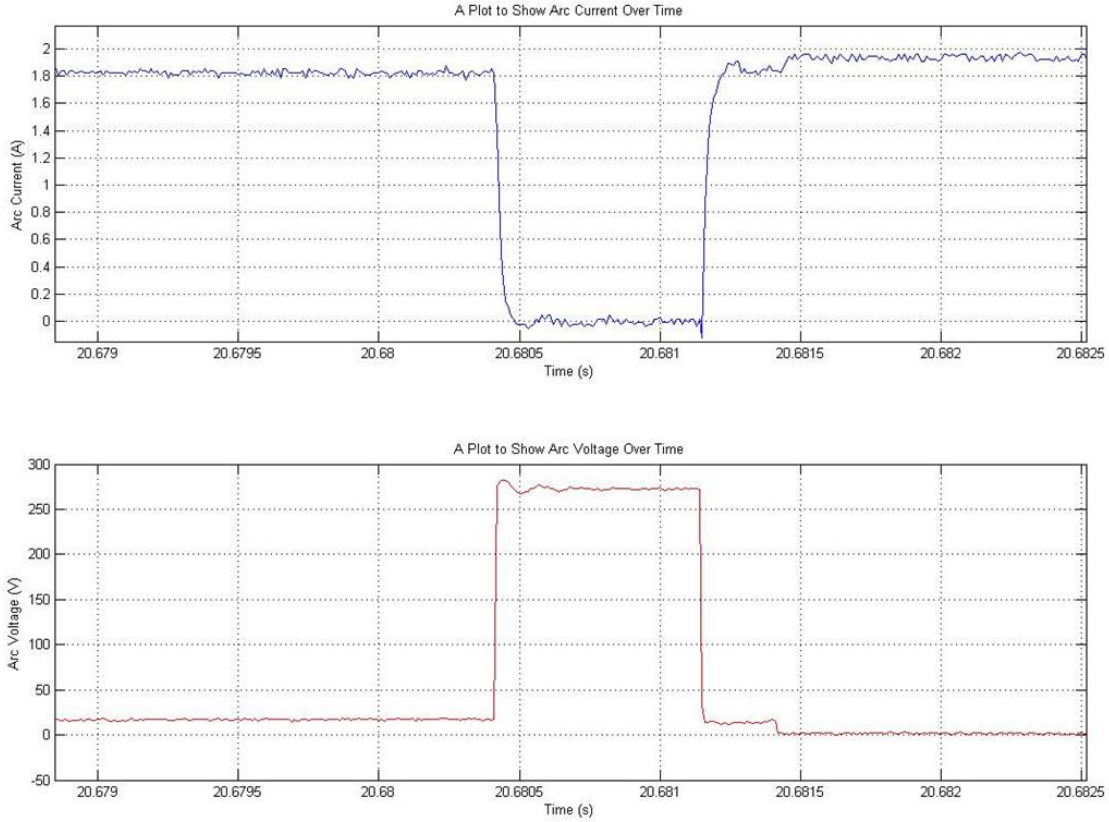

Figure 7.22: Stable Arc followed by quenching then re-establishing

The above figure shows an arc established from the very beginning of the traces, again the arc voltage is approximately 20V. and when time reaches 20.684s the arc is quenched only to be re-established at 20.6812s. However, at 28.6814s electrical connection was re-established and the arc voltage reduces to 0V.

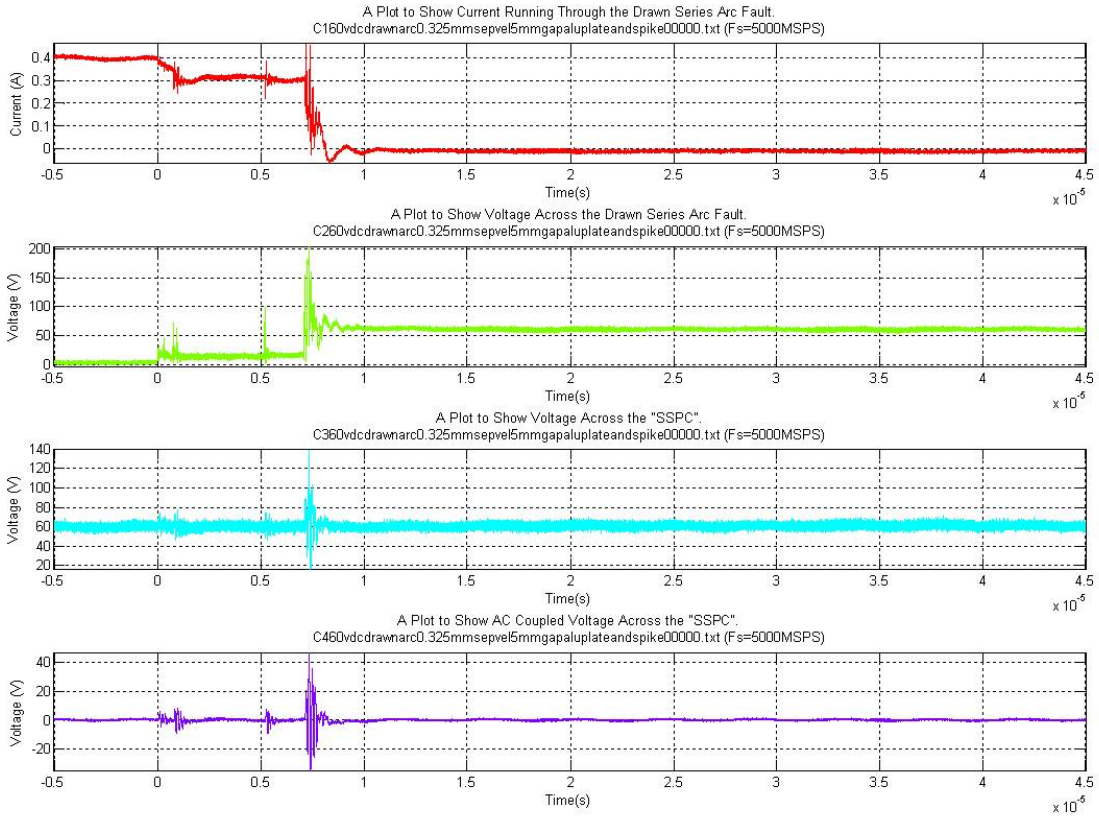

Figure 7.23: Tests producing a Drawn arc

The above figure was again produced using a set up as shown in figure 7.19. The supply voltage was set to 60V, however, this time the element labeled 'series arc gap' is actually two electrodes touching one another that can be pulled apart at programmable

rates by virtue of a stepper motor under PC control. This is similar to the shaker table discussed previously, however, this set up only provides a sample of one arc each time it is operated.

Chapter

8 Conclusion and Further Work

8.1 Conclusion

As detailed in Chapter 3, the currently accepted theory does not result in an equation that predicts the experimental 'Paschen' curve [18]. The equations that do result from the current accepted theory require further curve fitting and are therefore not considered fundamental in their treatment to the partial discharge phenomenon.

The current accepted design guidelines consider multiple variables that could result in electrical discharge, unfortunately these variables (e.g gas type, contamination) are not made explicit in the guidelines and are therefore unable to be separated out should modern design practices be employed negating some variables such as contamination. This has directly impacted many designs for aerospace, resulting in many of them being over engineered requiring larger volume equipment than should be necessary [8].

The proposed theory that is detailed in Chapters 4 and 5 attempts to provide a

fundamental understanding to the theory of partial discharge. The resulting equation from the proposed theory is given below in equation 8.1. This equation is that of the minimum conditions that will result in the probability of electrical discharge becoming none zero. The resultant curve of equation 8.1 is given below in figure 8.1.

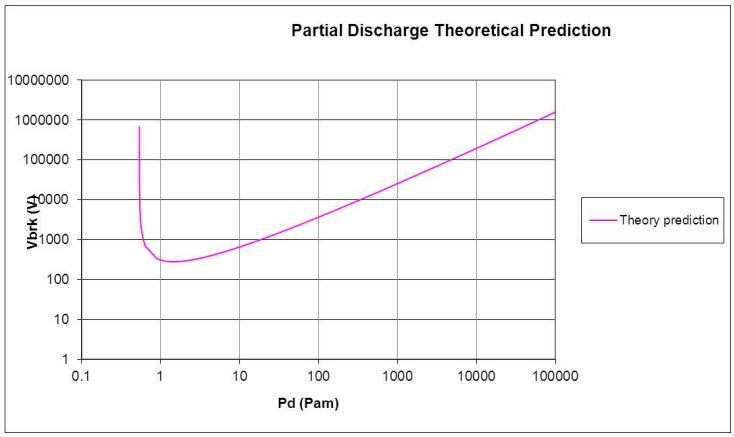

Figure 8.1: Curve showing theoretical partial discharge prediction

$$V_{pd} = \frac{4\pi\rho\sigma^2 epd}{3m_e\epsilon kT \cdot \left[\left(1 + ln\left(\frac{kT}{\sigma}\right)\right) + ln(pd)\right]} \tag{8.1}$$

From Figure 8.1 it can be seen that Equation 8.1 holds true for '*pd*' products greater than '0.7', however for *pd* products ≤ 0.7 the theory appears not to hold. At these very low '*pd*' products the mean free path λ of the gas is equal to and becoming greater than the distance '*d*' of the gap itself. This is probably a good definition of a vacuum. At these very low '*pd*' products alternative mechanisms may be taking place, such as;

- Electric Tunnelling
- Vacuum Breakdown

To put things in perspective the minimum achievable clearance on manufactured printed circuit boards is typically 0.15mm. Aircraft, however, are expected to fly at altitudes of 16781m (55000ft) ($p = 9170Pa$). This translates into a pd product of 1.4 Pam. This, therefore sets the upper limit for the 'pd' product.

Note: RTCA DO-160F section 4 temperature, altitude category D3 requires electrical equipment to be qualified to 15000m. [5]

At sea level(Altitude = $0m$ & $p = 101330Pa$) the corresponding pd product is Pd = 15.2 Pam, again assuming a 0.15mm clearance, this translates to a 'pd' range of $1.4 < pd < 15.2$. Referring this range of 'pd' product to that given in Figure 8.1, no violations to Equation 8.1 have been observed and good agreement can be found with that of IPC-2221A [8] and EN-60664 [25].

As a point of note the theory derived here provides an explanation as to how and why the variable that Paschen applied to the breakdown curve is 'pd'. But a variable that the Paschen curve does not account for is how the discharge voltage varies with temperature (T). From Equation 8.1 it can be seen that the voltage responsible for partial discharge will reduce if the temperature is raised.

Referring to Figure 4.5 it can be seen that the probability of a plasma formation on an individual flux line meeting the charge distribution criterion detailed in this paper, must be proportional to the quantity of flux lines themselves, therefore the area over which the E-field exists is an influencing factor and the larger the area where partial discharge can occur the greater its probability. As the tests themselves were conducted using relatively

small spherical electrodes, the probability of partial discharge occurring would be much reduced and this may account for the results being showing higher breakdown voltages than the theoretical predicted minimum.

Therefore over the regions of '*pd*' product that are practical and achievable no violations to the theory have been observed, even with statistical extrapolation so as to account for an even wider results range, no violations could be realised.

Referring again to figures 7.16 & 7.17, these figures provide a graphical representation of the guidance documents (IPC-2221A and EN-60664), overlaid with the extrapolated statistical worst case minimum discharge voltages which were derived from experimental results and the proposed theoretical minimum discharge curve. In the region where the mean free path λ is less than the air gap distance d, the theoretical curve sits between the experimental results and the documented guidance of IPC-2221A and EN-60664. This is a very encouraging result in that, no experimental results (statistically extrapolated to predict a worst case result), violate the theoretical minimum discharge curve. Also the guidance documents (IPC-2221A and EN-60664) fall below the theoretical minimum, this shows that the guidance is good, albeit conservative.

What is interesting is that the guidance given for system voltages for 300V or below, becomes extremely conservative and appears to show clearly the potential case for over designing in this region. Referring again to figure 2.19 which is the guidance table for IPC-2221A, for 31V and above columns B4 and A5 provide the same guidance, where column B4 relates to bare PCB requirements and A5 for an assembled variant. What is interesting is that the guidance given in both columns B4 and A5 for system voltages

of 300V and above, agree well with the theoretical predictions and experimentally validated results, as shown in figures 7.16 & 7.17, such that the guidance documents provide a consistent, albeit moderately conservative, guidance for design. However, below 300V all other guidance is extremely conservative, compared to experimental results and theoretical predictions. This provides a good indication that these documents are guiding designers to over engineered solutions.

In summary, adhering to the design guidelines as provided in IPC-2221A or EN-60664 will provide guidance for safe designs, in terms of clearance requirements. However, this guidance will prohibit density improvements in aviation equipment, this will further be exacerbated as system voltages rise, causing a reduction is equipment density. The theory presented here in this thesis, provides encouragement that increased densities can be realised, that still provide the same inherent safety margins as would be expected for aviation.

8.2 Further Work

Although the work presented in this thesis correlates well with experimentation and design guidelines (IPC-2221A and EN-60664), over the range of 'pd' products that are achievable and practicable for aviation applications. The experimentation has by no means provided conclusive results for the theory, however, the experimentation has neither disproved the theory also. This means that further experimentation would certainly be beneficial to further substantiate the claims made in this thesis. This is also true to the theories application to arcs, which also correlates well with experiment and observation, but would

also benefit from further experimentation.

The theoretical curve shown in figure 8.1 shown two inclinations centered around a minimum. To the right of this minimum, good, albeit conservative agreement with experiment and guidance has been presented. Variations, however, in Gas and Temperature are predicted but have not been experimentally verified. This would certainly be beneficial to substantiate the proposed theory and will discussed further below.

Results to the left of the theoretical minimum shown in figure 8.1, do not correlate well, where disruptive discharges have been observed below the theoretical minimum. Although the left side of the curve is beyond what is practicable and achievable for aviation purposes, it is still a theory that has been violated experimentally in this region. So further understanding is required in this area, either finding modifications to the proposed theory or a detailed study of alternate discharge methods such as electric tunnelling or vacuum discharge.

8.2.1 Effects of Gas variation and Temperature

The mean free path (λ) of the gaseous dielectric between two electrodes has featured extensively throughout the formulation of equation 8.1 and as Nitrogen is the most abundant molecule found in air, all of the analysis was conducted using Nitrogen exclusively. It would therefore be of great interest to conduct the whole suit of tests again in a Nitrogen filled chamber.

Other types of gases should also be considered in order to understand further how they influence partial discharge under varying pressures.

8.2.2 Polarisation effects throughout dielectric

The whole theory of plasma formation is tightly coupled to the interaction of polarisation forces on the gas molecules themselves. Applying the same theory as shown in earlier chapters, where the plasma has not progressed as far as described in the analysis the same equation 8.1 results.

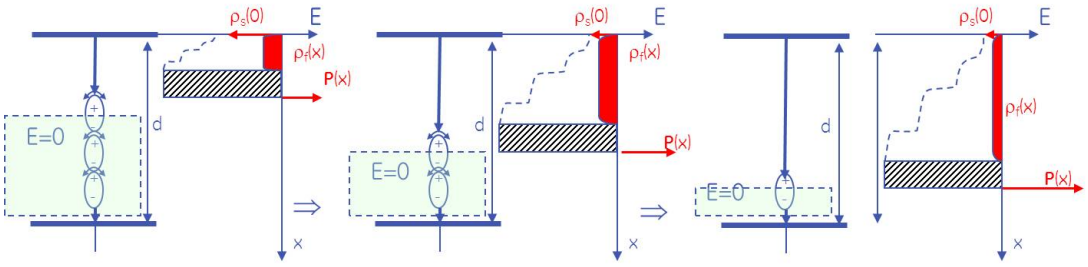

Figure 8.2: Three possible states of varying plasma distance

From figure 8.2 three possible states of vaying distances of plasma/dielectric combinations can be seen, all of which yield the same resulting equation. What would be of great interest is to observe this effective 'polarisation chain' whereby all of the polarised molecules interact and attract to one another.

Therefore if an experiment is set up as shown above where an E-field is applied to a gaseous dielectric, in order to polarise the air molecules, optical spectroscopy would

provide an insight into this hypothesis of a 'polarisation chain'

8.2.3 Time dependence of partial discharge

The theory presented here is probabilistic in nature and time invariant, which is fine under normal conditions, however, leads to further potential over engineering when considering transients, such as lightning strike. If, for example, equipment is being operated below the minimum voltage required for partial discharge or breakdown, but may experience transient voltages in the form lightning strike of up to 2000V for approximately 120 μs. Then as the theory is time invariant the only sensible conclusion would be to architect the system to be able to withstand 2000V, even though the transient event is over in such a short time.

Therefore, could time be incorporated into the analysis, whereby certain '*pd*' combinations will take a certain minimum amount of time to observe partial discharge events. Analysis in this area may prevent potential over engineering in any given solution.

8.2.4 Non uniform structures

The analysis throughout this thesis has applied the general theory to partial discharge with parallel plate electrodes. However, it would be of interest to demonstrate the theory to other non-uniform structures that will be observed in realistic situations.

It would be reasonable to expect that at near points the E-field will have greater intensity. Here the conditions may be appropriate for plasma formation, however, these conditions will be very local to the point and not allow plasma formation all the way to

the anode electrode. This may go some way to explaining non-visible corona.

8.2.5 Arcs

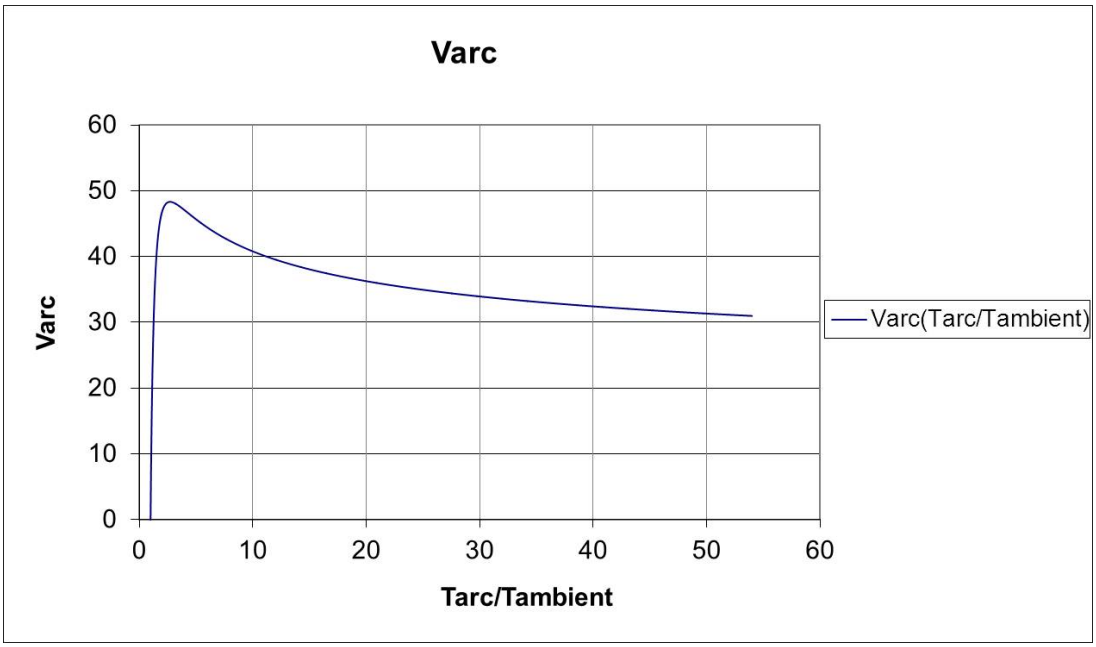

Figure 8.3: Varc over moderate arc temperature gain

The above figure shows the theoretical arc voltage as a function of temperature gain, over a moderate temperature range. Limiting the temperature range allows the continuous nature of the proposed arc voltage to be observed.

Chapter 6 has provided a possible relationship between partial discharge and arcs, this however, has not been exhaustive, therefore this is an area where much more work should be carried out to provide a fuller treatment and analysis in this area.

The equation 6.3 correlates the temperature gain of the arc temperature to the surrounding environment, to that of the arc voltage. The equation is shown graphically in figure 6.5. Now if temperature gain is a function of current, this curve would represent a negative impedance to the circuit as a whole. Referring now the the experimental results shown in figure 7.21, it can be seen that the transition from arc to quenched arc is quite abrupt, this may be due to the fact that temperature gain of the arc reduces extremely rapidly and was unable to be observed with the equipment used and its associated sampling speed.

Therefore further experiments to try and exaggerate the quenching of the arc, in an attempt to observe its continuous nature would be of great interest. This would still require a set up similar to that shown in figure 7.19, however, more inductance may be required to help sustain the arcing event. The shaker table or the drawn arc test set up may be used. The drawn arc test set up can only result in a single quenched arc but the shaker table does provide more results.

The theory presented here was derived over one mean free path λ at an extremely high gas temperature. Arc phenomena has been observed exceeding this distance, e.g. lightning. It is for this reason why the test set up giving the results shown in figure 7.23 was limited to 60V so that with all of the system losses, the available arc voltage was only just above the theoretical limit of 48V and therefore a true 'drawn arc' would not be observed. It would therefore be a interest to further understand the process by which a drawn arc propagates.

As stated earlier, it is reasonable to accept that the temperature of the arc is related

to the current passing through the circuit, however, I am not aware of any work that has correlated these two variables. Understanding this correlation would permit an arc model to be formed. It has be pointed out many times in this thesis that it is the interruption of a given circuit by means of an air gap that gives rise to an arc. Even relays and contactors experience arcing events every time that they open, unless mitigating circuits are incorporated to suppress this, such as snubber circuits. Understanding and correlating the relationship between circuit current and arc temperature would be of great interest, as it would provide input requirements to wiring insulation providers, which currently can only be conducted experimentally.

References

[1] A. Snow, "The first national grid," *Engineering Science and Education Journal*, pp. 215 – 224, 1993.

[2] The history of electrical power in aviation. GE Aviation. [Online]. Available: http://www.ge.com/audio_video/ge/technology/history_of_electric_power.html

[3] M. Mountney, "Ngcw technical report," TSB, Tech. Rep., 2010.

[4] R. Kolodziejczyk, "Protection and certification of aircraft avionic systems from lightning indirect effects," in *13th International Wroclaw Symposium and Exhibition on Electromagnetic Compatibility*, 1996.

[5] *RTCA DO-160F Environmental Conditions and Test Procedures for Airborne Equipment*, RTCA Std., 2007.

[6] F. A. Administration, "1999 structures der conference airframe breakout session," 1999.

[7] D. Walen, "Aircraft lightning, hirf and emc issues," in *FAA Propulsion Safety Workshop*, 2000.

[8] *IPC-2221A Generic Standard on Printed Board Design*, IPC Std.

[9] A. Qureshi and J. Dayton, "Insulation requirements of high-voltage power systems in future spacecraft," NASA, Tech. Rep., 1995.

[10] I. Cotton, "High voltage systems for the more electric aircraft," in *University of Manchester Short Course*, 2007.

[11] J. M. Kennedy, "Report on the operations of the proposed central electricity board," *Electricity Council Archive*, 1926.

[12] M. Sinnett, "787 no-bleed systems: Saving fuel and enhancing operational efficiencies," 2007. [Online]. Available: http://www.boeing.com/commercial/aeromagazine/articles/qtr_4_07/AERO_Q407_article2.pdf

[13] Louis karl heinrich friedrich paschen (january 22, 1865 - february 25, 1947), was a german physicist, known for his work on electrical discharges.

[14] A.-H. Zaki, "Power transmission to distant offshore facilities," *IEEE Transactions on Industry Applications*, vol. 47, pp. 1180–1183, 2011.

[15] T. Robbins, "Circuit breaker model for over current protection simulation of dc distribution systems," *Intelec*, 1995.

[16] R. M. B Gengenback and G. Horn, "Erosion characteristics of silver-based contact materials in a dc contactor," *IEEE Transactions on Components, Hybrids and Manufacturing Technology*, vol. CHMT-8, pp. 64 – 69, 1985.

[17] J. Sekikawa, T. Kitajima, T. Endo, and T. Kubono, "Observation of arc-emitted light between slowly opening electrical contacts using a high-speed camera," *Proceedings of the 50th IEEE Holm Conference on Electrical Contacts and the 22nd International Conference on Electrical Contacts*, pp. 47–52, 2004.

[18] E. Husain, "Analysis of paschen curves for air, n2 and sf6," *IEEE Transactions on Electrical Insulation*, vol. EI-17, pp. 350 – 353, 1982.

[19] H. Toyota, "Gaseous electrical discharge characteristics in air and nitrogen at cryo-gknic temperature," *IEEE Transactions on Dielectrics and Electrical Insulation*, vol. 9, pp. 891 – 898, 2002.

[20] V. Choulkov, "Effect of natural surface roughtness on electron emissin from metal in electric field," *IEEE*, pp. 17–20, 2004.

[21] J. P.L. Bellaschi Paul Evans, "Effect of altitude on impulse and 60 cycle strength of electrical apparatus," *Transactions of the American Institute of Electrical Engineers*, vol. 63, pp. 236 – 241, 1944.

[22] *MIL-STD-810*, Department of Defence Std.

[23] *MIL-HDBK-217*, Department of Defence Std.

[24] *Aircraft Lightning Environment and Related Test Waveforms*, SAE Std.

[25] *EN 60664-5 Insulation Coordination for equipment within low voltage systems*, European Standard Std.

[26] F. A. Bettelheim, W. H. Brown, M. K. Campbell, and S. O. Farrell, *Introduction to General, Organic and Biochemistry*, Brooks/Cole, Ed. Cengage Learning, 2009, 2009.

[27] J.S.Townsend, *Electricity in Gases*, C. Press, Ed. Oxford University Press, 1915.

[28] E. Kuffel and W. Zaengl, *High Voltage Engineering - Fundamentals*, N. York, Ed. Pergamon Press, 1884.

[29] M. Akyuz, "Positive steamer discharges in air and along insulating surfaces: experiment and simulation," Ph.D. dissertation, ACTA Universitatis Upsaliensis, 2002.

[30] A. Hammoud and M. Stavnes, "Effects of thermal and electrical stressing on the breakdown behavior of space wiring," NASA, Tech. Rep., 1995.

[31] G. Petraconi, H. S. Maciel, R. S. Pessoa, G. Murakami, M. Massi, C. Otani, W. M. I. Uruchi, and B. Sismanoglu, "Longitudinal magnetic field effect on the electrical breakdown in low pressure gases," *Brazilian Journal of Physics*, vol. 34, pp. 1662 – 1666, 2004.

[32] D. Parsons, "Corona/partial discharge handbook, design review, specification and test plans," Smiths Aerospace, Tech. Rep., 2004.

[33] C. Belnap, "High voltage packaging design for electric flight control surface actuator components," NASA, Tech. Rep., 2001.

[34] J. M. Mesina, "Determination of electrical clearances for permissable equipment operating in gassy mines and tunnels," *IEE Transactions on Industry Applications*, vol. 30, pp. 1339 – 1350, 1994.

[35] R. G. LONGWITZ, "Study of gas ionization in a glow discharge and development of a micro gas ionizer for gas detection and analysis," Ph.D. dissertation, COLE POLYTECHNIQUE FDRALE DE LAUSANNE, 2004.

[36] V. Lisovskiy, S. Yakovin, and V. Yegorenkov, "Scaling law for a low-pressure gas breakdown in a dc electric field in oxygen," kharkov National University.

[37] B. K. Das, B. G. Arambhadiya, M. S. Khan, S. B. Bhatt, and D. C. Reddy, "Electron impact breakdown of hydrogen gas," institute for Plasma Research, Bhat, Gandhinagar, Gujarat, India.

[38] Y. I. Davydov, "On the first townsend coefficient at high electric field," Joint Institute for Nuclear Research, 141980, Dubna, Russia, Tech. Rep., 2006.

[39] W. G. Dunbar, "Aerospace high voltage development," *IEEE AES Magazine*, pp. 2 –6, 1986.

[40] W. Khachen, J. Suthar, A. Stokes, and R. Dollinger, "Aerospace-specific design guidelines for electrical insulation," *IEEE Transactions on Electrical Insulation*, vol. 28, pp. 876 – 886, 1993.

[41] D. Kasten, S. Sebo, and X. Liu, "Partial discharges at sub-atmospheric pressures insulation evaluation procedures for aerospace applications," IEEE, Tech. Rep., 2007.

[42] F. Alrumayan, I. Cotton, and A. Nelms, "Partial discharge testing of aerospace electrical systems," *IEEE TRANSACTIONS ON AEROSPACE AND ELECTRONIC SYSTEMS*, vol. 46, pp. 848 – 863, 2010.

[43] R.S.Dhariwal, J.M.Torres, and M. Desmulliez, "Electric field breakdown at micrometre separations in air and nitrogen at atmospheric pressure," *IEE Proc.-Sci. Meas. Technol.,*, vol. 147, pp. 261 – 265, 2000.

[44] B. G. Rodriguez-Mendez, R. Lopez-Callejas, R. Pena-Eguilu, A. Mercado-Cabrera, R. V. Alvarado, S. R. Barocio, A. de la Piedad-Beneitez, J. S. Benitez-Read, , and J. O. Pacheco-Sotelo, "Instrumentation for pulsed corona discharge generation ap-

plied to water," *IEEE TRANSACTIONS ON PLASMA SCIENCE*, vol. 36, pp. 185 – 191, 2008.

[45] E. Wagenaars, "Plasma breakdown of low-pressure gas discharges," Ph.D. dissertation, Technische Universiteit Eindhoven,, 2006.

[46] G. B. Schmit, "Modelling particle behaviour in electric field stabilized fluidized beds," TUDelft, Tech. Rep., 2002.

[47] R. H. Fowler and D. L. Nordheim, "Electron emission in intense electric fields," *Proceedings from the Royal Society*, pp. 173 – 181, 1928.

[48] G. A. Mesyats and I. V. Uimanov, "Field emissions from metals in strong electric fields," *XXIIInd Int. Symp on Discharges and Electrical Insulation in Vacuum - Matsue*, pp. 29 – 32, 2006.

[49] P. A. Tipler and G. Mosca, *Physics for Engineers, Volume 1*, Macmillan, Ed. W.H Freeman and Company, 2008.

[50] Chemicool. (2011, June) Nitrogen chemicool periodic table. chemicool.com. ¡http://www.chemicool.com/elements/nitrogen.html¿.

[51] M. Lindmayer, A. Mutzke, and T. Ruether, "Some aspects of arc behavior in low voltage arc chutes," in *XVIth Symposium of Physics of Switching Arc*, 2005.

[52] S. Kulkarni, "An investigation into the dependence of the arc voltage on the parameters of the short-circuit current and the design of the vacuum interrupter," in *XXIIIrd International Symposium on Discharges and Electrical Insulation in Bacuum*, 2008.

[53] R. Rui, I. Cotton, L. Zhang, and C. Ilias, "Electrical machine and drive insulation system design issues for the more electric aircraft," *IET Electric Power Applications*, 2009.

[54] J. E. Harry, "Measurement of electrical parameters of ac arcs," *IEEE TRANSACTIONS ON INDUSTRY AND GENERAL APPLICATIONS*, vol. 5, pp. 594 – 599, 1969.

[55] X. Yan, C. Wang, and W. Chen, "Testing and modeling of low current arc in free air," *International Conference on High Voltage Engineering and Application*, pp. 136 –139, 2008.

[56] S. Kulkarni, S. Rajan, L. Andrews, R. Rajhans, and J. T. M, "An investigation into the dependence of the arc voltage on the parameters of the short-circuit current and the design of the vacuum interrupter," *XXIII-rd Int. Symp. on Discharges and Electrical Insulation in Vacuum Bucharest*, 2008.

[57] J. F. Lancaster, "The physics of fusion welding part 1: The electric arc in welding," *IEE REVIEW*, vol. 134, pp. 233 – 254, 1987.

[58] J. Sekikawa and T. Kubono, "Voltage-current characteristics of breaking arc at constant opening speed in the air," *IEEE TRANSACTIONS ON COMPONENTS AND PACKAGING TECHNOLOGIES*, vol. 27, pp. 167 – 171, 2004.

[59] C. Soelver, "Electric arcs and arc interruption," Chalmers University of Technology, Department of Electric Power Engineering, Tech. Rep., 2002.

[60] I. I. Beilis, "Present state of the theory of vacuum arcs," *IEEE 19th 1nt.Symp. on Discharges and Electrical Insulation in Vacuum-*, pp. 150 – 159, 2000.

[61] K. E. Crouch and L. C. Whitman, "The effect of wave shape on the electric breakdown of nitrogen gas," *IEEE TRANSACTIONS ON ELECTRICAL INSULATION,*, vol. 2, pp. 114 – 120, 1967.

[62] N. Zamanan and J. K. Sykulski, "Modelling arcing high impedances faults in relation to the physical processes in the electric arc," *WSEAS Transactions on power systems*, vol. 1, pp. 1507 – 1512, 2006.

[63] V. V. Terzija and H. J. Koglin, "Newapproach to arc resistance calculation," *IEEE*, pp. 781 – 787, 2001.

[64] H. Zhan, C. Wang, G. Wang, and H. Ai, "Research on relationship between arc length and arc voltage in the plasma deposition manufacture process," *Progress In Electromagnetics Research Symposium, Beijing, China*, pp. 959 – 963, 2009.

[65] M. Naidu, T. J. Schoepf, and S. Gopalakrishnan, *Electrical Wiring Harnesses and Electronics and Systems Reliability*, SAE, Ed. SAE, 2005.

[66] J. Zhange, C. Wang, G. Wang, and H. Ai, "Research on relationship between arc length and arc voltage in the plasma deposition manufacture process," in *Progress in Electromagnetics Research Symposium*, 2009.

[67] T. Robbins, "Circuit-breaker model for over-current protection simulation of dc distribution systems," in *IEEE - Intelec*, 95.

[68] J. Sekikawa, T. Kitajima, T. Endo, and T. Kubono, "Observation of arc-emitted light between slowly opening electrical contacts using a high-speed camera," *IEEE*, pp. 47 – 52.

[69] C. Strobl and P. Meckler, "Basic experiments for detecting arc faults in dc aircrafbasic aircraft networks," ICE, Tech. Rep., 2008.

[70] H. Fang, J. Jiang, and R. Mou, "The study of the relationship between arc duration and arc energy of relay and microswitch contacts," Department of Electrical Engineering, Xian Jiaotong University Xien, Shaanxi 710049 People's Republic of China, Tech. Rep., 1992.

[71] H. Toyota, S. Zama, and Y. Akamine, "Gaseous electrical discharge characteristics in air and nitrogen at cryogenic temperature," *IEEE Transactions on Dielectrics and Electrical Insulation*, vol. 9, pp. 891 – 898, 2002.

[72] D. F. Peelo, "Current interruption using high voltage air-break disconnectors," Ph.D. dissertation, Technische Universiteit Eindhoven, 2004.

[73] R. Jerome, C. Stephane, and A. M'Hammaed, "The modeling of the cathode sheath of an electrical arc in vacuum." Laboratoire de Recherches sur la Ractivit des Solides, UMR 5613 CNRS Universit de Bourgogne 21078 Dijon (France), Tech. Rep., 2002.

[74] I. Cotton, "Ge aviation electrical discharge on circuit boards," University of Manchester, Tech. Rep., 2011.